Adsorption of Naphthenic Acids from Oil Sand Process-Affected Water (OSPW) using Synthesized Activated Carbon

A Thesis Submitted to the Committee on Graduate Studies in Partial Fulfillment of the Requirements for the Degree of Doctor of Philosophy in the Faculty of Arts and Science

TRENT UNIVERSITY

Peterborough, Ontario, Canada

Materials Science Ph.D. Graduate Program

January 2025

Abstract

Adsorption of Naphthenic Acids from Oil Sand Process-Affected Water (OSPW) using Synthesized Activated Carbon

Elmira Nazari

This thesis explores the remediation of naphthenic acids (NAs) from oil sands process-affected water (OSPW) using activated carbon (AC) derived from petroleum coke (PC) chemically activated with potassium hydroxide. The research aims to identify the most effective method for the adsorptive removal of NAs by optimizing the use of economically viable KOH quantities and to apply Fourier Transform Ion Cyclotron Resonance Mass Spectrometry (FT-ICR-MS) for species-specific detection and characterization of NAs, crucial for targeting specific NAs in future studies.

Prior research focused on single-species adsorption, establishing a foundational understanding of non-competitive adsorption before applying these findings to more complex NA mixtures and OSPW. This study builds upon this foundation, addressing a significant gap in the literature concerning the use of petcoke-derived AC with low KOH ratios and short activation times, which are economically advantageous for large scale applications.

In this thesis, a comprehensive investigation into the kinetics and isotherms of NA adsorption on various ACs including PAC (petroleum coke AC), PWAC (pore-widened AC), HAC (heat-treated wood-based AC), and CAC (commercial AC) was conducted. The study specifically examines the adsorption behaviors of seven model NAs, reflecting the diverse molecular structures present in real world OSPW. The research also explores the impact of pore widening

techniques on the adsorption efficiency of ACs, hypothesizing that increased mesoporosity enhances the adsorption of NA compounds.

The findings demonstrate that FT-ICR-MS is an essential tool for precisely characterizing the NA species in OSPW, revealing that pore-widened ACs significantly improve the adsorption of NAFCs. This thesis contributes to the field of environmental remediation by offering new insights into the optimization of AC for NA removal, emphasizing the importance of surface chemistry and mesoporosity in enhancing adsorption efficiency. The study's outcomes have significant implications for the treatment of OSPW, providing a scalable and cost-effective solution to mitigate the environmental impacts of oil sands production.

Keywords

Oil Sands Process-Affected Water (OSPW), Naphthenic Acids (NAs), Activated Carbon (AC), Petroleum Coke (PC), FT-ICR-MS, Adsorption Kinetics, Environmental Remediation.

Acknowledgment

This PhD journey has been one of the most challenging and rewarding experiences of my life, and I am deeply grateful to the many people who have supported me along the way.

First and foremost, I would like to express my sincere gratitude to my supervisor, Prof. Andrew Vreugdenhil, for his unwavering support, guidance, and encouragement throughout my research. His insightful advice and constructive feedback have been invaluable, and his belief in my work has kept me motivated even during the most challenging times. Thanks a million for the opportunity you provided for me.

I am also thankful to the members of my thesis committee, Prof. Brad Easton and Prof. Aaron Slepkov, for their time, effort, and invaluable feedback, which have significantly improved the quality of my research.

I would like to extend my thanks to my colleagues and fellow researchers in the IMRL The friendship, shared experiences, and stimulating discussions have enriched my academic journey and made this process more enjoyable.

A special thank you goes to the technical staff at Water Quality Centre Specially Dr. Naomi Stock, whose support and assistance have been crucial in navigating the logistical aspects of my research.

I am deeply grateful to my family for their endless love, patience, and encouragement. My siblings for being always there for me. My parents have always been my biggest supporters, and their unwavering belief in my abilities has been a constant source of strength. You are my everything. I love you forever.

To my love, MReza, your unwavering support, patience, and understanding have been my greatest source of strength throughout this journey. You've been by my side through the late nights, the moments of doubt, and the celebrations of success, always encouraging me to keep going. Your belief in me, even when I struggled to believe in myself, has been a constant reminder of the love and partnership we share. Thank you for being my rock, my confidant, and my greatest cheerleader. I couldn't have done this without you, and I am endlessly grateful for your love. This thesis is as much yours as it is mine. Thank you for everything.

To my wonderful kids, Nila and Shayan. Thank you for being my greatest gifts and constant sources of inspiration. I am so proud of you two and will always support you in achieving your dreams. I love you more than words can express.

Lastly, I would like to acknowledge the financial support from Paul Pede, from Carbonix Inc. for his support throughout this research. which made this research possible.

To everyone who has been part of this journey, whether mentioned here or not, your support has meant the world to me. Thank you.

Table of Contents

Abstract ..... **ii**

Keywords ..... ***iii***

Acknowledgment ..... **iv**

List of Figures ..... **ix**

List of Tables ..... **xi**

List of Abbreviations ..... **xii**

Chapter 1 – Introduction and Research Objectives **1**

1.1 General Introduction to Oil Sands Process-Affected Water (OSPW) ***1***

1.1.1 Oil Sands in Alberta 1

1.1.2 Process of Extracting Oil 2

1.2 Oil Sands Naphthenic Acids ***5***

1.2.1 Origin 5

1.2.2 Properties of Naphthenic Acids 5

1.2.3 Toxicity and Corrosiveness of Naphthenic Acids 7

1.2.4 Analytical Methods for Detection and Quantification of NAs 8

1.2.5 Remediation Techniques of OSPW 11

1.3 Production of Activated Carbon from Petroleum Coke ***12***

1.4 Thesis Objectives ***15***

Chapter 2 - Methodology and Characterization Techniques **18**

2.1 Characterization Techniques ***18***

2.1.1 Total Organic Carbon Analyzer (TOC) 18

2.1.2 Surface Area and Pore Size Distribution Characterization 20

2.1.3 X-Ray Photoelectron Spectroscopy (XPS) 23

2.1.4 Fourier Transform Ion Cyclotron Resonance Mass Spectrometry (FT-ICR MS) and Electroscopy Ionization (ESI) 24

2.1.5 Point of Zero Charge 26

2.2 Adsorption Study ***28***

2.2.1 Adsorption Kinetics 28

2.2.2 Kinetics Modelling 29

2.2.3 Adsorption Isotherms 30
2.3 Production of Activated Carbon 34
2.3.1 Production of Potassium Hydroxide (KOH) Petroleum Coke Activated Carbon 34
2.3.2 Production of Heat-Cycled KOH Petroleum Coke Activated Carbon 35
2.3.3 Production of Heat-Treated Phosphoric Acid (H_3PO_4) Activated Carbon 36
Chapter 3 – Kinetics and Isotherms Study of Naphthenic Acid Adsorption on Various Synthesized Activated Carbons 38
3.1 Introduction 38
3.2 Materials and Methods 40
3.3 Results and Discussion 40
3.3.1 Textural Properties of each Activated Carbon 40
3.3.2 Surface Functionality of each Adsorbent 43
3.3.3 Kinetics of Adsorption 45
3.3.4 Isotherms Study 50
3.4 Conclusion 58
Chapter 4 – Adsorption Kinetics of Model Naphthenic Acids on Pore Widened Activated Carbons 59
4.1 Introduction 59
4.2 Materials and Methods 60
4.3 Results and Discussion 61
4.3.1 Kinetics Study 61
4.3.2 Adsorption study of Model Compounds and Their Characterization by FT-ICR-MS . 69
4.4 Conclusion 75
Chapter 5 - Removal of Naphthenic Acids from OSPW Using Pore-Widened Activated Carbons: An FT-ICR-MS Study 76
5.1 Introduction 76
5.2 Material and Methods: 77
5.2.1 Chemical and reagents 77
5.2.2 Activation of petroleum coke with KOH and subsequent cycling experiments 77
5.2.3 Adsorption test: TOC 78
5.2.4 Liquid-Liquid Extraction of Naphthenic Acids 78
5.2.5 Point of zero charge (PZC) 79

5.2.6 Characterization techniques 79
5.2.6.1 Brunauer-Emmet-Teller (BET) surface area analysis 79
5.3 Results and Discussion ***82***
5.4 Conclusion ***91***
Chapter 6 – Conclusion **93**
6.1 General Conclusion ***93***
6.2 Future Work ***95***
6.3 Contributions to Science ***96***
6.3.1 Publications 96
6.3.2 Conferences 96
References **98**

List of Figures

Figure 1.1. Major oil sands areas in Alberta, Canada, Source: (Alberta Energy Regulator and Alberta Geological Survey) 2

Figure 1.2. Examples of classical NAs where R represents an alkyl chain. 6

Figure 1.3. Three types of adsorption mechanisms on the surface of activated carbon: a) physisorption; b)H-bonding; and c)chemisorption. 14

Figure 2.1. TOC Analyzer to measure the residual organic carbon in naphthenic acid solution. 18

Figure 2.2. Schematic diagram showing TOC measurement using TOC Analyzer 19

Figure 2.3. IUPAC 6 types of isotherms (Taken from ref [96]) 21

Figure 2.4. Schematic of procedures involved in generating a mass spectrum through FT-ICR-MS analysis (Taken from ref [72]) 25

Figure 3.1. Particle size distribution of all three adsorbents of a)PAC; b)CAC; and c)HAC. 43

Figure 3.2. C 1s XPS Survey Scans of a) PAC; b) HAC; and c) CAC 45

Figure 3.3. Adsorption kinetics of model NAs onto three types of ACs: 1) PAC; 2) CAC; and 3) HAC. 48

Figure 3.4. Isotherms illustrating the absorption of model NA species on (a) CAC, (b) PAC, and (c) HAC. 52

Figure 3.5. The highest adsorption capacities for each model NA, as determined through experimentation, normalized against the total specific surface area of each type of activated carbon. 54

Figure 4.1. Adsorption kinetic plots for model naphthenic acids of a) diphenylacetic acid (DPA); b) cyclohexaneacetic acid (CHA); and c) heptanoic acid (HA) on three heat-cycled ACs with showing the initial up to 2h. Single, double and triple AC are activated carbons subjected to one, two and three cycles of heat treatments, respectively. 64

Figure 4.2. Adsorption kinetics with adsorption capacity normalized to surface area of each activated carbon for a) diphenylacetic acid (DPA); b) cyclohexaneacetic acid (CHA); and c) heptanoic acid (HA). 67

Figure 4.3. Mass spectral analysis of a) DPA, b) DHA, c) SA, d) 1,4-CHA, e) ACA, and f) PCA compounds treated with single and triple-cycled ACs. 74

Figure 5.1. An illustration of ultrahigh resolving power is evident in the detection of four distinct peaks within a 018 Da range in a negative-ion ESI FT-ICR mass spectrum acquired for an acid-extracted OSPW sample. This data was obtained using magnitude mode. 84

Figure 5.2. Broadband mass spectra for NA extracts of: a) non-treated OSPW; b) OSPW treated with single cycled AC; and c) OSPW treated with triple cycled AC acquired in negative mode by FT-ICR mass spectrometer. 86

Figure 5.3. Negative ion ESI-FT-ICR-MS heteroatom class distribution for OSPW, treated OSPW with single-cycled AC and triple-cycled AC. the relative standard deviation based on triplicate run of the same sample was less than 10% of the measured values. 88

Figure 5.4. Comparison of OSPW treated with single and triple cycled ACs with non-treated OSPW for the 5 most abundant NAFC classes as follows: a) O2; b) O3; c) O4; d) O2S and e) O3S in Negative-ion ESI-FT-ICR-MS analysis. 91

List of Tables

Table 3.1. Analysis of the BET surface area of the utilized activated carbon adsorbents. 41

Table 3.2. Atomic Percent Composition by XPS 43

Table 3.3. Adsorption half times for model naphthenic acids onto each activated carbon calculated using m-exp modelling. *CAC was not modelled by m-exp, and thus adsorption half times are approximated by experimental adsorption kinetics. 50

Table 3.4. Assessment of Optimal Isotherm Models for Each Adsorption System. 57

Table 3.5. Parameters Determined from Isotherm Modeling of the Most Representative Models for Each Adsorption System. 57

Table 4.1. An overview of model NA compounds used in this study. 61

Table 4.2. Adsorption half times for three model naphthenic acids of DPA, CHA and HA on surface of het-cycled ACs 68

Table 5.1. Surface properties of single and triple cycled PWACs 78

Table 5.2. Summary of NA concentration, # of assigned formulas, mass accuracy and total intensities in pre-treated OSPW and OSPW treated with single and triple cycled AC. 83

List of Abbreviations

1,4-CHA	1,4-cyclohexanedicarboxylic acid
AC	Activated Carbon
ACA	9-anthracenecrboxylic acid
AIC	Akaike Information Criterion
APPI	Atmospheric Pressure Photoionization
BET	Brunauer-Emmet-Teller Surfaace Area Analysis
CAC	Commercial Activated Carbon
CHA	Cyclohexaneacetic Acid
DBE	Double Bond Equivalency
DFT	Density Functional Theory
DHA	Dicyclohexylacetic Acid
DPA	Diphenylacetic Acid
ESI	Electroscopy Ionization
FT-ICR-MS	Fourier Transform Ion Cyclotron Resonance Mass Spectrometry
FTIR	Fourier transform infrared Spectroscopy
GC-MS	Gas Chromatography-Mass Spectrometry
HA	Heptanoic Acid
HAC	Heat-Treated Wod-based Activated Carbon
HPLC	High-Performance Liquid Chromatography
IMRL	Inorganic Materials Research Lab
IUPAC	International Union of Pure and Applied Chemistry
KOH	Potassium Hydroxide
MCH	2-methyl-1-cyclohexanecarboxylic acid
MW	Molecular Weight
NA	Naphthenic Acid
NAFC	Naphthenic Acid Fraction Compounds
NLDFT	Non-Local Density Functional Theory
NMR	Nuclear Magnetic Resonance
NPOC	Non-Purgeable Organic Carbon
OSPW	Oil Sands Process-Affected Water
OSTWAEO	Oil Sands Tailings Water Acid-Extractable Organics
PAC	Petroleum Coke-derived Activated Carbon
PAH	Polyaromatic Hydrocarbons
PC	Petroleum Coke
PCA	1-pyrenecarboxylic acid
POC	Purgeable Organic Carbon
PWAC	Pore-Widened Activated Carbon
PZC	Point of Zero Charge
RP	Redlich-Peterson

SA	Succinic Acid
SAGD	Steam Assisted Gravity Drainage
TOC	Total Organic Carbon
UV	Ultraviolet
VAPEX	Vapor Extraction Process
XPS	X-Ray Photoelectron Spectroscopy

Chapter 1 – Introduction and Research Objectives

1.1 General Introduction to Oil Sands Process-Affected Water (OSPW)

1.1.1 Oil Sands in Alberta

The northern Alberta oil sands possess the world's third-largest oil reserves, trailing only Venezuela and Saudi Arabia. These reserves are estimated to contain approximately 2.5 trillion barrels of recoverable bitumen, a dense and viscous form of crude oil.[1,2]. As per a government report, in northern Alberta, three primary oil sands deposits—Athabasca, Cold Lake, and Peace River—span a surface area of approximately > 140,000 km^2 (Figure 1). The bitumen production from Alberta's oil sands industry reached 2.15 million barrels per day in 2014 and is projected to increase to 3.95 million barrels per day by 2030[3,4].

Figure 1.1. Major oil sands areas in Alberta, Canada, Source: (Alberta Energy Regulator and Alberta Geological Survey)

The surge in demand, coupled with technological advancements, has resulted in the swift expansion of the oil sands industry[3]. Over the period from 1999 to 2013, investments totaling around $201 billion were injected into the industry[5]. As the ongoing growth and expansion persist, growing concerns emerge regarding the remediation of tailings ponds containing hazardous wastewater and the significant extraction of fresh water from the nearby Athabasca River[3,6].

1.1.2 Process of Extracting Oil

The oil sands are comprised of compressed deposits of sand, silt, clay, water, and bitumen. Typically, they consist of approximately 6 to 14% bitumen by weight, with 80 to 85% constituting mineral solids, and the remaining balance composed of water[7,8]. Bitumen is characterized as a naturally occurring, highly viscous mixture of hydrocarbons that cannot be recovered in its natural state through conventional oil well production methods, including currently employed enhanced recovery techniques[3].

In Alberta, bitumen extraction typically involves two methods: surface mining (open pit mining) and *in-situ* extraction utilizing thermal recovery methods[9].The primary method of oil extraction employed by the two major oil producers in Alberta, namely Suncor Energy Inc. and Syncrude Canada Ltd., is surface mining which significantly transforms the landscape[3,10]. Open-pit mining is employed for oil sand deposits located within 75 meters of the surface. Initially, oil sands material from shallow deposits is transported to crushers by large trucks. Subsequently, it is commonly conveyed as a slurry from the mining area to the extraction plant[11]. The bitumen, a dense mixture of hydrocarbons that undergoes transformation into crude oil, is extracted using the Clark Hot Water Process[12,13]. Water sourced from the Athabasca river is heated, and a caustic

soda (NaOH) is introduced into the slurry to enhance bitumen separation and facilitate the release of surfactants[9,14]. The slurry is subsequently transported through pipelines to primary separation vessels, where bitumen separation is achieved through flotation. The isolated bitumen is then conveyed to the froth treatment plant, where it undergoes upgrading to become crude oil[14,15]

While this approach proves highly effective for bitumen extraction, it comes with the drawback that approximately 3 barrels of water are utilized for one barrel of crude oil produced. This produced water, known as oil sands process-affected water (OSPW), exhibits high toxicity to biological organisms and represents a significant environmental and economic challenge for the ongoing development of this resource[15–17].

Suncor Energy Inc. and several smaller extraction companies have also adopted a second extraction method known as *in-situ* mining. *In-situ* operations distinguish themselves from open-pit mining by extracting bitumen from ore deposits situated at depths below 75 meters through drilled wells[3,13]. *In-situ* operations have the capability to recover and recycle approximately 90% of the water employed, with the remaining portion being lost into the ground[3,18]. Three commonly employed *in-situ* methods include Cycle Steam Stimulation (CSS), Steam Assisted Gravity Drainage (SAGD), and the Vapor Extraction Process (VAPEX)[3,9,12]. In Cycle Steam Stimulation, a single well is alternated between production (extraction) and steam injection. This method yields relatively low bitumen recovery, typically ranging from 20-25%, with cycle times averaging 6-8 months[3,19]. Steam Assisted Gravity Drainage utilizes horizontal drilling techniques initially developed for petroleum production. Steam Assisted Gravity Drainage proves more cost-effective than Cycle Steam Stimulation and achieves superior recovery rates. Currently, companies are exploring

combinations of both methods to enhance recovery rates [13]. Another method utilizing a heat carrier is the Vapor Extraction Process, akin to Steam Assisted Gravity Drainage but employing vaporized solvents instead of steam to liquefy bitumen for subsequent extraction[3,12]

The resultant OSPW is mildly alkaline, highly saline, and poses acute toxicity to aquatic organisms. This toxicity is primarily attributed to the elevated concentrations of organic compounds leaching from bitumen during the extraction process[20]. Tailings water produces at a daily rate of one billion liters, given that approximately 4 m^3 of OSPW are discharged per 1 m^3 of bitumen extracted from oil deposits [11,21]. This has led to the generation of over 720 billion liters of OSPW, which is currently stored in tailings ponds, covering an expansive area of 170 km^2[3,11,20]. Because of Alberta's zero discharge regulation, oil sands producers are unable to discharge the processed water back into rivers. Consequently, they are obliged to store all processed waters and tailings on-site, leading to the accumulation of substantial volumes of water in tailings ponds[9,12].

OSPW is composed of a combination of residual bitumen, dissolved salts, minerals, inorganic compounds, and a diverse array of organic compounds. These include polyaromatic hydrocarbons (PAHs), benzene, phenols, humic and fulvic acids, as well as toluene and naphthenic acids (NAs)[22,23]. The existence of NAs significantly contributes to the acute toxicity observed in OSPW[24,25]. therefore, treatment technologies focused on mitigating OSPW toxicity have specifically aimed at removing these compounds[13,26].

1.2 Oil Sands Naphthenic Acids

1.2.1 Origin

NAs constitute a natural component present in deposits of bituminous oil sands. While the oil sands industry has been increasingly adopting the *in-situ* SAGD process for bitumen recovery, surface mining and extraction methods have been more prevalent among companies in recent decades[27,28]. The latter approach has been argued to be more efficient, yet it also generates a larger volume of waste[7,8]. The reported range for the concentration of extractable organic acids in tailings ponds is between 40 and 125 mg/L[3,20]. Within the Athabasca oil sands leases, these organic acids are discharged under alkaline conditions.

1.2.2 Properties of Naphthenic Acids

NAs consist of a mixture of alicyclic and aliphatic carboxylic acids that are chemically stable and non volatile and serve as surfactants owing to their hydrophobic (non-polar aliphatic) and hydrophilic ends (carboxyl group)[11,29]. These substances are naturally present in petroleum, with varying concentration levels determined by the specific source of the petroleum[12,17,23,30]. These organic acids can be expressed by the general chemical formula $C_nH_{2n+z}O_2$, where 'n' signifies the carbon number, and 'z' is either zero or a negative even number, denoting the quantity of cyclic rings in a particular homologous series[17,29,31–33]. Figure 1-2 illustrates examples of fundamental acyclic, monocyclic, bicyclic, and tricyclic NAs.

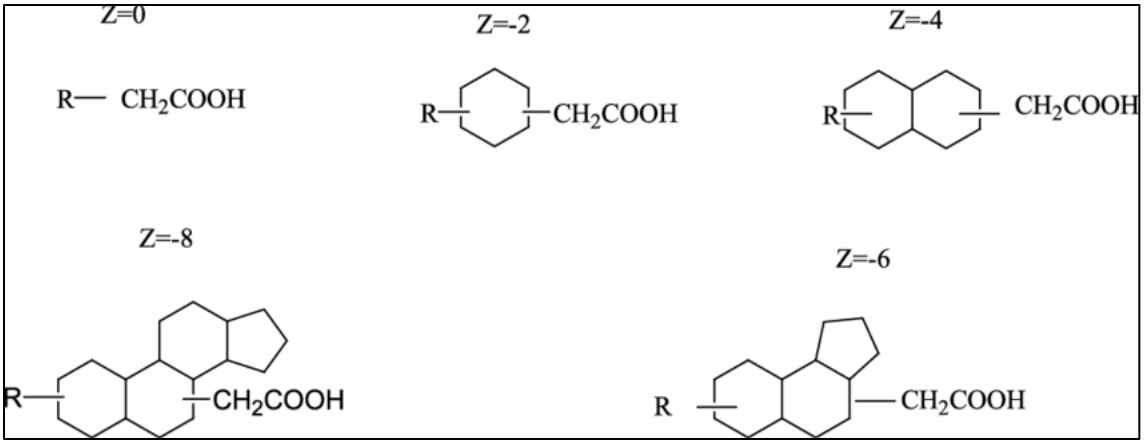

Figure 1.2. Examples of classical NAs where R represents an alkyl chain.

The ring structures present in NAs usually consist of 5 or 6 carbon atoms arranged in diverse combinations. Consequently, a wide variety of NAs exists, characterized by distinct functional groups and levels of aromaticity. There are numerous other NA compounds that do not follow the formula of classical NAs, like aromatic NAs and other heteroatom containing NA species. This diversity leads to variations in toxicity levels among different NAs species[23,34]. The molecular weight (MW) of NAs undergoes a change of 2 mass units (H_2) within the Z series and 14 mass units (CH_2) within the n series[35]. As reported, NAs originating from OSPW may possess numerous carboxylic acid groups, along with compounds containing nitrogen (N) and sulfur (S)[30,36]. Hence, the general formula employed to depict NAs is an oversimplification, encompassing not just the NA mixture but also traditional NAs. The Z-value may arise from factors such as aromaticity or double bonds, not solely the count of rings present[11]. The exact number of different types of NAs present in OSPW can be considerable, reflecting the complexity and diversity of these compounds in the environment[6,17]. Advanced analytical techniques, such as high-resolution mass spectrometry, have identified hundreds to thousands of distinct NA molecular species in OSPW[36].

The solubility of NAs in water is contingent on pH; nonetheless, they exhibit high solubility in organic solvents. Due to the alkaline pH of OSPW[37], NAs take on the form of water-soluble salts within the tailing's ponds. The acid dissociation constant of NAs falls within the range of 10^{-5} to 10^{-6} (pK_a= 5-6), rendering them weaker acids when compared to low molecular weight carboxylic acids like acetic acid (pK_a= 4.7). Nevertheless, their dissociation constants closely align with those of common fatty acids[3,37].

1.2.3 Toxicity and Corrosiveness of Naphthenic Acids

NAs are considered the primary toxic constituents of OSPW [3,6,11]. Their bioavailability and persistence are believed to be significant, contingent upon their specific structural characteristics[16]. Because of this, coupled with the discovery of NA concentrations ranging from 0.4 to 51 mg/L in the groundwater around the oil sands, as reported by Clemente & Fedorak (2005), numerous studies have explored the toxicity of NA mixtures in isolation. The water solubility promotes the transportation of NAs in both surface water and groundwater, facilitating potential uptake by plants and animals[23]. Toxicological studies have established that NAs are the predominant components of tailings pond water responsible for both acute and chronic toxicity in various organisms, including fish, amphibians, zooplankton, and certain mammals like rats and guinea pigs[23,38]. To underscore the level of toxicity observed in tailings pond water, Allen et al[3] noted that NAs concentrations exceeding 2.5-5 ppm were deemed toxic to fish species. Meanwhile, the concentration of NAs in tailings pond water typically falls within the range of 20-120 ppm. In contrast, the Athabasca River, a neighboring freshwater source, exhibits a NAs concentration of less than 0.01 ppm[31]. While the toxicity of NAs is specific to each species, and the degree of toxicity varies with structural composition, the leaching of OSPW into groundwater and nearby freshwater sources can pose significant environmental hazards[12,39].

1.2.4 Analytical Methods for Detection and Quantification of NAs

The diverse structural variability of oil sands NAs has presented challenges in achieving accurate quantification and characterization. Also, NAs exhibit considerable similarity in terms of potential chromophores, making it difficult to differentiate them using techniques such as Fourier Transform Infrared Spectroscopy (FTIR), Nuclear Magnetic Resonance (NMR), and UV-vis spectroscopy. To address this, various analytical techniques have been developed. Some are specifically employed to ascertain the overall concentration of NAs in the aqueous phase, while others can provide insights into their structural composition.

Standard techniques for identifying and quantifying NAs include Fourier transform infrared (FTIR) spectroscopy, gas chromatography-mass spectrometry (GC-MS), high-performance liquid chromatography (HPLC), negative ion electrospray ionization-mass spectrometry (ESI-MS), and high-resolution Fourier transform ion cyclotron resonance mass spectrometry (FT-ICR-MS)[12,33,40,41]. These methods provide an approximate response that can be correlated with the concentration of NAs in the absence of interferences. However, due to the compositionally similar but structurally unique nature of NAs, there is currently no specialized method for the comprehensive identification or precise quantification of individual acids within the mixture.

The primary method for detecting and quantifying NAs in general has been a Fourier-transform infrared (FTIR) spectroscopy-based approach developed by researchers at Syncrude Ltd. [42,43]. This method relies on the infrared (IR) absorbance of carboxylic acids in an organic solvent extract phase for detection. Therefore, NAs are extracted from the acidified aqueous phase (acidified the original filtered OSPW sample by adding concentrated HCl to lower the pH to 2) into dichloromethane[44]. The absorbance peak heights of the monomeric and dimeric forms are assessed at 1743 and 1704 cm^{-1} respectively[12,27]. The total peak height is directly correlated

with the concentration of NAs. Therefore, the concentration of NAs in an unknown sample is established by comparing the combined absorbance peak height of the sample with those in a calibration curve derived from FTIR analyses of solutions prepared using commercially available NAs[42].

Because of its robustness and cost-effectiveness, this FTIR technique has found extensive use in both the oil sands industry and the scientific community[12,42]. However, the technique has its limitations. As the detection relies on the IR absorbance of all carboxylic acids in a solution, it cannot distinguish between various NA species. In essence, it only quantifies the total concentration of NAs without providing details about the structural composition. Similarly, the technique is unable to distinguish between classical, oxygenated, and unconventional NAs containing phenol, thiophene, and pyrrole groups due to the same limitation[27].

Gas chromatography coupled with mass spectrometry (GC-MS) has been employed for the quantification and characterization of NAs. This approach necessitates a pre-derivatization step to produce t-butyldimethylsilyl esters of NAs, which are subsequently analyzed using GC-MS[45]. The reported detection limit for this method is 0.01 ppm[27,45]. Nevertheless, it should be noted that the method assumes the complete and equal derivatization of all the NA species by the derivatizing agent, which may not always be achieved.

Mass spectrometry stands out as the prevalent detection technique in NA analysis, and it can be utilized either independently, or as mentioned earlier, in conjunction with a chromatographic technique. Various forms of mass spectrometry are applied in NA analysis, with Electrospray Eonization MS (ESI-MS) being a favored technique. This preference arises because non-polar contaminants in NA mixtures encounter difficulty in forming ions within the ESI-MS process[46–48]. Several studies have determined that operating electrospray ionization mass spectrometry

(ESI-MS) in negative mode is more effective for NA detection[49]. However, it is worth noting that other dissolved organic acids may interfere with the detection process, and the elevated concentrations of inorganic salts in OSPW can potentially overwhelm the mass spectrometry system with charged ions, causing harm to the instrument[49].

Ultrahigh-resolution mass spectrometry with a resolution exceeding 100,000 has increasingly played a vital role in advancing our understanding of the molecular composition of petroleum. This expanding field of study, commonly referred to as "petroleomics"[50,51], incorporates techniques such as Fourier-transform ion cyclotron resonance mass spectrometry (FT-ICR-MS). FT-ICR-MS has been at the forefront of this field due to its exceptional resolving power and mass accuracy[50,52]. These characteristics are highly suitable for investigating complex mixtures. Electrospray ionization (ESI) enables the examination of both the acidic and basic components present in fossil fuels[52]. While examinations of OSPW have historically concentrated on characterizing NAs, it has become increasingly apparent that numerous additional components merit deeper investigation. Ultrahigh-resolution mass spectrometry has proven to be invaluable for analyzing mixtures related to the Athabasca region[53]. Headley et al. employed Electrospray Ionization Fourier-Transform Ion Cyclotron Resonance Mass Spectrometry (ESI-FT-ICR-MS) to emphasize the existence of sulfur-containing compounds in oil sands extracts[36,54]. Research conducted by Barrow et al. analyzed a specific OSPW sample using both Electrospray Ionization (ESI) and Atmospheric Pressure Photoionization (APPI). This study underscored the diversity of compound classes present and emphasized how the choice of ionization method significantly influences the observed components[55]. Subsequently, Grewer et al. utilized ESI Fourier-Transform Ion Cyclotron Resonance Mass Spectrometry (FT-ICR) to explore various water and OSPW samples. They concluded that less than 50% of the detected ions could be classified as

oxy-NAs, suggesting the adoption of the term "OSTWAEO" or oil sands tailings water acid-extractable organics to encompass the broad spectrum of compound classes involved[30].

1.2.5 Remediation Techniques of OSPW

As previously mentioned, OSPW is presently being stored in tailings ponds near the oil sands sites, and the volume of OSPW continues to grow[1,23]. There is a concern that contaminants may leach into the Athabasca River due to the close proximity of the tailings ponds to the river, posing a potential threat to the aquatic environment[3,30]. At some point, all oil sands companies will need to remediate OSPW for safe discharge into the environment because all lands used for oil sands operations, including tailings ponds, are expected to be required to be eventually reclaimed[3]. OSPW must adhere to standard guidelines to ensure its safe discharge into the environment. Consequently, the removal of organic compounds, including NAs, is identified as the top treatment priority[27]. To effectively eliminate contaminants such as dissolved and suspended solids, dissolved organic compounds, and insoluble hydrocarbons, a series of sequential treatment processes is expected to be required[7].

Successful remediation of NAs plays a crucial role in the reclamation endeavors associated with oil sands tailings ponds. Various techniques, including biodegradation, photocatalytic degradation, ozonation, nanofiltration, sequestration using cyclodextrin-based polymers, and adsorption by activated carbon (AC), have been explored and documented in the literature for remediating NAs from OSPW[38,39,56–60].

The microbial degradation of NAs usually results in the production of CO_2, fragmented organic compounds, and water[38]. Nevertheless, the degree of degradation depends on the molecular weight and chemical structure of the compounds. Scott et al. (2005) noted that low

molecular weight NAs are more prone to biodegradation compared to high molecular weight NAs[31]. It has been proposed that the biodegradation rate is predominantly influenced by the chemical structures of NAs. The more resistant NAs are those with higher degrees of aliphatic chains, methyl-substituted cycloalkane rings, and increased cyclicity[31]. The efficacy of photocatalytic degradation is constrained by its reliance on the molecular weights and cyclicity of the compounds. Ozonation of NAs does not result in complete degradation and consequently generates various by-products, including aldehydes, ketones, peroxides, and other carboxylic constituents[56,57]. Some of these by-products might even pose greater hazards than the original compound[31,57].

Adsorption stands out as one of the most efficient methods for remediating wastewater, thanks to its high efficacy in removing contaminants[21,27,61,62]. Unlike some of the remediation techniques mentioned earlier, adsorption allows for the complete removal of persistent contaminants, rather than breaking them down into smaller, potentially more harmful fragments [23,63]. Utilizing porous adsorbents like AC offers a significant advantage in that its physical and chemical properties can be customized to specifically target certain contaminant species. This customization enhances the overall adsorption affinity of the adsorbent for the contaminants[26,64].

1.3 Production of Activated Carbon from Petroleum Coke

Among all the different treatment methods for NA removal, adsorption has gained significant attention due to its high efficiency and fast removal rates. A very broadly useful adsorbent is AC which can be produced from a wide range of feedstocks. One possible feedstock related to the activities of the oil extraction industry is petroleum coke. Petroleum coke (PC) is a waste-product of the bitumen upgrading process. It is a carbonaceous solid (80-85 wt% carbon), non-porous and consequently, with very low specific surface area. In 2011, Alberta's oil sands

operations generated about 10 million tons of petroleum coke (petcoke) annually. Comparatively, the coal and other industries consumed around 5 million tons of petcoke each year. By the close of 2011, Alberta had amassed a petcoke stockpile of roughly 72 million metric tons. Given that between 15% and 30% of a barrel of bitumen from tar sands typically converts into petcoke, there's a notable chance to repurpose this petcoke into a more beneficial product. Through effective enhancement and precise chemical or thermal modification of its surface properties, it is possible to transform petcoke into economically and environmentally beneficial AC, which can be utilized in environmental cleanup efforts[63].Studies have indicated that petroleum coke can be thermally treated with an activating agent to produce AC with high specific surface area. The term “activated carbon” refers to a wide range of high carbon content amorphous materials. Through various chemical and physical methods, high carbon content feedstocks can be converted to a disordered inorganic carbon material which is typified by very high specific surface areas, varying pore size distribution and a range of surface functional groups.

Figure 1.3 shows three different types of interactions that describe how molecules are adsorbed onto the surface of activated carbons. As is shown in figure 1.3 (a), physisorption refers to the adsorption of diphenylacetic acid molecule onto the activated carbon’s surface through weak van der Waals forces. It is generally reversible and occurs without significant changes to the structure of the adsorbed molecule. Figure 1.3 (b) depicts the adsorption of cyclohexaneacetic acid onto the surface via hydrogen bonding which is a specific type of dipole-dipole interaction and occurs between a hydrogen atom covalently bonded to an electronegative atom like oxygen and another electronegative atom. The carboxylic acid group interacts with a hydroxyl (-OH) on the activated carbon surface, emphasizing the role of functional group in facilitating specific adsorbate-surface interactions. Figure 1.3 (c) demonstrates chemisorption

adsorption of a deprotonated molecule through a covalent bond formation with the activated carbon surface. This interaction represents a strong and irreversible chemical bonding process, altering the structure of the molecule.

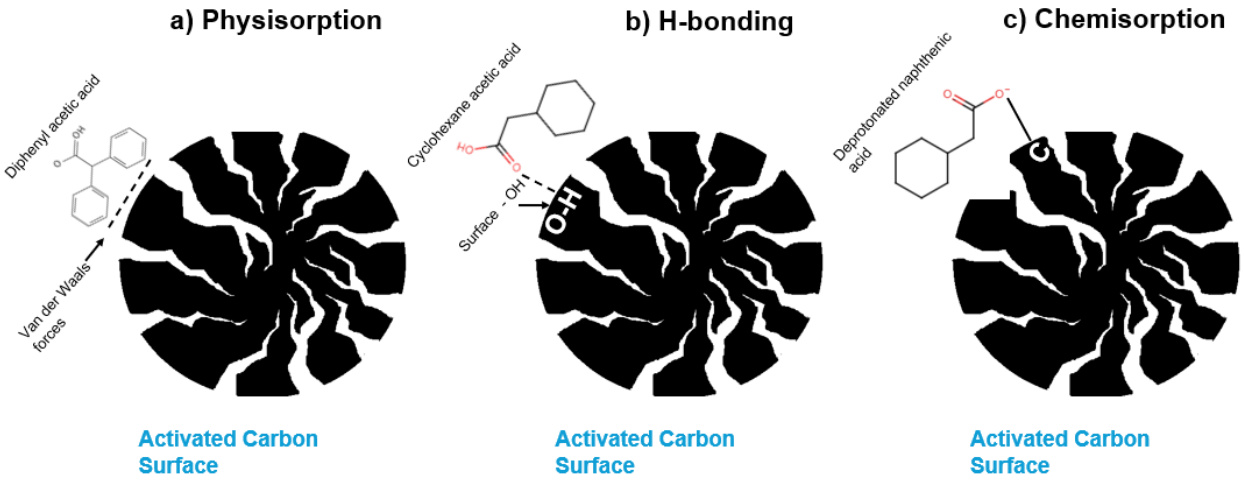

Figure 1.3. Three types of adsorption mechanisms on the surface of activated carbon: a) physisorption; b) H-bonding; and c) chemisorption.

Various activation methods have been adopted for increasing the specific surface area and pore size distribution, and customization of functional groups on the material's surface based on the target adsorbate. Most of the earlier research used chemical activation methods using KOH or some other alkali metal hydroxides. Barnard, et al. used petcoke to produce AC using KOH as a chemical activation agent for the uptake of NAs. Similarly, Niasar, et al used activated PC. Two different amination processes of the AC surface were used to vary the surface chemical functionality. They found that KOH activation of petroleum coke improved the adsorption of three specific NAs significantly using a KOH to PC mass ratio of 3:1. They found that although, generally KOH AC adsorbents with a higher specific surface area and pore volume provide better adsorption capacity, the textural properties of surface areas and pore volume are not the only parameters determining the adsorption capacity. Other parameters such as surface functionalities

and solution pH play important roles on the adsorption capacity of the produced adsorbents for NAs[6,26].

Takayuki et al. worked on improving the NA adsorptivity using KOH activated AC from petcoke feedstock. They revealed that the surface functionality as well as the textural properties were dependent on the KOH content, temperature and activation time. Similarly, Lu et al. examined the importance of preactivation treatment of the feedstock. They identified the presence of C–O, C–O–C, C–O–H and some alkyl species on the surface of the precursors. These surface functional species were proposed to play a key role in the pore development during KOH activation. They concluded that the surface area and the pore size distribution of the AC can be controlled by optimizing the conditions of activation processes[65].

1.4 Thesis Objectives

My overarching research goal is twofold:

1) To identify the best adsorptive removal of NAs from oils sands process-affected waters using petroleum coke-derived AC chemically activated with economically viable KOH quantities
2) To apply a species-specific detection method, in our case FT-ICR-MS, to precisely characterize the NA species as this is essential for subsequent research to target prioritized specific NAs.

Prior to the research described in this thesis, our lab group has primarily focused on the investigation of the adsorption of individual model NAs. This is so that the non-competitive adsorption process could be elucidated to establish a baseline understanding of single NA species before undertaking adsorption from more complex NA mixtures and actual OSPW. We were interested in evaluating which NAs are not adsorbed using ultrahigh resolution ESI-FT-ICR-MS

measurement technique to identify whether there is any kind of NA speciation dependant adsorption.

Currently very little has been reported on adsorption of NA's using petcoke derived AC with low ratios of KOH and short activation times both of which parameters result in a much more economically viable generation of AC. The context of our research is particularly relevant given the environmental challenges associated with oil sands production. One of the primary issues is the impact on water quality, where contaminants can severely affect ecosystems and human health. The petroleum coke that could be transformed into AC is situated at the same site as the tailings ponds requiring treatment. Given the large volumes of AC needed to address the tailings, it is beneficial to have the raw material nearby. Constructing a facility on-site would reduce both the financial and environmental costs associated with transporting the required adsorbent.

In our laboratory, a major industrial collaboration is underway to design, synthesize and characterize AC from petcoke feedstocks using more economically viable processing conditions. My research explores the application of these novel and economical AC materials for NA adsorption from OSPW. Our process uses chemical activation of PC using KOH with KOH/PC mass ratios of between 0.5 and 2 and maximizes the adsorption of NAs mixtures and actual OSPW by enhancing the surface chemistry of the AC, increasing mesoporosity, and increasing surface area.

To the best of my knowledge, the discussion of the ESI-FT-ICR MS results concerning the NAs extracts from (OSPW) after treatment with AC, as presented in the thesis, is novel. Ultrahigh resolution mass spectrometry with Electrospray Ionization (ESI) proves advantageous in characterizing NAs, providing an optimal analytical window for detecting polar, heteroatom-containing compounds. It offers chemical insights into the composition of NAs in OSPW,

information that is not easily attainable through traditional chromatographic analysis. Additionally, FT ICR MS has demonstrated its suitability as the most ideal technique for monitoring crucial environmental processes related to petroleum organics. This contributes to a better understanding of the environmental fate of NAs, especially in multi component systems like OSPW.

Chapter 2 - Methodology and Characterization Techniques

2.1 Characterization Techniques

The characterization of activated carbon materials and their adsorption properties necessitates the utilization of numerous analytical tools. In this chapter, an overview of the four instrumental techniques will be provided, focusing on their principles, methodologies, and applications in the analysis of these materials.

2.1.1 Total Organic Carbon Analyzer (TOC)

Figure 2.1. TOC Analyzer to measure the residual organic carbon in naphthenic acid solution

The measurement of Total Organic Carbon (TOC) is a widely employed method for assessing the level of organic contamination present in water. TOC serves as an indirect indicator of organic molecules within water, quantified in terms of carbon content[66]. The introduction of organic molecules into the wastewater occurs through various sources such as the initial water supply, purification processes, and materials within the waste management system. The analytical technologies employed for TOC measurement share the common goal of fully oxidizing organic molecules (using a catalytic oxidation combustion technique at 680 ºC) within a sample of water into carbon dioxide (CO_2), measuring the resulting CO_2 concentration, and presenting this outcome as carbon concentration[59,66]. It is imperative to differentiate between

inorganic carbon, potentially originating from dissolved CO_2 and bicarbonate in the water, and the CO_2 produced through this oxidation of organic molecules in the sample.

A method employed for TOC measurement includes subtracting the measured inorganic carbon (IC) from the total carbon (TC) measurement. The total carbon encompasses both organic and inorganic carbon components[10,59].

$$TOC = TC - IC \qquad \text{Eq (1)}$$

Figure 2.2 shows a schematic diagram showing TOC measurement using TOC analyzer.

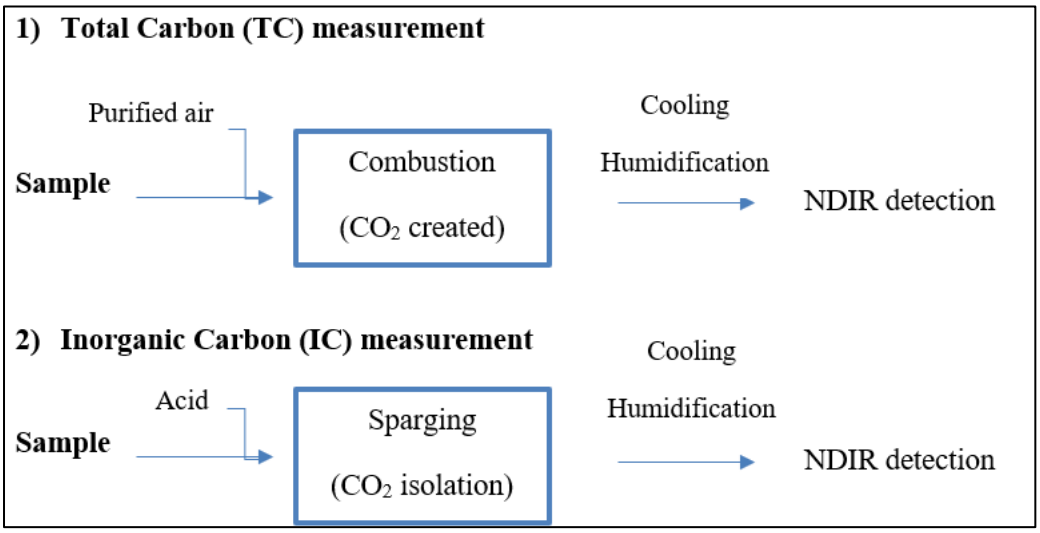

Figure 2.2. Schematic diagram showing TOC measurement using TOC Analyzer

By sparging samples with a slight HCl addition and reducing the pH to 2, the inorganic carbon in the sample undergoes conversion into carbon dioxide. After removing this carbon dioxide, the total organic carbon (TOC) is determined by measuring the total carbon (TC) in the treated sample. It is important to note that during the removal of carbon dioxide from the inorganic carbon (IC), some purgeable organic carbon (POC) may also be lost. Consequently, the TOC obtained through this method is known as Non-Purgeable Organic Carbon (NPOC).

In this work, all adsorption tests were conducted in triplicate, and the samples were filtered using disposable 45 μm syringe filters before being analyzed with a Shimadzu TOC-VCPH analyzer. The analysis was performed using either the Total Carbon /Inorganic Carbon (TC/IC) method or the Non-Purgeable Organic Carbon (NPOC) method.

2.1.2 Surface Area and Pore Size Distribution Characterization

BET (Brunauer-Emmett-Teller) surface area analysis is a widely used method for measuring the specific surface area of materials, particularly porous materials such as catalysts, adsorbents, and other nanostructured materials. The technique is based on the physical adsorption of gas molecules on a solid surface. Upon exposure of a solid surface to a gas, there is an initial surge in adsorption of the gas molecules onto the surface, followed by the establishment of equilibrium between adsorption and desorption rates. By maintaining a consistent temperature throughout this phenomenon, the equilibrium position becomes contingent only on the system's pressure. This relationship can be assessed through a volumetric technique, involving the introduction of a specified gas quantity to the adsorbent under constant temperature conditions[67]. At the pressure equilibrium (p), the quantity of adsorbed gas (n^{o}) is determined by subtracting the gas amount introduced from the amount necessary to occupy the space. A graphical representation of the amount of adsorbed gas versus the equilibrium relative pressure (p/p^{o}) of the gas, maintained at a constant temperature, enables the creation of an adsorption isotherm[68]. Adsorption isotherms play a crucial role in assessing various properties of an adsorbate, such as surface area, pore volume, pore size distribution, and heat of adsorption[67].

In accordance with IUPAC standards, most physisorption isotherms fall into six distinct types, as illustrated in Figure 2.3. The reversible Type I(a) and I(b) isotherms exhibit a rapid increase in adsorption at low p/p^{o} values, followed by a plateau as p/po approaches 1. This

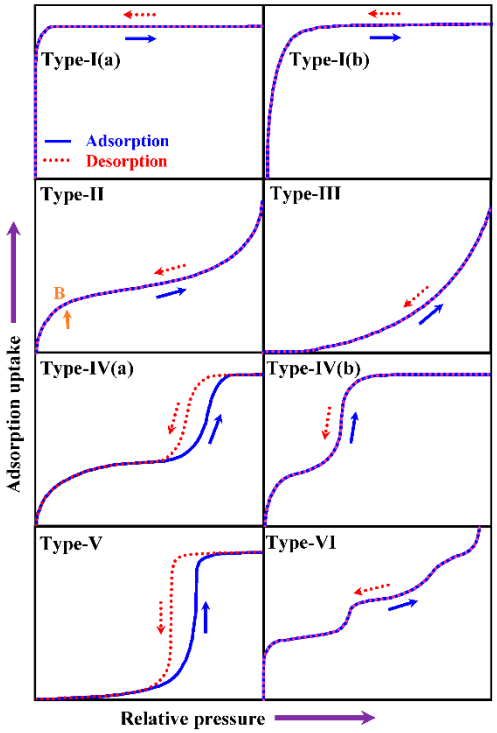

Figure 2.3. IUPAC 6 types of isotherms (Taken from ref [96])

isotherm pattern signifies the formation of a monolayer and is commonly observed in microporous materials with comparatively diminutive external surfaces. The swift adsorption rate at low p/p° values is attributed to the filling of micropores, and materials predominantly featuring narrow micropores exhibit a more rapid rate compared to those with wider micropores and potentially narrow mesopores[69]. The reversible Type II isotherm configuration is frequently observed in non-porous or macroporous adsorbents, allowing for unhindered monolayer-multilayer adsorption. In this isotherm, monolayer adsorption extends until point "B" on the graph, marking the commencement of multilayer adsorption[69]. The reversible Type III isotherm displays a convex shape concerning the p/p° axis, signifying mild interactions among adsorbate molecules. In this scenario, a monolayer doesn't develop, as the adsorbate molecules cluster around the most favorable sites on the surface of a nonporous or microporous solid[69]. Mesoporous adsorbents exhibit Type IV isotherms, marked by the presence of a hysteresis loop. Initially, there is adsorption of a monolayer-multilayer on the mesopore walls, followed by capillary condensation. Capillary condensation takes place as the gas transitions to a liquid-like phase within a pore, leading to multilayer adsorption originating from the liquid-like phase[69]. Type V isotherms exhibit a resemblance to Type III isotherms in the lower p/p^{o} range, indicating weak interactions between adsorbent and adsorbate. With increasing p/p°, molecular clustering is

succeeded by pore filling[69]. On the other hand, the Type VI isotherm signifies a gradual, stepwise multilayer adsorption on a uniform and non-porous surface[68].

The Brunauer-Emmett-Teller (BET) equation is a frequently employed tool for analyzing isotherm data, offering quantitative insights into the surface area[68]. The BET equation operates under the assumption of multilayer adsorption, with the linear format of the equation utilized to determine the BET monolayer capacity (n^a_m) (Eq 2),

$$\frac{p}{n^a(p^o-p)} = \frac{1}{n^a_m C} + \frac{(C-1)}{n^a_m C}\left(\frac{p}{p^o}\right) \quad \text{Eq (2)}$$

Here, n^a represents the amount adsorbed at the relative pressure p/p°, and C is a constant associated with the enthalpy of adsorption. In conjunction with monolayer adsorption, the equation necessitates a linear correlation between p/n° (p°-p) and p/p°. Typically, this constraint is applicable to p/p° values ranging from 0.05 to 0.30. Derived from the BET monolayer capacity, the specific surface area (a_s) can be computed using Eq (3).

$$a_s = \frac{A_s}{m} = \frac{n^a_m \cdot L \cdot a_m}{m} \quad \text{Eq (3)}$$

Here, A_s represents the surface area, and m denotes the mass of the adsorbent. The definition of A_s involves the multiplication of the BET monolayer capacity, the molecular cross-sectional area (a_m), and Avogadro's constant (L).

In this study, the specific surface areas of all activated carbon (AC) samples were determined using a Tristar II Plus surface area and porosity analyzer. N_2 adsorption at 77 K was employed for analysis, encompassing 50 points for adsorption spanning between 0.0065 p/p^0 and 0.995 p/p^0, and 52 points for desorption ranging from 0.995 p/p^0 to 0.104 p/p^0. The reported surface areas were determined through BET surface area analysis.

2.1.3 X-Ray Photoelectron Spectroscopy (XPS)

X-ray photoelectron spectroscopy (XPS) is a technique used to analyze surface characteristics, revealing details about a material's elemental and chemical composition, as well as the chemical speciation of its elements. This method involves bombarding the surface with X-ray photons, causing core electrons to be emitted. When X-ray light hits a material, it can transfer its energy to the electrons in the core shell part of the material, causing these electrons, known as photoelectrons, to be pushed out. Other electronic phenomenon may occur as well however XPS uses the information provided by the photoelectron to characterize the surface.[70].

The kinetic energy of the photoelectrons is measurable and can be defined by Eq 4.

$$E_k = hv - \Phi - BE \qquad \text{Eq (4)}$$

The process involves the photon energy (hv), interacting with the spectrometer's work function (Φ) and the electron's binding energy (BE), crucial for understanding the characteristics of the initial state of the photoelectron.

In our study, The XPS analyses were carried out with a Thermofisher Scientific K(alpha) spectrometer using a monochromatic Al K(alpha) source (15mA, 15kV). The instrument work function was calibrated using sputter cleaned Au, Ag and Cu to determine the absolute linearity of the binding energy scale, with 83.96 eV for the Au 4f7/2 line for metallic gold, 368.21 eV for Ag 3d5/2, and 932.62 eV for the Cu 2p3/2 line of metallic copper. Survey scan analyses were carried out with 200 eV pass energy and a 1 eV/step. High resolution analyses were carried out with an analysis area of 300 x 700 microns and a pass energy of 20 eV. Spectral analysis including peak fitting was done using CASA XPS Software (version 2.31) with the spectra being corrected to the main line of the carbon 1s spectrum at 284.85 eV.

2.1.4 Fourier Transform Ion Cyclotron Resonance Mass Spectrometry (FT-ICR MS) and Electroscopy Ionization (ESI)

2.1.4.1 Theoretical Foundations and Principles in Fourier Transform Ion Cyclotron Resonance Mass Spectrometry (FT-ICR MS)

Fourier Transform Ion Cyclotron Resonance Mass Spectrometry (FT-ICR MS) stands out as a highly effective analytical instrument for molecular analysis of intricate organic blends, including raw or weathered petroleum, non-aqueous phase liquids (NAFCs), and natural organic matter. Pioneered by Comisarow and Marshall in 1974, FT-ICR MS has played a crucial role in numerous scientific breakthroughs over the past five decades. When coupled with diverse ionization methods, it enables the identification of both polar and non-polar molecules that may not be readily detected through chromatographic measurements(McKenna et al. 2013).

Marshall et al. (1998) present a comprehensive elucidation of the physics and mathematical principles underpinning the design of FT-ICR MS instruments. Illustrated in Figure 2.4 is a simplified schematic delineating the various processes involved in generating a mass spectrum using FT-ICR MS instruments. In Figure 2.4(a) and Equation (5), ions move within a spatially uniform and static magnetic field, denoted as B, rotating in a confined space at a cyclotron frequency, v_c, measured in Hz or rad/sec. This frequency is parallel to the magnetic field and inversely proportional to the mass-to-charge ratio (m/z).

$$v_c = \frac{zB}{m} \qquad \text{Eq (5)}$$

Raising the magnetic field strength to several Tesla (T) results in enhancements to mass accuracy, dynamic range, and the duration of analysis[73]. The confined ions' cyclic motion is identified by gauging the image current generated as the ions traverse the detection plates. These

currents exhibit distinctive geometric waveforms, oscillating periodically. Consequently, the frequency, entirely distinctive to the ion's mass-to-charge ratio, can be determined from this characteristic pattern. In Figure 2.4a, the ensuing time-domain image current signal is showcased, a result of ions passing through electrodes. Fourier Transform data reduction is then employed to transform these current signals into a frequency, as depicted in Figure 2.4c. Ultimately, the ion cyclotron frequencies are translated into a mass spectrum through the application of a calibrated frequency-to-m/z conversion factor, outlined in Figure 2.5d.

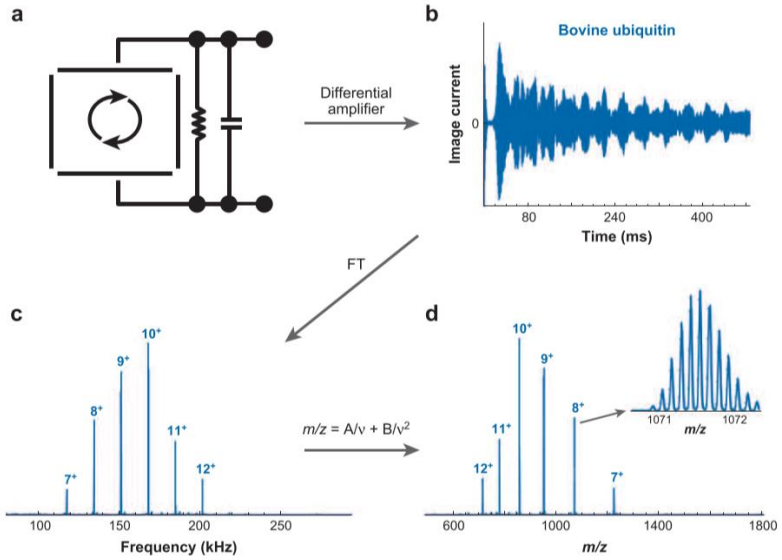

Figure 2.4. Schematic of procedures involved in generating a mass spectrum through FT-ICR-MS analysis (Taken from ref [72])

2.1.4.2 Electrospray ionization (ESI)

For optimal outcomes with FT-ICR MS instrumentation, a crucial stage involves the generation of charged ions through a chosen method of analyte ionization. Electrospray ionization (ESI) emerges as a widely employed method for ionizing polar, low molecular weight analytes in MS analysis(Yi-Wun Wang et al. 2022). When coupled with FT-ICR MS instruments,

it enables the discrimination of minute mass variations between isobaric compounds, such as C_3 and SH_4 or O_2 and S [75]. In their comprehensive work, Prabhu et al. (2023) offers a detailed scientific introduction to the configuration, mechanism, and prospects of electrospray ionization (ESI). The liquid sample is introduced into the ESI capillary, where it encounters a high voltage, leading to the generation of large, charged droplets within the Taylor cone. The utilization of a nebulizer and drying gases leads to solvent evaporation, resulting in the reduction of droplet size and the production of gas-phase ions suitable for introduction into the mass analyzer. Depending on the specific analyte of interest, it is crucial to carefully select the appropriate ionization mode, whether positive or negative, considering whether the analytes ionize as positively or negatively charged ions, respectively. Various factors may act as constraints on the applicability of ESI, including sample pH, matrix effects, and the existence of non-volatile salts and molecular adducts(Yi-Wun Wang 2022;Prabhu et al., 2023). These factors should be considered, both before and during the analysis, particularly when undertaking ESI-FT-ICR MS analysis of polar analytes like non-aqueous phase liquids.

In this research, we use negative-mode Electrospray Ionization Fourier transform ion cyclotron mass spectrometry (ESI (-) FT-ICR MS) to further characterize the species in the NA extracts of pre-treated and post-treated OSPW samples with two different synthesized AC adsorbents.

2.1.5 Point of Zero Charge

The point of zero charge (PZC) is a key indicator that helps understand how charged a material's surface is. PZC refers to the pH value at which a solid surface exhibits a net zero surface charge. At this specific pH, the number of positive charges on the surface equals the number of negative charges[76]. Knowing the PZC can identify whether certain charged

substances, like NAs and AC, will interact well, or poorly with each other. When the pH of the solution is above the PZC of AC, the surface of the carbon will predominantly carry a negative charge. If the NAs (which are negatively charged at a higher pH due to deprotonation) are introduced into the solution, the electrostatic interaction between the negatively charged carbon surface and the NAs may reduce the efficiency of adsorption. Conversely, if the pH is below the PZC of AC, the surface will have a net positive charge. Depending on the charge state of the particular NA, this can create an attractive force between the positively charged carbon surface and the negatively charged NAs, enhancing the likelihood of adsorption. At the pH corresponding to the PZC, the surface of AC has a neutral charge, which may result in reduced electrostatic interactions with the NAs. However, other forces, such as van der Waals forces or hydrophobic interactions, may still facilitate the adsorption process. That's why measuring the PZC is crucial for all the adsorbing materials discussed in this thesis.

The (PZC) for each type of AC was calculated using the pH drift method[77]. Here, a 0.01 M NaCl solution was prepared, and nitrogen gas was used to remove dissolved carbon dioxide. Then, 50 mL of this solution was poured into several 100 mL beakers, with the pH being adjusted between 2 and 12 using HCl or NaOH. Each beaker received 150 mg of AC. These mixtures were stirred for 48 hours at 250 rpm, after which they were filtered, and the final pH levels were recorded. The change in pH (ΔpH), calculated as the difference between the final pH and the initial pH, was plotted against the initial pH. The point at which ΔpH equals zero was identified as the point of zero charge.

2.2 Adsorption Study

2.2.1 Adsorption Kinetics

Adsorption kinetics describe the rate at which a substance is adsorbed onto a surface, detailing how quickly the adsorption process reaches equilibrium. This is crucial in understanding how quickly pollutants, ions, or molecules adhere to adsorbents in various environmental and industrial processes. It encompasses the steps involved in the movement of adsorbate molecules from the bulk phase to the surface of the adsorbent and is often modeled to optimize the design of adsorption systems for water treatment, gas purification, and chemical separation[13].The transfer of mass from the solution to the adsorbent particles' adsorption sites is controlled by mass transfer resistances. These resistances determine the time required to reach equilibrium and are crucial factors in designing fixed-bed or flow-through systems(Worch et al. 2012). The pace of adsorption is typically restricted by diffusion processes both towards the external surface of the adsorbent and within the porous particles of the adsorbent.

In this work, adsorption kinetics experiments for each model NA were conducted over a duration ranging from 5 minutes to 48 hours. A fixed adsorbent dosing of 0.5 g/L of AC was stirred at 200 rpm with a 40 mg/L solution of each model NA in 125 ml beakers, sealed with parafilm. All adsorption tests were pH-buffered to a value of 8 using a phosphate buffer to mimic the pH conditions found in authentic OSPW.

The calculation of the percentage of removal through adsorption was determined using the provided Eq(6):

$$\%Removal = \frac{C_0 - C_t}{C_0} * 100 \qquad \text{Eq (6)}$$

Here, C_0 and C_t denote the initial and time-dependent TOC) concentrations in the solution, respectively.

2.2.2 Kinetics Modelling

There are several kinetics models such as zero-order kinetics, first-order kinetics, second-order kinetics and multi-exponential model (m-exp) to understand adsorption mechanism and rate better. M-exp model was used in this study among other models simply because it can account for the complexity and heterogeneity of real-world systems and provides a comprehensive understanding, making it more accurate for predicting and analyzing complex behaviors in contaminated water systems. m-exp model is often considered a set of parallel pseudo-first-order mechanisms designed to align with the kinetics of adsorption as determined through experimental observations[79].

$$q_t = q_e - q_e \sum_{i=1}^{n} f_i \exp(-k_i t) \qquad \text{Eq (7)}$$

Where,

$$\sum_{i=1}^{n} f_i = 1$$

Here, f_i is defined as the segment of the adsorption kinetics that is determined by the distinct rate constant k_i (min^{-1}). Equation 7 served solely as an empirical method to calculate the half-life times of adsorption, represented as $t_{(1/2)}$ (in minutes), independent of the model. These calculated times were then utilized for conducting comparative analyses among different model NAs.

2.2.3 Adsorption Isotherms

Choosing an appropriate adsorbent for a specific separation task is a complex challenge. The primary scientific criterion for adsorbent selection is typically the equilibrium isotherm, with the diffusion rate generally considered of secondary importance[27,80]. An isotherm signifies the connection between the quantities of adsorbate on the adsorbent at equilibrium, and these isotherms serve to articulate adsorption phenomena[80]. Understanding the adsorption isotherm allows for the determination of the adsorbent's carrying capacity, regeneration techniques, the extent of unusable bed length, and product purities(Ayawei et al., 2017; Iranmanesh, 2013). Hence, establishing the equilibrium isotherm holds significance in formulating the entire process design. The equation below was used to determine adsorption capacity:

$$q_e = \frac{V^*(C_0 - C_e)}{m} \qquad \text{Eq (8)}$$

The volume of solution used is denoted by V, the initial concentration is represented as C_0, the equilibrium concentration is denoted as C_e, q_e is an adsorbent capacity at equilibrium and m signifies the mass of the adsorbent.

Adsorption isotherms serve as a tool for assessing and contrasting the adsorption capacities of diverse adsorbents concerning a specific adsorbate species. Experimentally, acquiring q_e and C_e values for an isotherm can be accomplished through two approaches: (1) introducing a constant adsorbent dosage into a series of solutions with differing initial concentrations, or (2) maintaining a constant initial adsorbate concentration across a series of solutions while adjusting the adsorbent dosage for each solution[80,81].

Throughout this study, all isotherm experiments were conducted with constant concentrations of NAs at 60 mg/L. This particular value was chosen as it fell within the experimental range

commonly observed in model NA adsorption isotherms and it is also close to the typical concentrations of NAs in OSPW(Sarkar et al., 2013; Iranmanesh, 2013).

In the upcoming sections, we will delve into descriptions of isotherm models widely utilized and referenced in the literature.

2.2.3.1 Langmuir Model

Originally devised to elucidate gas-phase adsorption, the Langmuir isotherm model has found widespread application in explaining the adsorption phenomena within aqueous systems[81]. The model establishes explicit assumptions, stipulating that adsorbed species exclusively create a monolayer devoid of interactions with neighboring adsorbed species. Additionally, it posits that the energy associated with adsorption at each site on the surface of an adsorbent remains constant, suggesting a homogeneous surface.

$$Q_e = \frac{Q_0 K_L C_e}{1+K_L C_e} \qquad \text{Eq (9)}$$

In the given equation, Q_0 (mg/g) and K_L (L/mg) represent the monolayer saturation capacity and Langmuir constant, respectively.

2.2.3.2 Freundlich Model

The practical Freundlich isotherm model (Eq 10) is frequently employed to depict adsorption on AC, primarily because of the heterogeneous nature of the adsorbent's surface(Worch, 2012). This model anticipates a limitless augmentation in adsorption capacity as the equilibrium concentration rises, suggesting the occurrence of multilayer adsorption.

$$Q_e = K_F C_e^{1/n} \qquad \text{Eq (10)}$$

Within Equation (10), K_F (mg/g)/(L/mg)$^{1/n}$) serves as the Freundlich constant characterizing adsorption strength, and 1/n represents the heterogeneity factor. Values closer to zero for 1/n indicate a surface with greater heterogeneity.

2.2.3.3 Redlich-Peterson Model

Although the Langmuir and Freundlich models are frequently employed, there are instances where they may fall short in explaining the equilibrium behavior in adsorption systems. The Redlich-Peterson and Sips isotherms, both being three-parameter models, are unique combinations of the Langmuir and Freundlich models. This distinctive feature imparts greater flexibility to these models, enabling them to better accommodate and fit adsorption isotherm data(Foo & Hameed, 2010; F. C. Wu et al., 2010).

$$Q_e = \frac{K_R C_e}{1+a_R C_e^g} \quad \text{Eq (11)}$$

In the Redlich-Peterson model presented in Equation 11, K_R (L/g) and a_R (L/mg) serve as the Redlich-Peterson constants, while the parameter g denotes the heterogeneity factor.

2.2.3.4 Sips Model

To establish an upper boundary for the Freundlich isotherm, Sips (1948) introduced an equation resembling the Langmuir equation by incorporating an additional parameter 'n'. When 'n' equals one, the Sips equation transforms into the Langmuir equation. The parameter 'n' is commonly interpreted as the degree of system heterogeneity. Consequently, as the magnitude of 'n' approaches 1, the adsorption system behaves more like Langmuir and thus implies a more homogeneous surface. It is important to note that the accuracy of the Sips equation diminishes within low concentration ranges.

$$Q_e = \frac{Q_{mS} K_S C_e^{\beta S}}{1 + K_S C_e^{\beta S}} \quad \text{Eq (12)}$$

In the provided equation, Q_{mS} (mg/g) and K_S (L/mg)$^{\beta S}$ represent the maximum monolayer saturation capacity and Sips constant, respectively, with βS serving as the heterogeneity factor.

The analysis of all isotherm models was performed using the non-linear curve fitting function in the OriginPro Software (2022, version 9.9.0.225). Employing a range of different evaluation techniques is recommended for a thorough assessment of isotherm modeling[81]. In this study, we initially applied the Akaike Information Criterion (AIC_c) to assess the fit of the model(Eder et al., 2021). The model that most accurately represents the isotherm data, in comparison to alternative models, is indicated by the lowest AIC_c value. Typically, the comparison of AIC_c values involves applying Equation 12.

$$\Delta_i = AIC_{c_i} - AIC_{c_{min}} \quad \text{Eq (13)}$$

In this context, AIC_{cmin} represents the isotherm model with the minimum AIC_c value. Comparing this value with the AIC_c values of other isotherm models helps in determining how well these other models represent the isotherm data relative to the model with the lowest AIC_c. Given that various models frequently appeared appropriate for depicting the isotherm data, we additionally employed both the reduced Chi-squared (X^2) and the adjusted coefficient of determination (R^2) to further evaluate the fit of the models.

2.3 Production of Activated Carbon

2.3.1 Production of Potassium Hydroxide (KOH) Petroleum Coke Activated Carbon

In the field of environmental science, one promising area of research is the development and utilization of adsorbent carbon materials, particularly from unconventional sources. Our research team is at the forefront of this innovative exploration, focusing on the use of petroleum coke.

One of the key processes in converting petcoke into an effective adsorbent material involves activation. Activation enhances the adsorptive properties of the carbon material, making it more effective in capturing contaminants. Our research has shown that when petcoke is activated using potassium hydroxide (KOH), it yields a more substantial amount of AC compared to other materials, such as KOH-activated lignocellulosic materials. This difference is primarily due to the pre-carbonized nature of petcoke, which results in less mass loss during the activation process.

In this chapter, we will delve into the specific methodologies for producing AC from petcoke. These methods are both environmentally and economically sustainable, making them ideal for widespread application. The processes we explore are integral to our thesis and have practical implications in addressing environmental challenges, particularly in adsorbing NA compounds commonly found in Oil Sands Processed Water (OSPW).

2.3.1.1 Activation Procedure

The activation of petcoke using KOH is a multistep process. Initially, the petroleum coke (PC) is ground to achieve particle sizes below 0.308 mm. This fine particle size is crucial for ensuring uniformity in the activation process. Before activation, the ground PC undergoes a

pretreatment step where it is heated at 400°C in the presence of air for one hour. This step eliminates volatile compounds that might interfere with the activation process.

Following pretreatment, the PC is mixed with dry KOH at a mass ratio of 1:1. This mixture is then loaded into crucibles and subjected to a controlled heating process. Initially, the temperature is increased at a rate of 40°C/min until reaching 410°C under a nitrogen atmosphere. The KOH is converted to potassium oxide (K_2O), at this stage. The activation itself involves further heating the mixture at a rate of 90°C/min until it reaches 900°C. This temperature is maintained for 15 minutes, allowing for thorough activation of the petcoke.

After the heating process, the activated material undergoes a washing procedure. This step involves using 20 mL of water per gram of the untreated activated product, followed by vacuum filtration. The final product, referred to as single-cycle AC exhibits enhanced adsorptive properties, making it suitable for environmental remediation applications, particularly in water treatment processes.

2.3.2 Production of Heat-Cycled KOH Petroleum Coke Activated Carbon

Our previous work, as detailed in Strong et al. (2023), builds upon the standard procedure for creating AC from petcoke using KOH, with an additional focus on creating pore-widened activated carbon (PWAC). The process begins similarly to the standard activation process, where the petcoke is activated at a temperature of 900ºC for 15 minutes. After the initial activation cycle and once the product cools down to room temperature, subsequent cycles of activation are initiated without the addition of any extra chemical reagents.

These subsequent cycles involve several key steps. First, the unwashed product from the initial single-cycle activation is exposed to the atmosphere. It is then crushed and remixed,

followed by a repetition of the activation heating cycle under an inert atmosphere. This process allows for the gradual expansion of the pores in the AC. The samples then undergo either a washing procedure or additional heating cycles.

After the washing procedure, the AC with widened pores (PWAC) is dried overnight at a temperature of 110 °C. Our study particularly emphasizes the use of single and triple cycles of activation to understand the differences in adsorption characteristics for NA compounds between these two types of adsorbents.

2.3.3 Production of Heat-Treated Phosphoric Acid (H_3PO_4) Activated Carbon

In our recent research, as detailed in the work of [84], we explored the application of this method using waste wood collected from construction sites in Ontario, Canada. The waste wood was initially subjected to size reduction until it was small enough to pass through an 18-mesh screen, equating to particle sizes of less than 1.0 mm. This size reduction is a crucial step, ensuring uniformity in the subsequent treatment processes.

Following size reduction, a dry mass ratio of 1:1, consisting of 25% phosphoric acid (H_3PO_4) and waste wood, was prepared[85]. This blend underwent a digestion process for 20 hours at a temperature of 35°C. The extended digestion period allows for thorough interaction between the acid and the wood, initiating the activation process.

After digestion, the treated waste wood was subjected to a muffle furnace for thermal treatment. This step involved heating the samples for 30 minutes at 400°C under a nitrogen flow of 5L/min. The controlled heating under an inert atmosphere is crucial for the development of the desired porous structure in the AC.

Once the thermal treatment was completed, the samples underwent further processing, including grinding, to ensure uniformity. The samples were then washed sequentially, first with 0.1 M hydrochloric acid (HCl) at a ratio of 10 mL per 1 g of the initial unwashed product. This wash was conducted at 80°C for 1 hour with agitation. The purpose of the HCl wash is to remove any residual phosphoric acid and other impurities.

Following the HCl wash, the samples were subjected to a wash with 0.1 M sodium hydroxide (NaOH) at the same ratio and temperature, and then a final wash with deionized (DI) water. These washing steps are critical for neutralizing the pH of the AC and removing any remaining impurities. After washing, the AC samples were dried overnight at a temperature of 110°C.

The final step in the process involved a heat treatment phase aimed at reducing the oxygen functionality on the surface of the AC. This step involved heating 5 grams of the product to 900°C for 15 minutes under a nitrogen atmosphere. The high-temperature treatment under an inert atmosphere further enhances the properties of the AC, making it more effective for adsorption applications.

Subsequent to this heat treatment, the samples underwent a final washing and drying process at 110°C. This comprehensive process, from the initial collection of waste wood to the final production of activated carbon, demonstrates a sustainable approach to creating high-value materials from waste.

Chapter 3 – Kinetics and Isotherms Study of Naphthenic Acid Adsorption on Various Synthesized Activated Carbons

3.1 Introduction

In this chapter a comprehensive exploration of the kinetics and isotherms characterizing the adsorption of seven model naphthenic acids (NAs) was investigated. This investigation was conducted using three distinct activated carbons (ACs): a potassium hydroxide petroleum coke AC (PAC), heat-treated wood-based activated carbon (HAC) and a commercial activated carbon (CAC), with a particular focus on elucidating the complexities of the adsorption process. NAs, abundant in oil sands process water (OSPW), present significant environmental challenges, emphasizing the importance of understanding their interactions with tailored ACs for effective water treatment strategies[1,6,28,31,86].

AC stands out as a versatile and highly efficient adsorbent, renowned for its porous structure and extensive surface area[34,87]. In the context of this study, the synthesized ACs are designed with unique textural and chemical properties, reflecting a deliberate effort to unravel the molecular mechanisms governing their interactions with NAs.

Canada's substantial production of waste wood, estimated at around 2.5 million tons annually, primarily originates from industrial, commercial, land clearing, and demolition activities. This amount of waste wood is significant, as it accounts for nearly half of all demolition materials that end up in landfills each year. The prevalence of waste wood in landfills highlights a critical environmental issue but also presents an opportunity. Given its abundance, waste wood becomes a prominent candidate as a cost-effective and sustainable resource for

producing novel materials, especially in the context of environmental remediation and sustainability.

One promising avenue for utilizing waste wood is through the process of phosphoric acid activation. This method, particularly effective for cellulose-based materials like wood, has been shown to be efficient in achieving activation at relatively low temperatures. Such a process results in higher yields of the desired product, enhanced porosity, and a substantial increase in surface area. These properties are particularly advantageous for adsorption applications, including the adsorption of NA compounds, a prevalent contaminant in industrial processes. Veksha et al. (2016) have noted the efficacy of this method, highlighting its potential in environmental remediation.

NAs, characterized by their complex molecular structures and functionalities, represent a key class of contaminants in OSPW[50]. The selection of seven model NAs for this study allows for a comprehensive examination as they represent a diverse range of solubilities, molecular structures, and properties, to understanding the complexity found in real-world environmental matrices.

The fundamental concept of adsorption, wherein molecules adhere to a solid surface, serves as the foundation for understanding the interactions between NAs and ACs[59,62]. This chapter places a particular emphasis on the kinetics of the adsorption process, exploring the rate at which NAs interact with the ACs as is shown in our earlier work[84]. Additionally, four prominent isotherm models—Langmuir, Freundlich, Sips, and Redlich-Peterson—are employed to characterize the equilibrium distribution of NAs on the synthesized ACs. These isotherm models provide a systematic framework for understanding the nature of sorption phenomena, including monolayer and multilayer adsorption[80].

The study presented in this chapter is derived from our previous paper which aims to contribute insights into the adsorption behavior of NAs by evaluating structurally different model species[84]. These NAs were explored to understand the variability in their adsorption onto AC at the relevant pH of OSPW. This investigation provided further insights into the favorable and unfavorable interactions between NAs and AC.

3.2 Materials and Methods

Diphenylacetic acid (DPA) (CAS# 117-34-0), dicyclohexylacetic acid (DHA) (CAS# 52034-92-1), cyclohexane acetic acid (CHA) (CAS# 5292-21-7), 2-methyl-1-cyclohexanecarboxylic acid (2-MCH) (CAS# 56586-13-1), 1,4-cyclohexanedicarboxylic acid (1,4-CHA) (CAS# 1076-97-7), heptanoic acid (HA) (CAS# 111-14-8), and succinic acid (SA) (CAS# 110-15-6) were all procured from Sigma Aldrich (St. Louis, MO) The ACs employed in this investigation are categorized as follows: commercial activated carbon (CAC) (CAS# 7440-44-0), obtained directly from Strem Chemicals and utilized without further modification; KOH petroleum coke activated carbon (PAC); and heat-treated wood-based activated carbon (HAC), for which activation procedures are detailed in the preceding chapter. The adsorption experiments and their respective conditions are described in Chapter 2.

3.3 Results and Discussion

3.3.1 Textural Properties of each Activated Carbon

3.3.1.1 Surface Properties of Adsorbents

In this study, several key techniques were employed to characterize the adsorbents used to assess model NA adsorption. Among these techniques were the BET method for analyzing surface area and the pore size distribution as detailed in Table 3.1, PAC stood out due to its

relatively low surface area, which was approximately 950 m^2/g. Furthermore, PAC was characterized by the lowest percentage of mesoporosity, around 20%, among the adsorbents tested. This suggests that PAC might have limitations in adsorbing NA molecules due to its restricted pore structure both in terms of overall capacity and the kinetics of adsorption.

On the other hand, CAC and HAC presented more favorable characteristics for the adsorption process. Both of these adsorbents showed similar surface area metrics, yet they differed significantly in their mesoporosity levels. The CAC exhibited a mesoporosity level of about 50%, indicating a well-balanced distribution of pore sizes that can accommodate a variety of molecular sizes. This feature makes CAC a versatile adsorbent for different types of contaminants, including NAs. Meanwhile, the HAC demonstrated an even higher level of mesoporosity, reaching 75%, which marks it as the adsorbent with the highest proportion of mesoporosity among the ones analyzed. Furthermore, variations in surface charge are anticipated owing to the differences in the point of zero charge (pzc) as shown in Table 3.1.

Table 3.1. Analysis of the BET surface area of the utilized activated carbon adsorbents.

Adsorbent	**Total Surface Area**	**Total Pore Volume**	**Micropore Volume**	**Mesopore Volume**	**Point Of Zero**
	(m^2/g)	(cm^3/g)	(cm^3/g)	(cm^3/g)	Charge
PAC	956 ± 34	$0.402 \pm 1.3*10^{-2}$	$0.322 \pm 1.2*10^{-2}$	$0.080 \pm 7.0*10^{-2}$	6.5
HAC	1440 ± 78	$0.761 \pm 1.5*10^{-2}$	$0.190 \pm 6.7*10^{-3}$	$0.572 \pm 2.2*10^{-2}$	4.0
CAC	1310 ± 69	$0.476 \pm 1.0*10^{-2}$	$0.261 \pm 1.6*10^{-3}$	$0.215 \pm 1.2*10^{-2}$	9.0

3.3.1.2 Size Distribution of Adsorbents

In our comprehensive study of the properties of ACs derived from different precursor materials, we conducted a detailed size fraction test to evaluate the particle size distribution of each type of AC. The results of this size fraction test are in Figure 3.1 of our report. For most

particle sizes, the distribution patterns of all three adsorbents—namely heat-treated wood based activated carbon (HAC), commercial activated carbon (CAC), and KOH petroleum coke activated carbon (PAC)—were found to be remarkably similar. This similarity suggests that the activation process and the fact that the ACs were ground as stated earlier, irrespective of the chemical agent used, tends to produce ACs with comparable particle size distributions in most of the size ranges we examined.

However, a notable exception was observed for particles with a diameter greater than 0.381 mm. In this size range, HAC exhibited a distinct deviation from the pattern observed in CAC and PAC. Specifically, HAC was found to have a higher proportion of larger particles compared to the other two types of ACs. This divergence was not only statistically significant as evidenced by the data presented in Figure 3.1 but was also corroborated by a visual inspection of the adsorbent container.

In contrast, the containers for CAC and PAC revealed a more homogeneous mixture of particle sizes, with fewer large particles and a distribution that appeared to be more consistent with the majority of the size ranges we analyzed.

The presence of larger particles in HAC could be attributed to several factors, including differences in the precursor material, variations in the activation process, or the specific conditions under which the phosphoric acid activation was performed. Larger particles in an adsorbent can have both advantages and disadvantages, depending on the intended application. For instance, larger particles may reduce pressure drop in fixed-bed adsorption processes, but they might also exhibit lower surface area-to-volume ratios, potentially impacting the adsorption efficiency for certain contaminants[88,89].

This finding underscores the importance of careful selection and characterization of Acs for specific applications. Understanding the particle size distribution and other physical properties of ACs is essential for optimizing their performance in adsorption processes. This study contributes valuable insights into the physical characteristics of ACs, highlighting the need for detailed analysis and selection based on the specific requirements of the intended application.

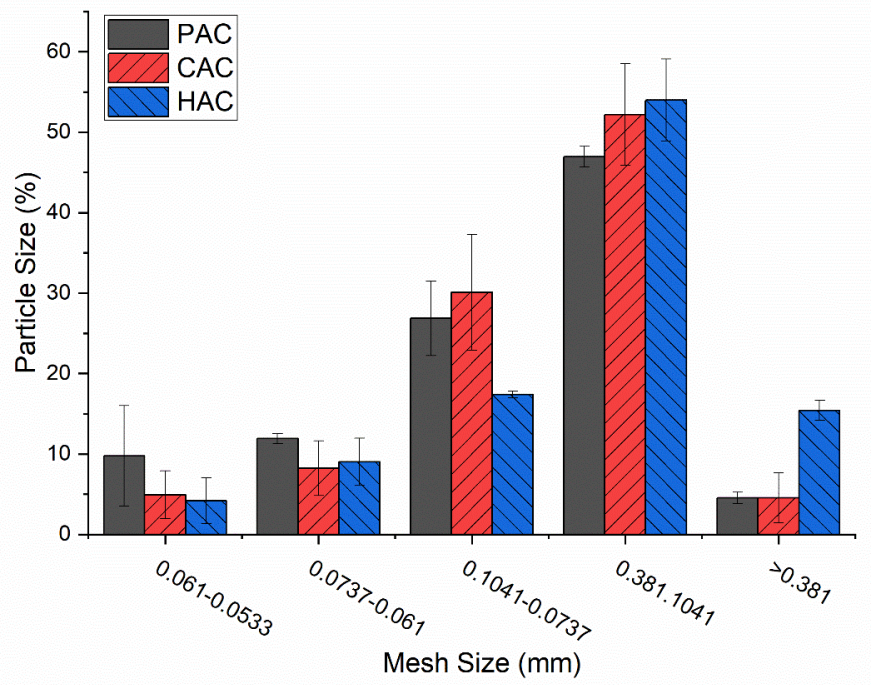

Figure 3.1. Particle size distribution of all three adsorbents of a)PAC; b)CAC; and c)HAC.

3.3.2 Surface Functionality of each Adsorbent

Table 3.2. Atomic Percent Composition by XPS

Adsorbent	*C (%)*	*O (%)*	*N (%)*	*P (%)*	*K (%)*	*S (%)*
HAC	93.9 ± 1.41	5.4 ± 1.08	0.30 ± 0.30	0.6 ± 0.09	/	/
CAC	84.5 ± 1.68	15.5 ± 1.68	/	/	/	/
PAC	85.5 ± 3.73	12.1 ± 2.31	0.4 ± 0.12	/	1.3 ± 0.53	0.6 ± 0.1

Table 3.2 presents atomic composition data from X-ray photoelectron spectroscopy (XPS) which offers insights into the surface elemental composition and chemical states of ACs from various activation processes, while the high-resolution C 1s spectrum with synthetic component fitting is shown in Figure 3.2. As shown in the table, all ACs share similar compositions, primarily consisting of carbon and oxygen functionalities. The high-resolution C 1s scans (Figure 3.2) reveal that while the types of oxygen functional groups are similar across all three ACs, their distributions vary slightly. These differences might explain the variations in adsorption performance observed among the ACs. Notably, HAC contains a small amount of phosphorus, which stems from the use of phosphoric acid during the activation process and has been integrated into the AC structure. Additionally, HAC displays a significantly lower level of oxygen functionality, as clearly shown in Table 3.2. Considering the different types of oxygen functionalities within these adsorbents, it is primarily the hydroxyl groups that facilitate favorable interactions with NAs through hydrogen bonding. Therefore, one reason for HAC's relatively poor adsorption performance compared to the other two ACs could be the fewer hydrogen bonding opportunities, owing to its lower oxygen content and consequently reduced hydroxyl functionality on the surface.

For CAC, the XPS survey scan reveals a composition predominantly consisting of oxygen and carbon. This indicates a high degree of purity with minimal impurities present. The predominance of oxygen suggests a significant amount of oxygenated functional groups on the surface, which can enhance the adsorption capabilities of the AC by providing additional sites for chemical interactions with contaminants.

In contrast, PAC demonstrates a different chemical profile. The XPS scan for PAC shows residual amounts of potassium, which is primarily present in the form of potassium carbonate.

This is likely a result of the potassium hydroxide activation process and the subsequent reactions occurring during the heat treatment. In addition to potassium, the PAC samples also exhibit some sulfur content. The presence of these elements indicates a more complex surface chemistry, which could influence the adsorption behavior of PAC, particularly in its interaction with specific types of contaminants.

The differences in the chemical compositions and surface properties of these ACs, as highlighted by the XPS survey scans, have significant implications for their use as adsorbents. The variety in elemental composition and functional groups present on the surface of the AC effect their adsorption efficacy, kinetics, and isotherms for specific contaminants, such as NAs. For example, the higher oxygen content in CAC might facilitate stronger interactions with polar contaminants, whereas the unique chemical functionalities in PAC and HAC could offer advantages for adsorbing other types of molecules.

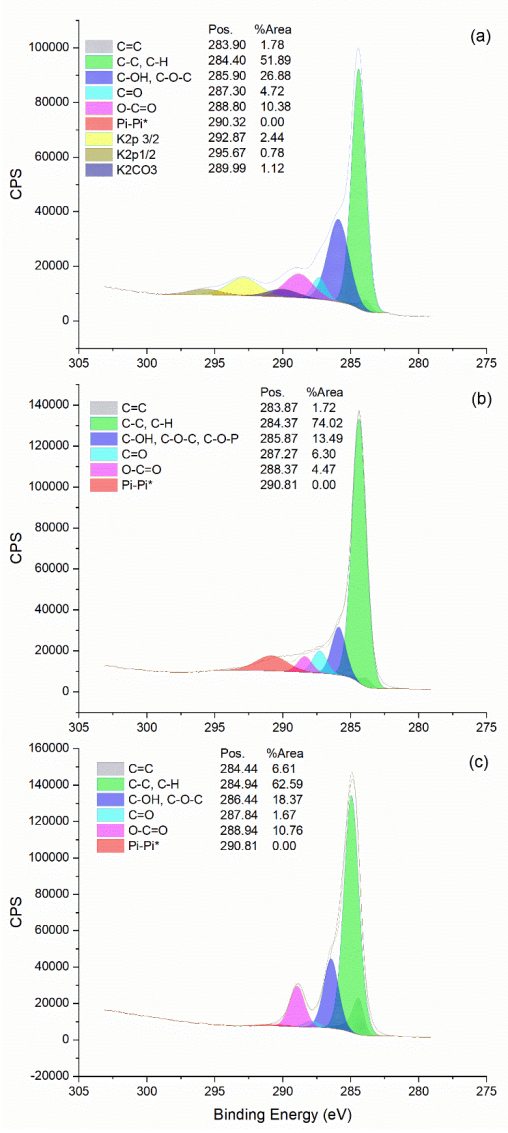

Figure 3.2. C 1s XPS Survey Scans of a) PAC; b) HAC; and c) CAC

3.3.3 Kinetics of Adsorption

The kinetics of NA adsorption on to the three AC materials was evaluated and the results are presented in Figure 3.3.

The kinetics of adsorption presented in Figure 3.3 reveal that the efficiency of NA uptake by each AC

strongly depends on the chemical structure of the given compound. Notably, DPA and DHA exhibited the highest adsorption capacities. In contrast, HA, CHA, and 2-MCH showed moderately lower adsorption percentages. 1,4-CHA and SA displayed minimal adsorption. Although these NAs represent only a fraction of potential NA compounds varieties in OSPW, this highlights the need for more targeted adsorption studies for optimal NA removal using AC.

The adsorption rate for each model NA also varied based on the surface properties such as pore size distribution and particle size of the AC adsorbent. Among the model NAs, CAC showed the quickest adsorption, reaching equilibrium within 30 to 60 minutes. PAC achieved equilibrium in 24 to 48 hours, depending on the NA, suggesting differences in pore size distribution compared to CAC. Despite having the highest mesoporosity, HAC took 2 to 8 hours to approach equilibrium. Table 3.1 illustrates that CAC and HAC possess a significantly larger mesopore volume in comparison to PAC's mesoporosity. This characteristic is expected to result in more rapid kinetics for these two adsorbents. Previously, we demonstrated that enhancing the mesoporosity of PAC without extra chemical additives leads to improved adsorption kinetics (Strong et al., 2023). This improvement is attributed to mesopores being more effective at promoting the internal diffusion of adsorbates than micropores[26]. As mentioned before, CAC and PAC share a similar distribution in particle sizes, but HAC displays a significant increase in its largest size fraction which could slow the kinetics of adsorption[26]. The larger particle size found in HAC probably accounts for the somewhat slower adsorption kinetics on this adsorbent compared to CAC, even though HAC possesses the greatest volume of mesoporosity. In general, particle size could be considered as a potential influencing factor in kinetics of NA adsorption.

This comparative analysis underscores the importance of selecting the right adsorbent based on its structural properties, including surface area and pore size distribution. These

characteristics directly impact the adsorbent's efficiency in capturing specific contaminants, highlighting the need for careful consideration in the design and selection of adsorbents for environmental remediation applications, particularly when targeting complex mixtures of pollutants like NAs.

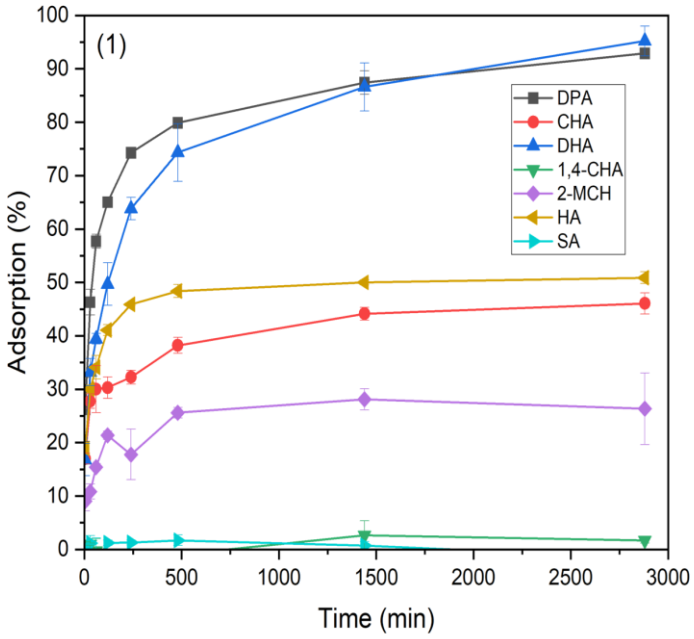

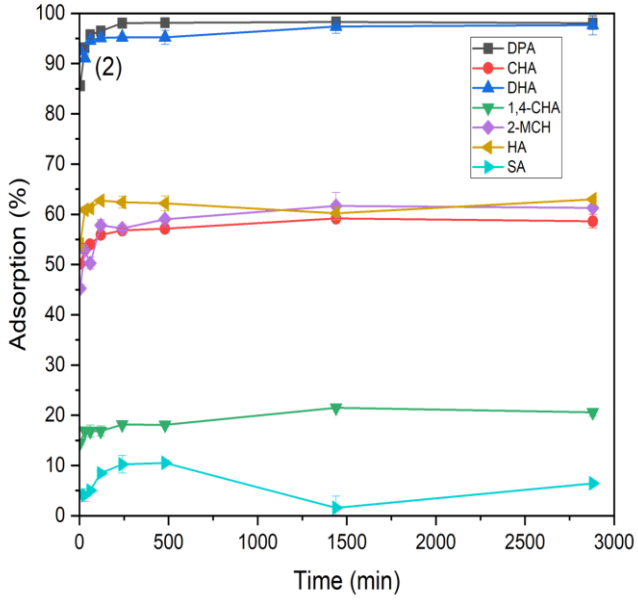

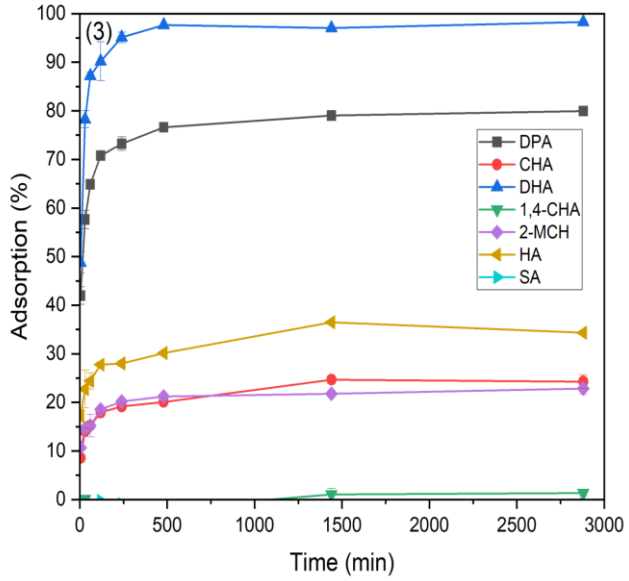

Figure 3.3. Adsorption kinetics of model NAs onto three types of ACs: 1) PAC; 2) CAC; and 3) HAC.

To understand the interaction between various NAs and activated carbons, we analyzed the rate at which these acids are absorbed using a technique known as kinetic modeling. More

specifically, we applied a model called the m-exp model, as outlined in Equation 7, to assess the adsorption "half-time," denoted as $t_{1/2}$. This term represents the estimated time required to reach 50% of adsorption equilibrium (Table 3.3). The M-exp model was chosen in this study for its ability to account for the complexity and heterogeneity of real-world systems, offering a more accurate prediction and analysis of behaviors in contaminated water systems. It is often viewed as a set of parallel pseudo-first-order mechanisms that align with the adsorption kinetics observed in experiments[79].

It is important to note that this modeling approach was not applied to all acids. We excluded SA and 1,4-CHA from our analysis due to their minimal adherence to the carbon surfaces, a phenomenon evident in Figure 3.3. Additionally, the interaction between CAC and the acids showed deviations from our model's predictions, likely due to the rapid and highly efficient adsorption process onto CAC. For the model to provide accurate insights, it is crucial to have data that spans the entire duration of the adsorption process, capturing the dynamics from beginning to end[76].

Upon evaluating the acids that aligned well with Equation 7, we calculated their $t_{1/2}$ values. It was observed that the PAC typically exhibited the longest adsorption half-times among the acids tested, particularly in comparison to HAC. Conversely, CAC stood out for its rapid adsorption rates, with the half-time for each acid tested on CAC occurring within the initial 5 minutes of agitation. This rapid performance of CAC relative to the other carbons offers valuable insights (most importantly pore size and particle size) into the interaction between different materials and

NAs, potentially guiding the selection of the most effective activated carbon for environmental cleanup efforts.

*Table 3.3. Adsorption half times for model naphthenic acids onto each activated carbon calculated using m-exp modelling. *CAC was not modelled by m-exp, and thus adsorption half times are approximated by experimental adsorption kinetics.*

	HAC		PAC		*CAC
Model NA	$t\frac{1}{2}$ (min)	R^2	$t\frac{1}{2}$ (min)	R^2	$t\frac{1}{2}$ (min)
DHA	6	0.9883	98	0.9914	< 5
DPA	4	0.9977	24	0.9960	< 5
HA	7	0.9621	11	0.9952	< 5
CHA	16	0.9725	7	0.9976	< 5
2-MCH	7	0.9883	53	0.9089	< 5

3.3.4 Isotherms Study

Kinetics modeling examines the rate at which adsorption occurs, providing insights into the mechanisms and factors influencing the speed of the adsorption process. Another essential parameter for adsorption is adsorption capacity and isotherm modeling which focuses on the equilibrium relationship between the concentration of adsorbate in the solution and its corresponding amount adsorbed onto a solid surface at constant temperature. This helps in understanding the capacity and affinity of the adsorbent. The interaction between various NAs and activated carbons significantly varies depending on the specific acid in question. For example, DHA and DPA demonstrated notable efficiency in adhering to activated carbons, with adsorption capacities ranging from 100 to 350 milligrams per gram (mg/g), indicating strong adsorption. However, the scenario was quite different for 1,4-CHA, where the adsorption capacity was significantly lower, as depicted in Figure 3.4, suggesting a lesser affinity for the carbon surfaces. SA presented an even more pronounced deviation, showing almost no inclination to either PAC or HAC, and only marginally better results with CAC. This could be

attributed to the soluble nature of SA and 1,4-CHA in water, making them less likely to detach from a liquid medium and bind to the hydrophobic surfaces of adsorbents.

Upon analyzing the performance of different activated carbon types in adsorbing these acids, several patterns emerged. CAC and PAC often performed comparably, effectively capturing a significant amount of acids. On the other hand, the HAC generally showed lower adsorption efficiency. It appeared that HAC, despite its unique preparation, did not perform as well in retaining the acids as its counterparts. This investigation underscores the fact that activated carbons and NAs are not all equivalent. The efficacy of adsorption depends greatly on the type of acid and the specific activated carbon used.

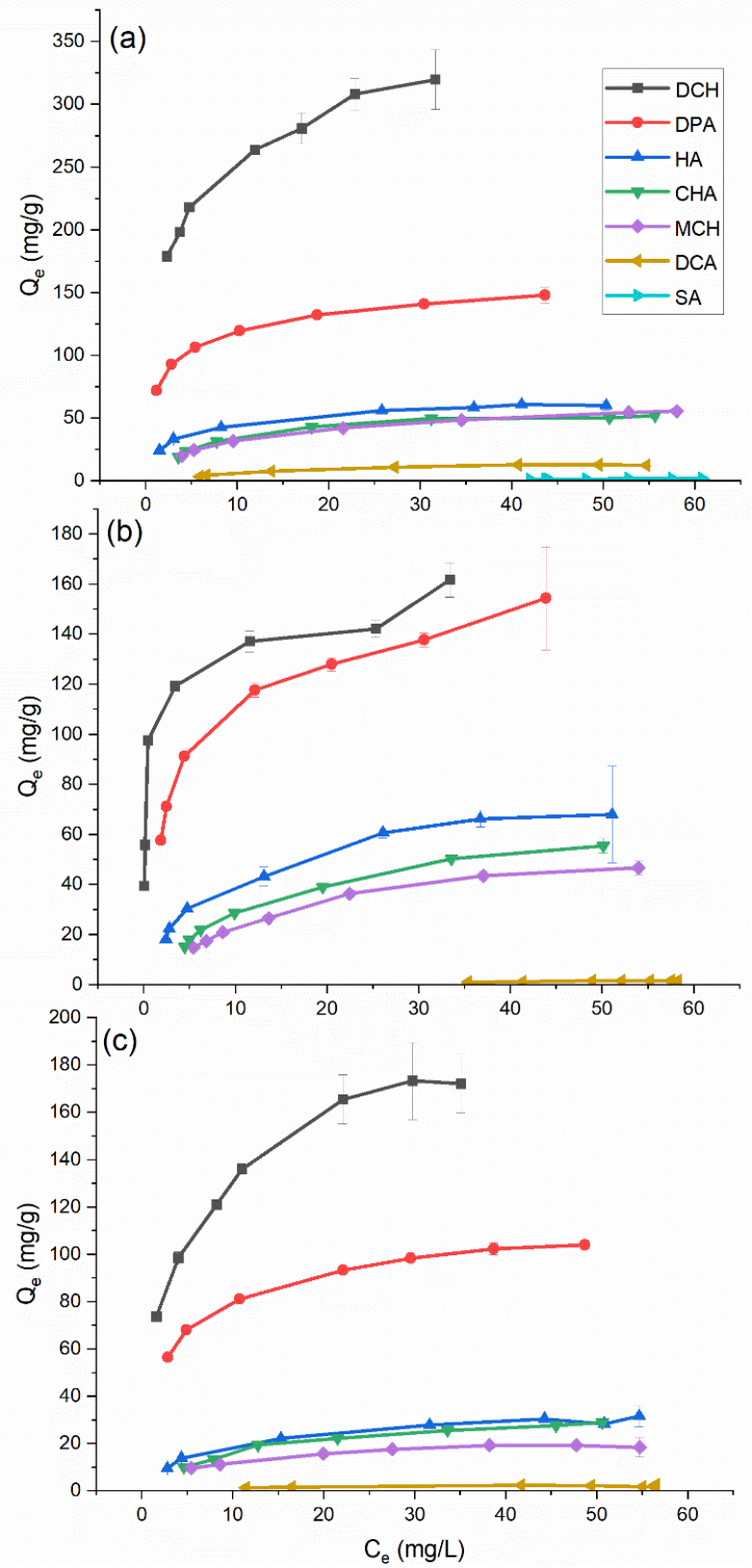

Figure 3.4. Isotherms illustrating the absorption of model NA species on (a) CAC, (b) PAC, and (c) HAC.

Figure 3.5 provides a more detailed comparison of how effectively each type of activated carbon can capture NAs. This figure showcases the maximum capacity of each activated carbon to adsorb NAs, using data derived from isotherm curves presented in Figure 3.4. Interestingly, we normalized these maximum capacities based on the surface area of each type of carbon, ensuring a fair comparison that accounts for the available surface for the NAs to adhere to.

From this analysis, we observed that PAC tends to outperform both the CAC and the HAC for a number of the NAs examined. This outcome is particularly intriguing as it challenges the assumption that a larger surface area is directly correlated with superior adsorption capability. Instead, it appears that the specific characteristics of the carbon's surface, along with the distinct physical and chemical attributes of the NAs, are the critical factors in determining adsorption efficiency.

This revelation significantly shifts our understanding of what to consider when selecting activated carbon for environmental cleanup tasks. It implies that merely looking at the surface area of activated carbon is not sufficient to gauge its effectiveness. Rather, attention must be paid to the interaction between the carbon's surface and the specific NAs in question. Certain surfaces may offer unique textures or chemical compositions that are particularly conducive to capturing specific NAs, despite not having the largest surface area.

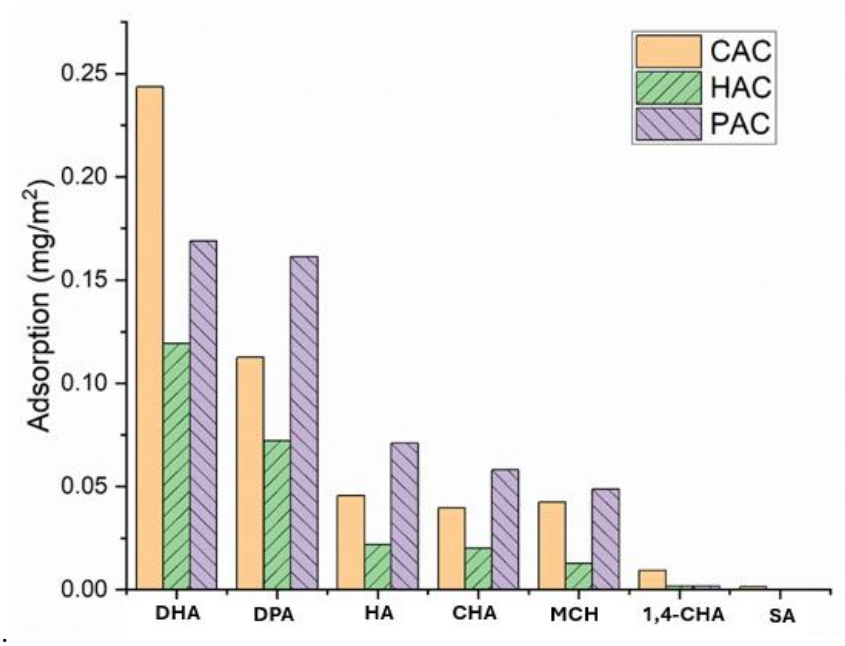

Figure 3.5. The highest adsorption capacities for each model NA, as determined through experimentation, normalized against the total specific surface area of each type of activated carbon.

In isotherm measurements, metrics like reduced chi-square (X^2), adjusted R-squared (R^2), and Akaike Information Criterion (AIC_c) are key for evaluating model fit and accuracy. Reduced X^2 assesses goodness-of-fit by comparing observed and predicted data, adjusted R^2 refines the fit by accounting for the number of predictors, and AIC_c balances fit with model complexity to identify the most efficient model. These tools collectively help select the most reliable isotherm model. Table 3.4 presents the assessment of adsorption isotherm modeling, showcasing the reduced X^2, adjusted R^2 and AIC_c values for the best fitted model of each adsorption system. In our study, Δi values from equation 12 that are less than 2 are typically deemed satisfactory, indicating that both isotherm models effectively represent the adsorption isotherm[83]. In numerous cases, this situation occurred, necessitating a comparison of

the reduced X^2 and adjusted R^2 to distinguish the most accurate isotherm model. Table 3.5 exhibits the fitted parameters for the optimal representative models for each adsorption system.

Although the Freundlich model is commonly used to describe adsorption onto activated carbon in existing literature[80], the Langmuir model was shown to best represent the adsorption isotherms for several of the model NA adsorption systems in this study. This preference may stem from the Freundlich model's limitations in accurately reflecting the relationship between low equilibrium concentrations (Ce) and equilibrium quantities (Qe), or in predicting saturation behavior at high Ce values when a complete isotherm is achieved[80]. The Langmuir model best represented the adsorption isotherms for HA, CHA, and MCH, as indicated by the low reduced X^2 and high adjusted R^2 values in Table 3.4. This suggests that the activated carbon surfaces have energetically uniform adsorption sites and a homogeneous surface, aligning with the fundamental assumptions of the Langmuir model.

The applicability of the Langmuir model is a surprising outcome as the assumptions of the model are not particularly consistent with the properties of AC surfaces. In particular, activated carbon lacks a consistent surface texture. Nonetheless, instances exist where the Langmuir model effectively describes adsorption systems using activated carbon, despite the deviation from the presumption of a homogenous surface(Worch, 2012). When considering adsorption sites influenced by hydrophobic or hydrogen bonding mechanisms, the associated energy spectrum is notably smaller compared to the larger energy interactions found in the specific chemical bonding between an adsorbent and an adsorbate. This might suffice to characterize the surface as uniformly consistent, especially in terms of the minor energy disparities among physisorption sites[80].

For both the MCH and HA isotherms on CAC, which are most accurately depicted by the Redlich-Peterson and Sips models respectively, the similarity of the heterogeneity factor to unity in both cases, as indicated in Table 3.5, suggests a higher degree of energy uniformity in the adsorption sites of the activated carbon. For DPA, despite its poor fit with the Langmuir model, the heterogeneity factors in the Redlich-Peterson and Sips models were also notably near to one, indicating a similar trend in uniformity. Isotherms of DHA were most accurately depicted using the Redlich-Peterson or Sips formulas. However, it is noteworthy that the heterogeneity factors derived from the Sips analysis of DHA on CAC and HAC indicated considerably lower values, suggesting the possibility of a broader range of energy distribution at the adsorption sites for this model species on these activated carbons. While the Langmuir expression effectively modeled 1,4-CHA's adsorption on CAC, the isotherm models applied to 1,4-CHA isotherms on PAC and HAC did not achieve a good fit. This is evident from Table 3.3, where even the most suitable isotherm model for 1,4-CHA on PAC and HAC yielded low R^2 values. The likely cause for this is the minimal adsorption observed on PAC and HAC, leading to an incomplete isotherm profile.

Table 3.4. Assessment of Optimal Isotherm Models for Each Adsorption System.

MODEL NA	ADSORBENT	BEST MODEL	X^2	ADJ R^2	AIC_C
DHA	CAC	Sips	20.36	0.9933	31.18
	PAC	RP	74.22	0.9645	40.23
	HAC	Sips	17.64	0.9883	30.17
DPA	CAC	RP	0.2683	0.9996	0.8738
	PAC	RP	15.97	0.9876	29.48
	HAC	Sips	0.6168	0.9982	6.700
HA	CAC	Sips	0.9872	0.9954	9.993
	PAC	Langmuir	7.962	0.9821	19.17
	HAC	Langmuir	1.501	0.9799	7.489
CHA	CAC	Langmuir	1.183	0.9936	5.824
	PAC	Langmuir	1.022	0.996	4.794
	HAC	Langmuir	0.5111	0.9904	-0.0539
MCH	CAC	RP	0.1800	0.9991	-1.921
	PAC	Langmuir	0.6351	0.9962	1.467
	HAC	Langmuir	0.4848	0.9692	-0.4234
1,4-CHA	CAC	Langmuir	0.4190	0.9736	-1.4442
	PAC	Langmuir	0.00528	0.8912	-32.05
	HAC	Langmuir	0.1165	0.4756	-10.404

Table 3.5. Parameters Determined from Isotherm Modeling of the Most Representative Models for Each Adsorption System.

			LANGMUIR		SIPS			RP		
MODEL NA	Adsorbent	Best Model	Q_0 (mg/g)	K_L (L/mg)	Q_m (mg/g)	K_s $(L/mg)^{\beta s}$	B_s	K_r (L/g)	A_r $(L/mg)^g$	g
DHA	PAC	RP						887.7	7.489	0.9275
	HAC	Sips			284.8	0.2624	0.5147			
	CAC	Sips			670.1	0.2682	0.3575			
DPA	PAC	RP						80.51	0.846	0.8673
	HAC	Sips			129.9	0.4191	0.5869			
	CAC	RP						244.6	2.605	0.876
HA	PAC	Langmuir	78.96	0.1205						
	HAC	Langmuir	34.26	0.1371						
	CAC	Sips			74.51	0.3746	0.628			
CHA	PAC	Langmuir	72.71	0.0639						
	HAC	Langmuir	35.06	0.0841						
	CAC	Langmuir	58.37	0.1485						
MCH	PAC	Langmuir	62.87	0.0571						
	HAC	Langmuir	22.05	0.1304						
	CAC	RP						11.21	0.3743	0.8259
1,4-CHA	PAC	Langmuir	7.736	0.0045						
	HAC	Langmuir	2.553	0.0877						
	CAC	Langmuir	17.67	0.0519						

3.4 Conclusion

This chapter highlights the diverse adsorption affinities of NA species to ACs, offering insights for identifying NAs resistant to adsorption. The importance of physicochemical properties, notably hydrophobicity, is emphasized as crucial for adsorption efficiency, suggesting physisorption as the dominant mechanism. Our findings indicate that while hydrophobic surface interactions are beneficial, hydrogen bonding with surface oxygenated groups also play a significant role, particularly evidenced by the lower adsorption rates of NAs on HAC compared to other carbons. This is attributed to the favorable presence of oxygenated species on the carbon surface, with future research directions aimed at enhancing surface functionalities to improve adsorption of recalcitrant NA species, thus optimizing ACs for environmental cleanup.

Chapter 4 – Adsorption Kinetics of Model Naphthenic Acids on Pore Widened Activated Carbons

4.1 Introduction

The demand for effective environmental remediation techniques has led to the exploration of various materials and methods capable of addressing the pervasive challenge of pollution, particularly from industrial sources. Among these, activated carbons (ACs) have emerged as a pivotal tool due to their high surface area, porosity, and adsorption capacity. This chapter delves into the adsorption kinetics of three model naphthenic acids (NAs) - diphenylacetic acid (DPA), cyclohexaneacetic acid (CHA), and heptanoic acid (HA) on pore-widened activated carbons, a study aimed at enhancing the understanding and efficiency of ACs in environmental applications.

Naphthenic acids, a class of compounds found in crude oil and oil sands process water, pose significant environmental hazards due to their toxicity and persistence. The remediation of these compounds is of utmost importance for environmental protection and sustainability. Activated carbon, derived from petroleum coke via chemical activation using potassium hydroxide (KOH), represents a promising material for this purpose. However, the intrinsic microporosity of the resulting ACs, while beneficial for certain applications, can limit the adsorption kinetics of larger molecular species, such as naphthenic acids, thereby restricting the material's effectiveness in rapid environmental remediation scenarios.

To overcome this limitation, our research has focused on a novel approach to modify the pore structure of activated carbons. By subjecting the KOH-activated carbon to additional heat cycles without introducing new chemical agents, we aim to enhance the mesoporosity of the material. This process leverages the oxidation of residual potassium metal, a byproduct of the initial

activation phase, to serve once again as an activating agent, promoting further development of the carbon's pore structure.

The effect of this pore-widening technique on the adsorption kinetics of DPA, CHA, and HA offers valuable insights into the potential of modified ACs for environmental applications. By increasing mesoporosity by 10–25% with each successive heat cycle, we hypothesize that the adsorption rates and capacities of the ACs for naphthenic acids will be significantly improved. This chapter presents a comprehensive examination of the adsorption behavior of single, double, and triple-cycled activated carbons, providing a critical assessment of their efficacy in the adsorption of model NAs. Through precise experimentation, including the utilization of Fourier Transform Ion Cyclotron Resonance Mass Spectrometry (FT-ICR-MS) to analyze the treated oil sands processed water (OSPW), this chapter also offers a thorough evaluation of the adsorption capabilities of single and triple-cycled activated carbons, especially with the remarkable adsorption behaviour and signal reduction observed for DPA, DHA, succinic acid (SA), 1,4-cyclohexanedicarboxylic acid (1,4-CHA), 9-anthracenecrboxylic acid (ACA) and 1-pyrenecarboxylic acid (PCA) which supports the promising role of modified ACs in the realm of environmental cleanup and sustainability.

4.2 Materials and Methods

Petroleum coke, sourced from the oil sands by Suncor Energy Inc. in Calgary, Alberta, Canada, served as the raw material for the potassium hydroxide (KOH) activation process. The chemicals used in the study, including potassium hydroxide and the naphthenic acids: DPA, CHA, 1,4-CHA, SA, DHA, PCA, ACA, HA, and dioctylsodium sulfoccinate as an internal standard were acquired directly from Sigma Aldrich in Milwaukee, WI, USA, and utilized without further modification. Table 4.1 presents a comprehensive overview of the naphthenic

acid compounds discussed in this chapter, including details on their chemical structures, chemical formulas, and molecular weights.

KOH petroleum coke activated carbon and Heat-cycled KOH petroleum coke activated carbon was prepared as described in chapter 2.3.1 and 2.3.2 respectively.

Table 4.1. An overview of model NA compounds used in this study.

Compound	DPA	DHA	CHA	1,4-CHA	SA	HA	PCA	ACA
Structure	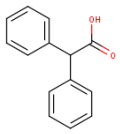	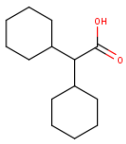	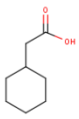	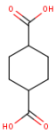	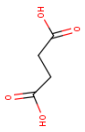		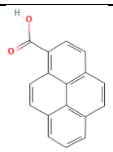	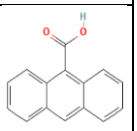
Chemical Formula	$C_{14}H_{12}O_2$	$C_{14}H_{24}O_2$	$C_8H_{14}O_2$	$C_8H_{12}O_4$	$C_4H_6O_4$	$C_7H_{14}O_2$	$C_{17}H_{10}O_2$	$C_{15}H_{10}O_2$
MW	212.0837	224.1776	142.0993	172.0735	118.0266	130.0993	246.0680	222.0680

4.3 Results and Discussion

4.3.1 Kinetics Study

In our research, as detailed in our previous publication[87], the effect of enlarging the pores on activated carbon and its impact on absorbing three types of naphthenic acids was explored. This investigation is crucial for the environmental safety of discharging water from oil sands operations into natural habitats. Our findings, illustrated in Figure 4.1, indicate that each naphthenic acid reached equilibrium, at approximately 24 hours after the adsorption experiment began. This observation is vital as it provides an estimate of the time required for the adsorption process to stabilize for these specific acids.

Upon analyzing the equilibrium state, we discovered little variance in the total amount of naphthenic acids adsorbed by the activated carbon, regardless of whether the carbon underwent one, two, or three cycles of pore enlargement. This suggests that increasing pore size does not significantly affect the total capacity of the activated carbon to bind with the acids over time. Although no significant differences in adsorption capacities on the pore-widened activated carbons were observed, the adsorption isotherms for these activated carbons were not fully explored, rendering this conclusion somewhat speculative.

However, an intriguing finding from our study is the noticeable difference in the initial adsorption rate based on the number of pore enlargement treatments the activated carbon received. Despite reaching similar equilibrium states, the initial rate at which the acids were adsorbed varied. Generally, the quicker an activated carbon begins to adsorb the acids, the more efficient and effective the water cleaning process may be. This aspect of our research emphasizes the importance of pore size and structure in enhancing the early stages of the adsorption process, as demonstrated in Figure 4.1.

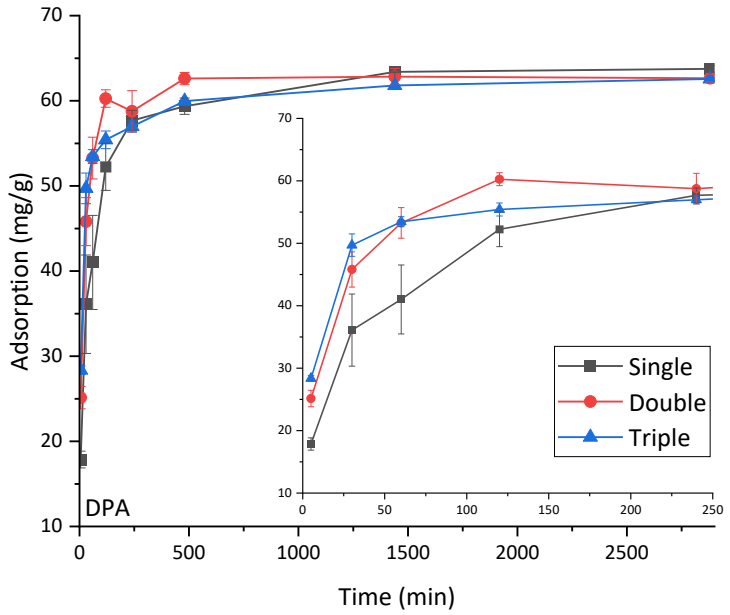
Adsorption (mg/g)
Time (min)
DPA
Single
Double
Triple

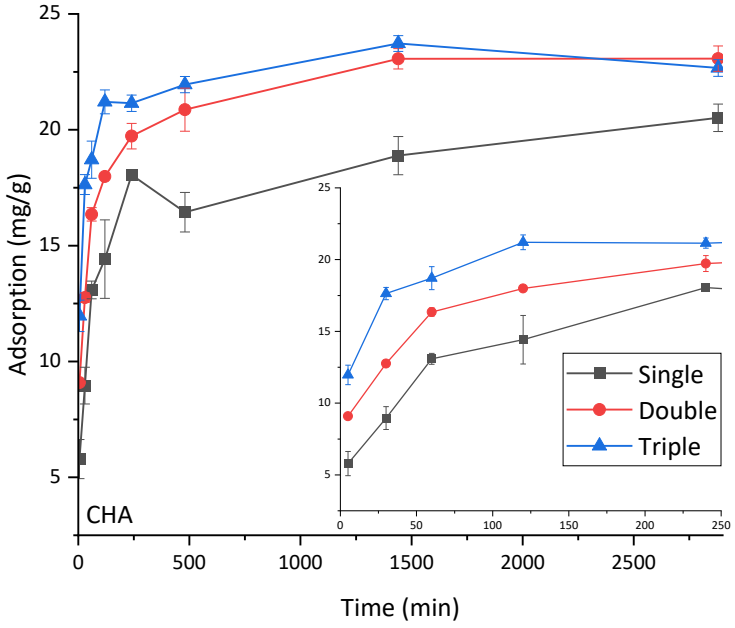
Adsorption (mg/g)
Time (min)
CHA
Single
Double
Triple

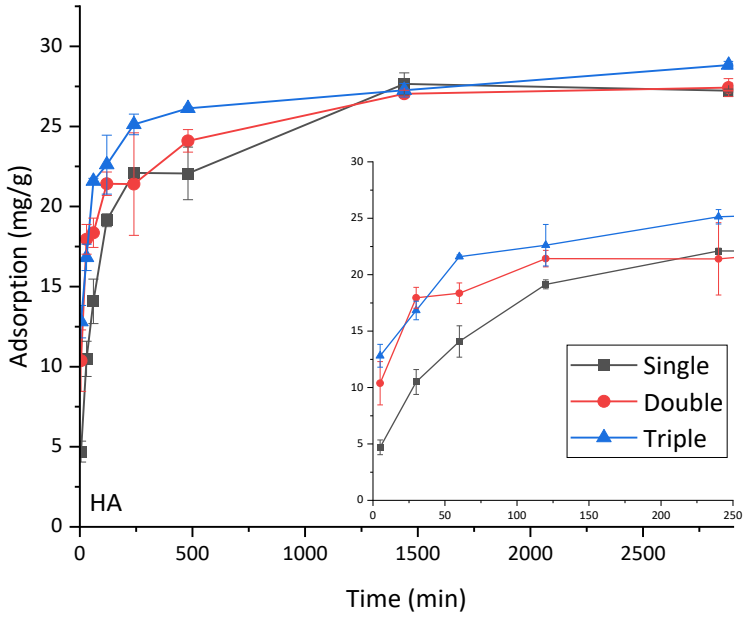

Figure 4.1. Adsorption kinetic plots for model naphthenic acids of a) diphenylacetic acid (DPA); b) cyclohexaneacetic acid (CHA); and c) heptanoic acid (HA) on three heat-cycled ACs with showing the initial up to 2h. Single, double and triple AC are activated carbons subjected to one, two and three cycles of heat treatments, respectively.

When the adsorption kinetics presented in Figure 4.1 are normalized to the specific surface area of each respective heat cycled PWAC, more distinct differences are seen in how quickly each type of carbon starts adsorbing naphthenic acids, as presented in Figure 4.2. This normalization allows us to make a more direct comparison on a per surface area basis. Among the three types of naphthenic acids that were examined, adsorption process appeared to be the fastest on the triple-cycled AC This was closely followed by the performance of the double cycled, and then the single cycled PWAC. This pattern highlights how the process of adsorption begins differently across these variations of activated carbon.

The most notable distinction among these three types of activated carbons lies in their pore size distribution. Specifically, the single, double, and triple cycled PWACs exhibit varying levels of mesoporosity, recorded at 25.1±2.3%, 39.4±0.2%, and 63.5±2.1% respectively. Figure 4.2 indicates a progressive increase in the amount of medium-sized pores across the series from single to triple cycled PWACs.

This variance in mesoporosity aligns with the observed differences in the initial adsorption kinetics for the model naphthenic acids across the three versions of PWAC. As mesoporosity increases, so does the efficiency of the internal diffusion process, which allows the adsorbate to more easily penetrate the activated carbon and reach the adsorption sites nestled within the microporous structure. Essentially, the increase in pore width enhances the ability of the activated carbons to quickly hold onto the naphthenic acids, making the initial stages of adsorption notably faster, especially in the triple cycled PWAC.

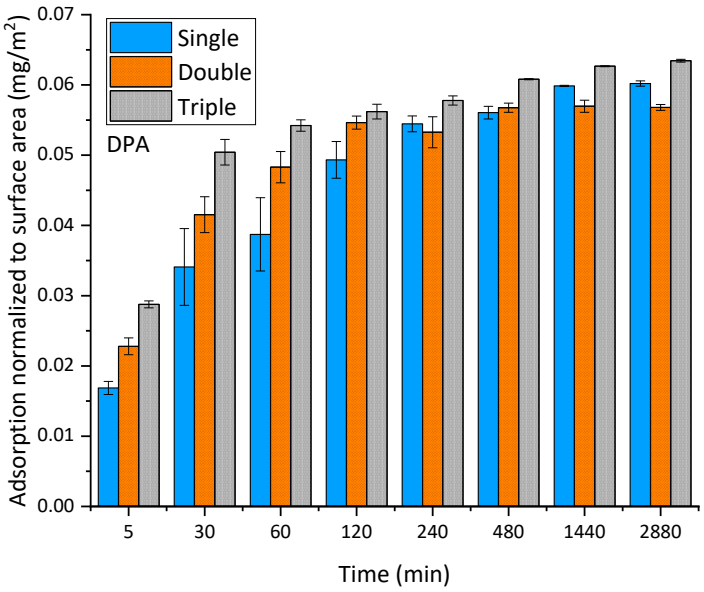
Single
Double
Triple
DPA
Adsorption normalized to surface area (mg/m^2)
0.00
0.01
0.02
0.03
0.04
0.05
0.06
0.07
5
30
60
120
240
480
1440
2880
Time (min)

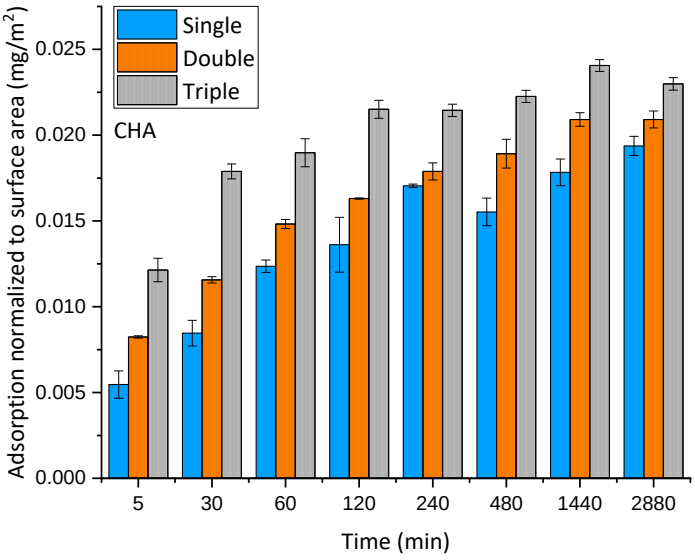
Single
Double
Triple
CHA
Adsorption normalized to surface area (mg/m^2)
0.000
0.005
0.010
0.015
0.020
0.025
5
30
60
120
240
480
1440
2880
Time (min)

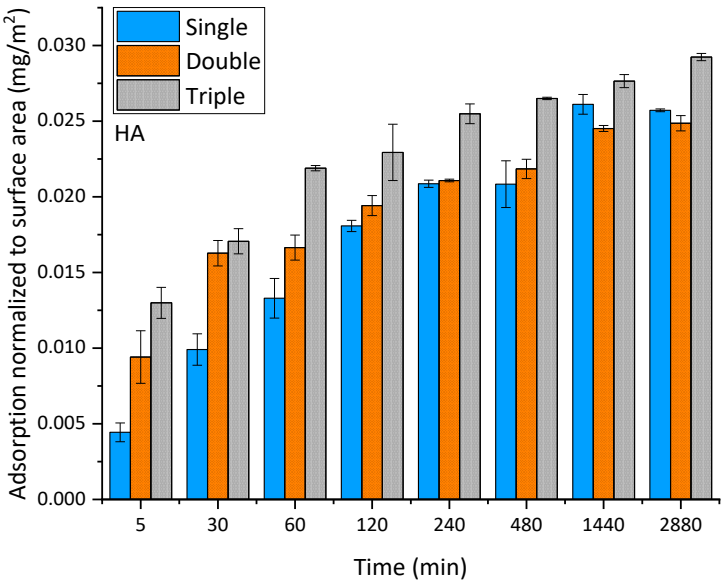

Figure 4.2. Adsorption kinetics with adsorption capacity normalized to surface area of each activated carbon for a) diphenylacetic acid (DPA); b) cyclohexaneacetic acid (CHA); and c) heptanoic acid (HA).

As described in chapter 3, the m-exp model was again used to calculate the half-life times ($t_{1/2}$) of adsorption, enabling us to compare the rates of uptake among different samples. According to the data presented in Table 4.2, there's a noticeable trend where the adsorption half-life times decrease as the activated carbons undergo more heat cycles. This trend aligns with the enhancements in mesoporosity detailed before, suggesting that more porous carbons adsorb naphthenic acids more quickly.

An interesting observation was made regarding the adsorption of HA, where the transition from the double-cycled petroleum coke activated carbon to the triple-cycled version didn't follow the expected pattern of reduced adsorption half times as strictly as other comparisons did. Nonetheless, the shift from the single-cycled to double-cycled AC revealed a significant drop in

the adsorption half time for heptanoic acid, underscoring a substantial improvement in adsorption speed after the first cycle of heat treatment.

It's important to highlight that despite these changes in adsorption rates and mesoporosity, the surface chemistry of the activated carbons appeared to remain stable across all heat treatments. X-ray photoelectron spectroscopy (XPS) analysis showed minimal variation in the carbon and oxygen components on the surface of these materials[87]. This observation suggests that the observed improvements in adsorption kinetics can be attributed primarily to the physical changes in the carbons' porosity rather than any chemical modifications.

These findings demonstrate the significant impact that increasing mesoporosity through repeated heat cycles has on enhancing the kinetics of adsorption. By widening existing micropores, the activated carbons can more rapidly capture and hold onto naphthenic acids, showcasing the pivotal role of physical structure in the adsorption process.

Ultimately, our study sheds light on the ways that modifying activated carbon, such as through pore enlargement, can enhance the removal of harmful naphthenic acids from wastewater. Understanding the equilibrium time and initial adsorption rates is essential for selecting and preparing the most suitable activated carbon for the purification of water from oil sands operations, ensuring the process is both safe and efficient.

Table 4.2. Adsorption half times for three model naphthenic acids of DPA, CHA and HA on surface of het-cycled ACs

DPA	**$T_{1/2}$ (min)**	**Adjusted R^2**	**Reduced X^2**
Single	20	0.9922	0.399
Double	8.4	0.9959	0.122
Single	6.6	0.9996	0.008

CHA	$T_{1/2}$ (min)	Adjusted R^2	Reduced X^2
Single	34.3	0.9761	0.292
Double	18.5	0.9984	0.034
Single	4.5	0.9946	0.108
HA	**$T_{1/2}$ (min)**	**Adjusted R^2**	**Reduced X^2**
Single	51.4	0.9915	0.184
Double	8.7	0.9941	0.116
Single	12	0.9956	0.109

4.3.2 Adsorption study of Model Compounds and Their Characterization by FT-ICR-MS

In our research, a synthetic mixture comprising seven individual naphthenic acid (NA) compounds specifically CHA, 1,4-CHA, SA, DPA, DHA, PCA and ACA. Many of these compounds were previously examined in Chapter 3, with the addition of a new compounds introduced in this chapter to expand our study, . As previously described, samples were formulated by dissolving 10 ppm of each compound into a buffered solution, followed by a thorough mixing process that lasted 24 hours to ensure uniform distribution of the compounds. Subsequently, we introduced 0.1 grams of AC, both single-cycled and triple-cycled varieties, into 100 milliliters of this NA mixture. The solution was then agitated on a shaker table for an additional 24 hours to facilitate the adsorption process, with each sample being prepared in triplicate to ensure the reliability of our results.

To quantitatively assess the effectiveness of the adsorption process in reducing the concentration of these NA compounds in the solution, we employed FT-ICR-MS. This allowed us to precisely characterize the composition of the residual mixture post-adsorption. Through this

approach, the goal was to obtain a clear visual representation of the changes in NA concentrations, providing concrete evidence of the capability of AC, in both its single and triple-cycled forms, to purify water solutions by adsorbing naphthenic acid compounds before undertaking more complex mixtures like OSPW which will be discussed in the next chapter.

Figure 4.3 presents a comprehensive analysis of seven FT-ICR-MS mass spectra showcasing the effects of single and triple-cycled activated carbons on the adsorption of seven model naphthenic acids in a buffered synthesized solution. To facilitate accurate comparisons of adsorption efficiency across different activated carbons and among various compounds, the signal intensities were adjusted using an internal standard as a reference point. This normalization ensures that the observed reductions are directly attributable to the adsorptive actions of the activated carbons, highlighting their effectiveness in removing compounds from the solution.

Across all spectra, a notable reduction in the relative response is observed, with single-cycled ACs followed by even greater decreases with triple-cycled ACs. This pattern highlights the efficacy of the AC treatment in reducing the presence of NAs in the solution. What stands out from our analysis is the consistency in the behavior of the NAs between this synthesized mixture and the individual adsorption results detailed in Chapters 3 and 4 which showcases that adsorption pattern of each NA on heat cycled ACs remain remarkably similar. Particularly, DPA and DHA, identified as the most hydrophobic NAs among those tested, exhibit significant signal reductions in the spectra. Figure 4.3(a) and (b) present the mass spectral analysis of DPA and DHA after treatment of OSPW with both single and triple-cycled activated carbons. The results indicate a significant adsorption efficiency, with DPA showing 86% removal using single-cycled

AC and a remarkable increase to 98% with triple-cycled AC This observation underscores their strong interaction with the ACs and their propensity to be efficiently adsorbed.

Conversely, SA and 1,4-CHA demonstrate the lowest affinity towards the AC surfaces, mirroring findings from previous chapters. Figures 4.3(c) and (d) focus on SA and 1,4-CHA, both of which exhibit minimal adsorption below 10% for both types of ACs. This minimal adsorption underscores their low attraction to AC surfaces, likely due to their more water-friendly (hydrophilic) characteristics, which hinders their ability to leave the aqueous phase and adhere to the hydrophobic surfaces of the ACs. Further analysis in Figures 4.3(e) and (f) showcase the adsorption rates for two polycyclic aromatic compounds, ACA and PCA and, with ACA achieving 81% adsorption with single-cycled AC and 98% with triple-cycled AC, and PCA showing 78% adsorption with single-cycled and a notable increase to 97% with triple-cycled AC. The high adsorption rates of these compounds can be attributed to their hydrophobic nature and structural aromaticity, which enhances their affinity for the similarly hydrophobic surfaces of AC. This observation highlights the critical role of hydrophobic interactions in the adsorption process, especially for compounds with polycyclic aromatic structures.

Figure 4.3 not only validates the consistency of NA adsorption behaviors across different experimental setups but also emphasizes the role of molecular characteristics such as hydrophobicity in determining adsorption efficiency. By comparing these patterns to earlier findings (although kinetics study has not been done yet on these NAs and these findings are only based on adsorption experiments at equilibrium), this figure enriches our understanding of how specific NA properties and the type of AC treatment influence adsorption processes, promising insights into future works on optimizing the use of activated carbon in water treatment applications.

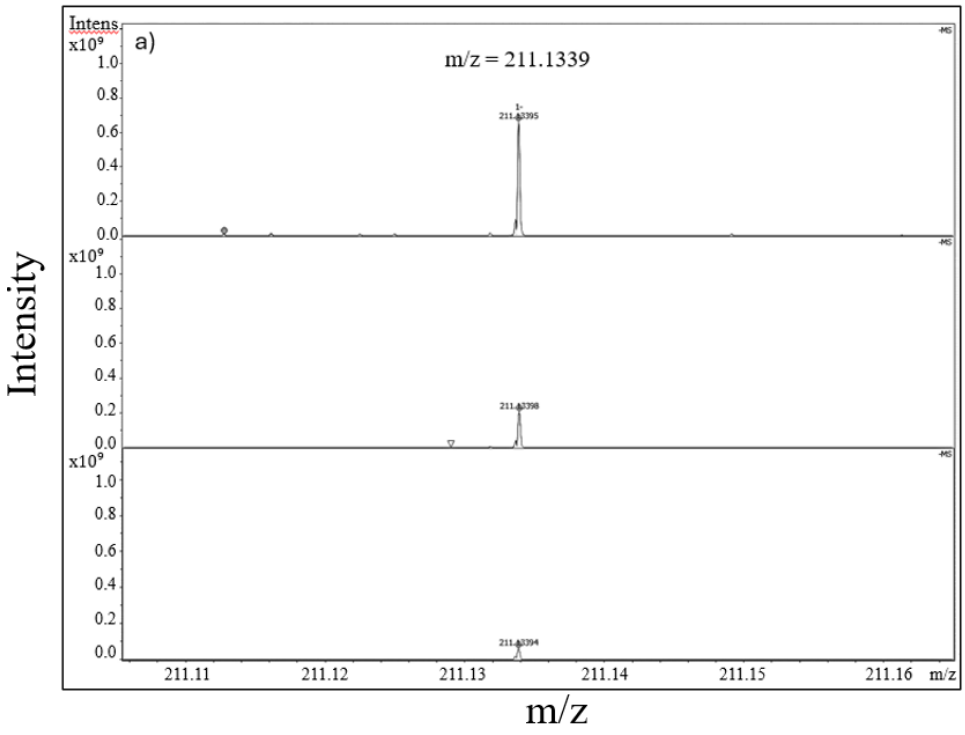
Intens.
x10^9
a)
m/z = 211.1339
1.0
0.8
0.6
0.4
0.2
0.0
211.11
211.12
211.13
211.14
211.15
211.16
m/z
Intensity
m/z

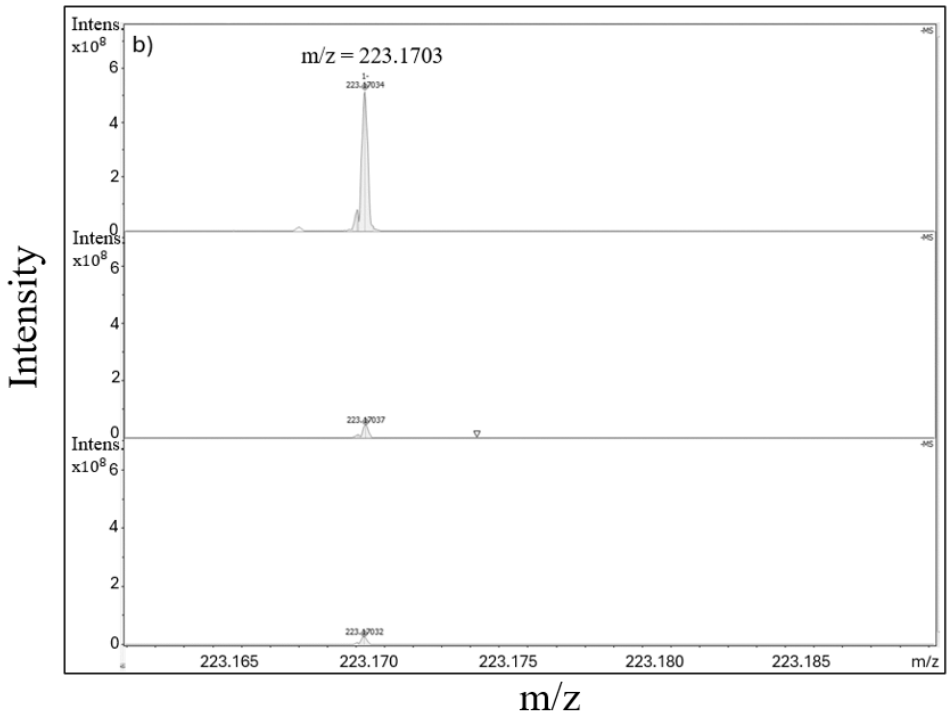
Intens.
x10^8
b)
m/z = 223.1703
6
4
2
0
223.165
223.170
223.175
223.180
223.185
m/z
Intensity
m/z

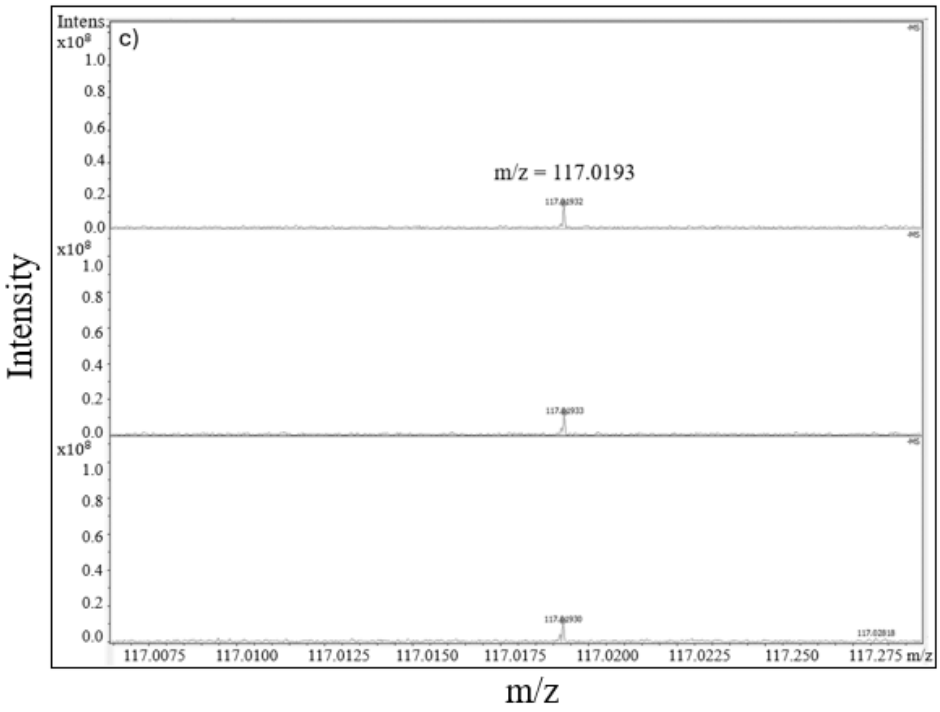
c)
m/z = 117.0193
Intens
x10^8
1.0
0.8
0.6
0.4
0.2
0.0
117.0075
117.0100
117.0125
117.0150
117.0175
117.0200
117.0225
117.250
117.275 m/z
Intensity
m/z

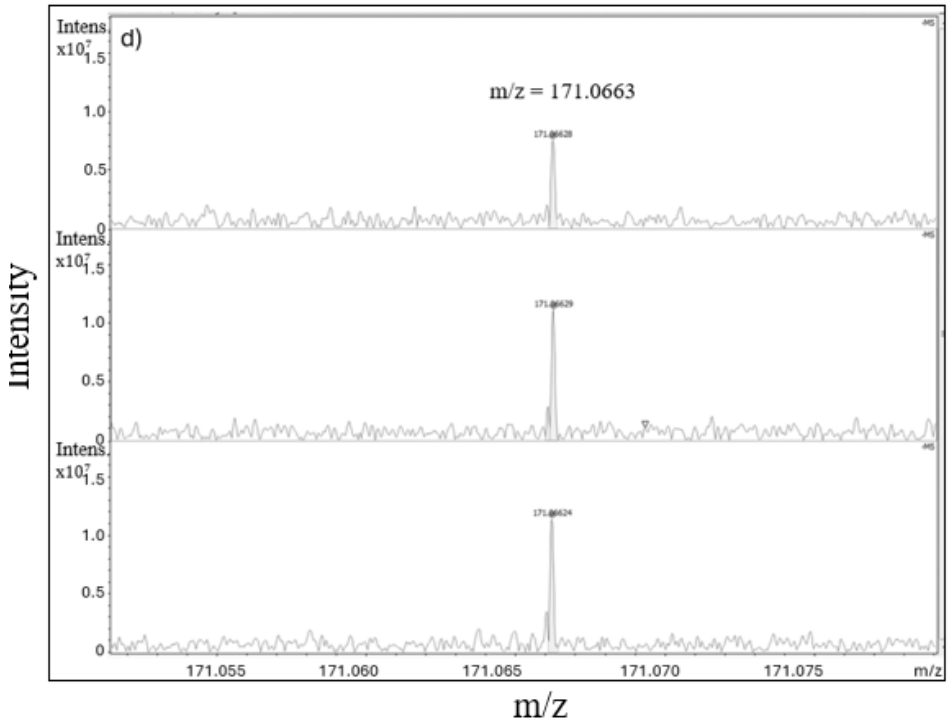
d)
m/z = 171.0663
Intens
x10^7
1.5
1.0
0.5
0
171.055
171.060
171.065
171.070
171.075
m/z
Intensity
m/z

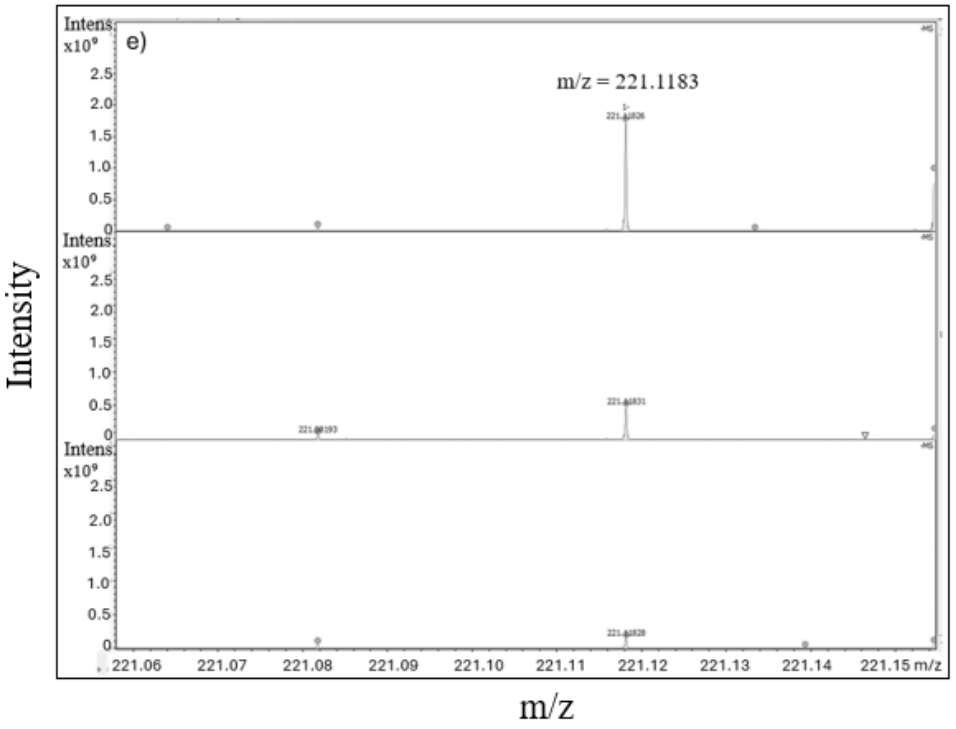

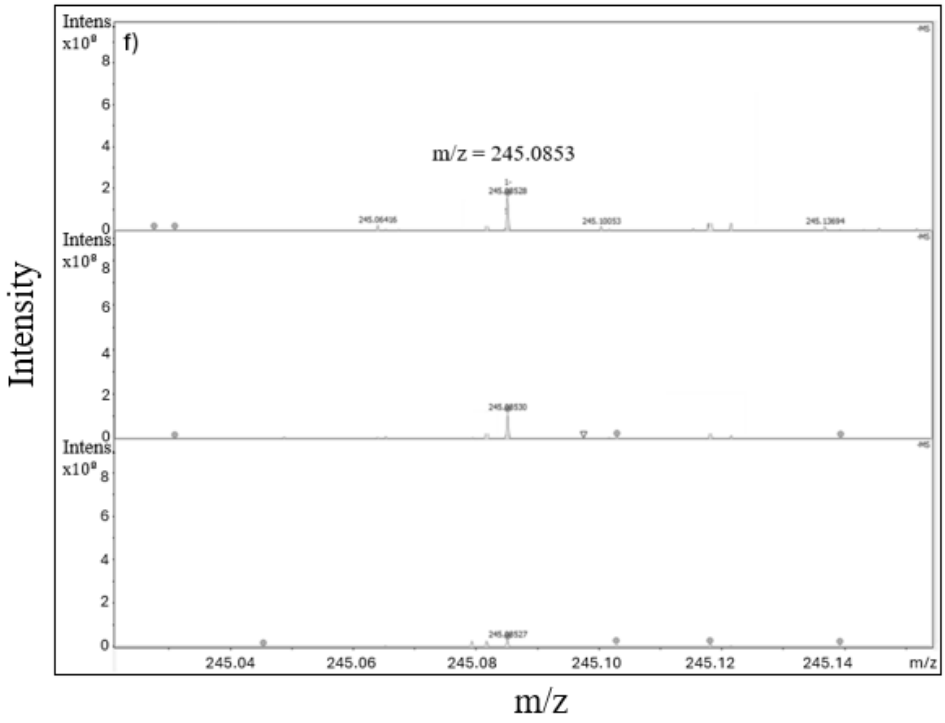

Figure 4.3. Mass spectral analysis of a) DPA, b) DHA, c) SA, d) 1,4-CHA, e) ACA, and f) PCA compounds treated with single and triple-cycled ACs.

4.4 Conclusion

In summary, our investigation into the adsorption behavior of naphthenic acids on heat-treated activated carbons has provided valuable insights for improving activated carbon's effectiveness in environmental cleanup. By using the m-exp model to evaluate adsorption half-life times, a consistent pattern was identified where increased heat treatment enhances mesoporosity, thereby accelerating adsorption rates, particularly noted with heptanoic acid. Despite these structural changes, the surface chemistry of the carbons remained stable, suggesting that the faster adsorption is mainly due to physical rather than chemical alterations. This advancement underscores the potential of optimizing activated carbon through heat treatment to boost its performance in removing naphthenic acids from Oil Sands Processed Water (OSPW), marking a significant step forward in the development of more efficient water treatment solutions. These insights, in line with prior studies, validate our approach and provide valuable guidance for optimizing the use of AC in treating NA-contaminated water.

Chapter 5 - Removal of Naphthenic Acids from OSPW Using Pore-Widened Activated Carbons: An FT-ICR-MS Study

The work in this chapter has been published as Elmira Nazari, Jacob L.A. Bothen, Greg F. Slater, Paul R. Pede, Andrew J. Vreugdenhil with the title of: "Removal of Naphthenic Acids from OSPW Using Pore-Widened Activated Carbons: An FT-ICR-MS Study", in the journal of Energy and Fuels.

5.1 Introduction

In Canada, the oil sands resources represent one of the world's largest crude oil reserves, located primarily in Alberta. The extraction of crude oil from oil sands generates substantial quantities of oil sands process water (OSPW) and tailings, which must be managed according to a zero-discharge policy. OSPW contains various organic and inorganic contaminants, with naphthenic acids being recognized as the primary organic environmental contaminants. These acids, along with other Naphthenic Acid Fraction Compounds (NAFCs), are challenging to degrade and can have toxic effects on aquatic organisms and infrastructure.

Given the complexity of OSPW, various treatment methods have been explored to remove NAFCs, including adsorption techniques using activated carbons. This study specifically investigates the effectiveness of heat-cycled activated carbons in removing NAFCs from OSPW. The activated carbon was produced from petroleum coke, activated with KOH under inert conditions to enhance mesoporosity and adsorption capabilities.

Recent advancements in analytical methodologies, such as ultrahigh-resolution mass spectrometry combined with electrospray ionization (ESI) and Fourier transform ion cyclotron

resonance mass spectrometry (FT-ICR-MS), have improved the characterization of NAFCs in OSPW. However, there is a lack of studies focusing on the FT-ICR-MS characterization of NAFC adsorption in activated carbon-treated OSPW.

The primary objective of this research is to evaluate the efficacy of heat-cycled activated carbons in removing various classes of NAFCs from OSPW, using FT-ICR-MS to profile the polar organic substances that remain after treatment. This study aims to compare different activated carbon types and identify which characteristics are most effective for the remediation of OSPW.

5.2 Material and Methods:

5.2.1 Chemical and reagents

OSPW was received from Alberta's oil sands Suncor Energy Pond. HPLC grade methanol (99%, CAS number: 67-56-1), toluene (99%, CAS number: 108-88-3), dichloromethane (99%, CAS number: 75-09-2), 28% ammonium hydroxide solution (CAS number: 1336-21-6), hydrochloric acid (CAS number: 7647-01-0) and dioctylsodium sulfosuccinate as an internal standard (CAS number: 577-11-7) were purchased from Sigma-Aldrich (St. Louis, MO).

5.2.2 Activation of petroleum coke with KOH and subsequent cycling experiments

KOH petroleum coke activated carbon and Heat-cycled KOH petroleum coke activated carbon was prepared as described in chapter 2.3.1 and 2.3.2 respectively. The surface properties of single-cycled and triple-cycled PWAC are presented in Table 5.1. The most significant change being the increase of 29.6% in the percent mesoporosity of the triple-cycled AC relative to the single-cycled AC.

Table 5.1. Surface properties of single and triple cycled PWACs

AC Type	Surface Area (m^2/g)	Total Pore Volume (cm^3/g)	Mesoporosity (%)	Point of Zero Charge (PZC)
Single-cycled	1382 ±49	0.557	26.4 ± 0.6	7.8
Triple-cycled	1289 ± 28	0.593	56.0 ± 2.3	7.8

5.2.3 Adsorption test: TOC

The adsorption study was carried out in plastic cups. 100 ml of the OSPW was contacted with 100 mg ± 0.5 mg of single or triple cycled PWAC for 24 hours. Samples were continuously agitated on a shaker table at 200 rpm and filtered into TOC sample vials using 0.45 μm syringe filters to determine residual NA carbon content via a Shimadzu TOC VCPH analyzer using Non Purgeable Organic Content (NPOC) analysis.

5.2.4 Liquid-Liquid Extraction of Naphthenic Acids

The NAFC extraction procedure from OSPW employed in this research is a minor modification of that described by Grewer et al [30]. In summary, following the adsorption tests described in previous section, 20 mL of each water sample were filtered through disposable 0.45 µm syringe filters. The pH of the solution was adjusted to 2 by incrementally adding concentrated HCl. Subsequently, the prepared samples were transferred to 250 mL separatory funnels for the liquid-liquid extraction procedure. The organic layer was allowed to settle for 5 minutes, followed by subjecting the samples to four washes with 5 mL of dichloromethane each (4 x 5 mL). After collecting the organic phase and transferring it into 25 mL glass jars, these extracts underwent evaporation in a hot water bath under gentle blowing of N2 until dry. Finally, the dry samples were reconstituted in a 10 mL organic solution consisting of a 3:1 ratio of

methanol to toluene. After mixing the stock solvent solutions for 3 minutes, a 0.5 mL portion from the pre-treated OSPW stock solution was diluted to a final volume of 10 mL using the 3:1 MeOH:Tol stock to reduce the NA concentration. In contrast, extracts from post-treated OSPW with ACs were left undiluted. Trace contamination was mitigated using a rigorous glassware cleaning protocol which involved immersing all glassware in acidified water for 24 hours, rinsing them with organic solvents, and ultimately placing them in a muffle furnace at 500 °C for 24 hours (Ruddy et al. 2018). Dioctylsodium sulfosuccinate was added to the samples as an internal standard

prior to each run due to its chemical stability, noninterference with the analytes of interest, providing a well-defined peak in the mass spectrum and its ionization efficiency for normalizing and quantifying NAFCs in OSPW.

5.2.5 Point of zero charge (PZC)

The method of pH drift was employed for measuring the PZC for every type of activated carbon[77]. In summary, this procedure entailed precise adjustments of consistent volumes of a 0.01 M NaCl solution to achieve pH levels ranging from 2 to 12, using either diluted NaOH or HCl. Following this, activated carbon was introduced into the solution and allowed to mix for 24 hours. The pH values were recorded both before and after the addition of activated carbon, enabling the estimation of the PZC.

5.2.6 Characterization techniques

5.2.6.1 Brunauer-Emmet-Teller (BET) surface area analysis

Surface area and pore size analysis were conducted using a Tristar II plus instrument. The samples underwent N_2 adsorption at 77 K, with 104 data points recorded for adsorption within

the range of 0.0065 p/p^0 to 0.995 p/p^0, and 52 data points recorded for desorption within the range of 0.995 p/p^0 to 0.104 p/p^0. All reported surface areas were determined using the BET surface area analysis, and pore size distributions were determined using Density Functional Theory (DFT) with slit geometry modeling 2D-NLDFT for N_2 adsorption in carbon finite pores [87].

5.2.6.2 Fourier Transform Ion Cyclotron Resonance Mass Spectrometer (FT-ICR-MS)

Before analysis, 20 µL of concentrated ammonium hydroxide solution and 20 µL of an internal standard was added to each sample vial to enhance ionization and deprotonation. All sample were analysed using a 7T Fourier Transform Ion Cyclotron Resonance Mass Spectrometer (SolariX XR, Bruker, Billerica, MA, USA). A 250 µL Hamilton syringe and the Apollo II ion funnel electrospray source were used for the whole instrument run at 180 µL per hour. The instrument was operated in negative-ion mode. ESI spray voltage was ± 4.5 kV with an end plate offset of -1 kV. The instrument was external calibrated at the beginning of each day using a 0.01 mg/L sodium trifluoroacetate (NaTFA) solution. Spectral size maximum was 8 million with mass resolutions of 450,000, 310,000, and 200,000 achieved at m/z values of 250, 400, and 600, respectively. The m/z values (for singly charged ions) of 100-600 with relative abundance greater than six times the standard deviation of the baseline noise was exported to a spreadsheet. For samples a total of 200 scans were accumulated, while process blanks underwent 80 to100 scans. To ensure accurate and consistent measurements, the ion accumulation time within the linear hexapole was adjusted in the range of 0.04 to 0.08 seconds for NAFC samples in ESI negative mode, aiming to achieve an optimal total ion count (TIC) of $1x10^9$ ions. For blank samples, the ion accumulation time was set to 0.5 seconds. Typical conditions for negative ionization were a dry gas temperature set at 200 °C with a flow rate of

4.0 L/min, and nitrogen utilized as the nebulizer gas at a pressure of 1.00 bar. In order to clean the tubing between sample runs, a cleaning process was used as follows: cleaning the syringe 5 times, flushing the tubing and the capillary with isopropyl alcohol, methanol and Type 1 ASTM water, and finally, the syringe was primed for the next solvent system with several rinses. All samples were run in triplicate and no significant difference was observed in the FT-ICR-MS data.

5.2.6.3 Data Processing

After conducting ESI (-) FT-ICR-MS measurements, the mass spectra were subsequently transferred to Data Analysis Software (Bruker Daltonics version 5.0) for the purpose of processing and elemental formula assignment. The signal-to-noise (S/N) ratio was set at 6 or higher when establishing the working mass list for utilization in the SmartFormula™ molecular assignment function. The settings for running SmartFormula™ in ESI(-) mode were as follows: The number of formulae per m/z = 1, charge = -1, ppm error threshold = ±1 ppm, only molecular ions of [M -H]- were taken into consideration, the number of carbons ranged from 0 to 100, the number of hydrogens ranged from 0 to 200, the number of oxygens ranged from 0 to 20, the number of nitrogen's ranged from 0 to 1, and the number of sulfurs ranged from 0 to 3. During the analysis in ESI (-) mode, it became evident that SmartFormula™ failed to detect several peaks that met the criteria described earlier. Consequently, we concluded that a comprehensive and precise interpretation of the data required manual selection of chemical formulas using the same criteria. The manually processed data was exported and typically plotted in a Van Krevelen plot. The raw data was analyzed using separate Excel sheets and Python code, which allowed us to identify all classes and species of NAFCs present in OSPW.

5.3 Results and Discussion

The aim of this study was to provide a quantitative measure of the overall reduction in NAFC portion of OSPW using TOC analysis, with complementary results of ultrahigh-resolution negative-ion electrospray ionization FT-ICR-MS measurements for detailed analysis of the NAFC class specific adsorption. The following results assess the efficiency of single and triple thermal cycled ACs in sequestering NAFCs and a qualitative breakdown of which specific NAFC species and molecular moieties were removed.

In their study, Headley et al. demonstrated that NAFCs in OSPW possess higher molecular weights compared to other sources such as technical mixtures (Fluka)[53]. Table 5.2 provides a summary of percentage of NAFC adsorption for each AC calculated with TOC analysis and the total number of species detected in OSPW before and after treatment with single and triple-cycled AC. With an increase in activation cycles, there is a notable decline in both the number of unique molecular formula's detected, as well as their total intensities as normalized to the signal of the internal standard. Despite a reduction in the surface area of the triple-cycled activated carbon (AC), as indicated in Table 1, this AC demonstrates effective removal of NAFCs (Table 5.2). This underscores the diminished significance of surface area in the adsorption of NAFCs and highlights the importance of AC properties such as surface functionality and pore size distribution for the adsorption of naphthenic acids from OSPW using these thermally cycled ACs[63,87]. As is evident from the adsorption percentages observed for each AC in Table 5.2, the number of detected peaks and the total intensities, the triple-cycled AC, distinguished by higher mesoporosity and a more hydrophobic surface compared to the single-cycled AC, facilitates better adsorption of non-polar naphthenic acid compounds onto its surface. XPS analysis of samples subjected to single and triple-cycled revealed nearly identical oxygen and carbon speciation, with

only minor reductions in C–OH and C–O–C bonding. This indicates that the surface chemistry remained largely unchanged, suggesting that any variations in adsorption are likely due to changes in surface morphology. The overall oxygen peak shape remained unchanged with a decrease in atomic % oxygen over successive cycles.

Table 5.2. Summary of NA concentration, # of assigned formulas, mass accuracy and total intensities in pre-treated OSPW and OSPW treated with single and triple cycled AC.

Sample	Adsorption using TOC (%)	# of Formula's Assigned	Mass Accuracy ($x10^{-5}$)	Total relative Intensities of Assigned Formulas
Pre-treated OSPW		1876	6.7	18367
OSPW treated with Single-cycled AC	33 ± 1.7	1254	7	526
OSPW treated with triple-cycled AC	71 ± 2.3	576	9	72

Figure 5.1 displays a typical plot demonstrating the mass accuracy and high resolution of the components obtained by FT-ICR-MS. All the species illustrated in Figure 5.1, each featuring ions at the nominal m/z of 299 for the pre-treated OSPW, lack classical monocarboxylic naphthenic acid characteristics as indicated by their elemental compositions which substantiates that OSPW encompasses various classes of NAFCs, aligning well with existing literature on the subject. This underscores the value of achieving high m/z resolution when determining the elemental compositions of the organic compounds linked to oil sands deposits and production[90]. Additionally, it is evident that four distinct peaks are separated with a resolution of 18 Da, revealing various components, including sulfur-containing and oxidized compounds, within the complex mixture. The elemental compositions for all species identified throughout this paper have been incorporated with a high degree of precision using FT-ICR-MS to generate the profiles depicted in the subsequent figures.

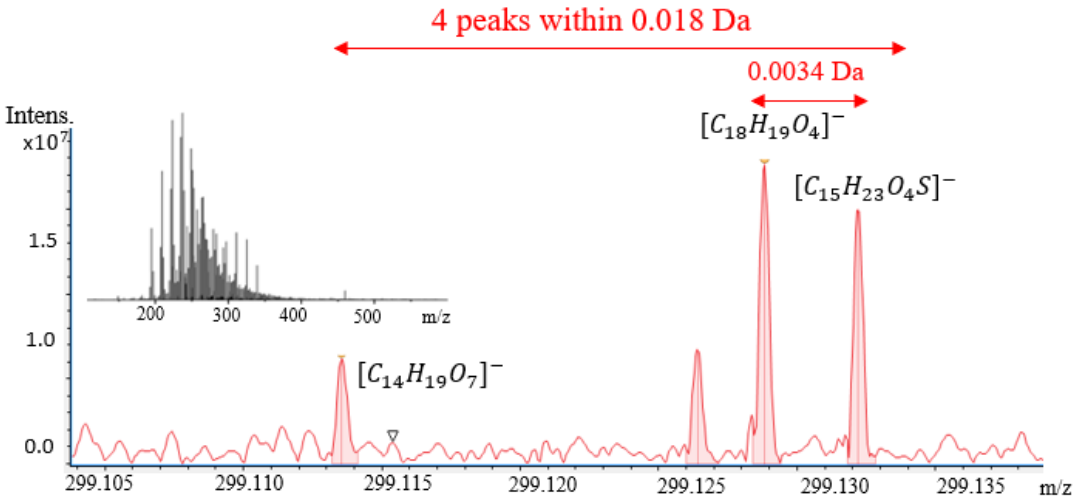

Figure 5.1. An illustration of ultrahigh resolving power is evident in the detection of four distinct peaks within a 018 Da range in a negative-ion ESI FT-ICR mass spectrum acquired for an acid-extracted OSPW sample. This data was obtained using magnitude mode.

For a more in-depth exploration of variations in the distribution of NA species between treated and untreated samples, three broad range FT-ICR mass spectra were acquired for compounds within the mass-to-charge ratio (m/z) range of 100 to 600 where n = 3 to 40 and Z = 0 to -12 as illustrated in Figure 5.2. A vast majority of the NAFC compounds (more than 90%) are in the mass range of 180-350 m/z. These spectra were examined to identify and characterize the NAFCs present in the extracts of the OSPW, both before and after treatment with single or triple cycled ACs.

As a demonstration of the capability of FT-ICR to track the fate of one species, $C_{14}H_{21}O_2$, Figure 5.2 vividly illustrates the changes in the distribution of NA compounds as a result of employing AC for adsorption and more importantly the effect of thermal cycling on the efficacy of the PWAC adsorption. It also highlights the trend in the diminishing sum of relative peak

intensities as the PWAC activation cycle is increased. The range of NAFCs distribution and the range of species observed are in a good agreement with other works[50,91]. The ion with a nominal m/z of 237 (known as oxygenated NA with highly nonpolar characteristic) serves as one clear example of FT-ICR-MS capability and a confirmation of the effectiveness of AC in eliminating NA compounds, as it illustrates a reduction in peak relative intensity when OSPW is treated with PWAC. This specific compound was selected due to its high intensity within the spectra of the untreated sample and the fact that it is highly nonpolar. Single-cycled and triple-cycled AC treatments achieved nearly 80% and 99% removal of this compound respectively.

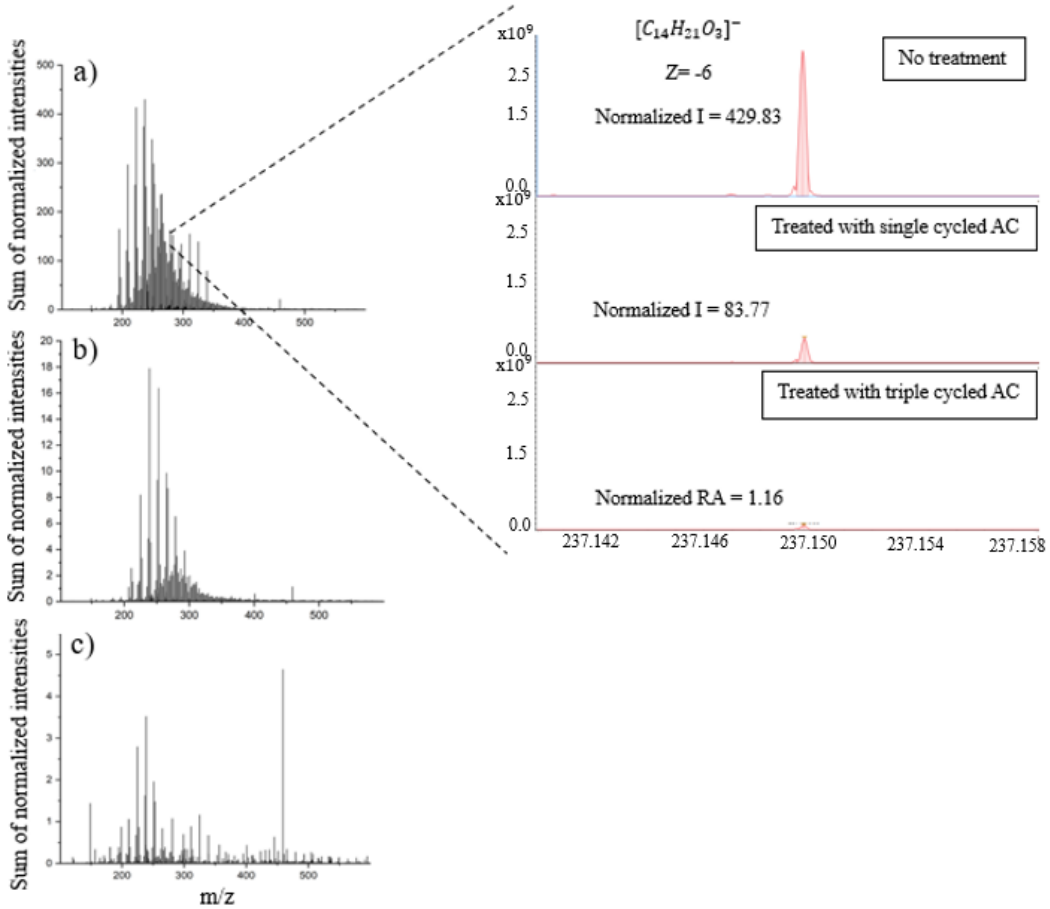

Figure 5.2. Broadband mass spectra for NA extracts of: a) non-treated OSPW; b) OSPW treated with single cycled AC; and c) OSPW treated with triple cycled AC acquired in negative mode by FT-ICR mass spectrometer.

Figure 5.3 shows that untreated OSPW contains diverse heteroatom-containing compounds, and that the classical naphthenic acids (i.e., O2) are just one of many classes encountered in OSPW[91,92]. Predominant compounds in OSPW NAFCs extracts are O_x and O_xS_y species (where x = 1 to 10 and y = 1 to 3), which could be acidic functional groups such as carboxylic acids in addition with other oxygen and sulfur functional groups. These acidic groups tend to be selectively ionized by ESI (-) and leads to the inhibition of the detection of nitrogen-containing compounds with relatively weaker acidity. Additionally, it cannot be ruled out that nitrogen containing NAFCs might be present in substantially lower concentrations within the processed water samples employed in this research[93]. The classes of O_2, O_3, and O_4 displayed the highest relative intensities, as determined based on the intensity relative to the intensity of the internal standard. Within the major NAFC classes in Figure 5.3, each class contained between 100 to 200 individual compounds over a diverse range of C# and Double bond equivalence (DBE).

As illustrated in Figure 5.3, all heteroatom classes showed a noticeable decrease in the sum of their normalized abundances, with almost a complete removal of O_2S_2, O_3S_2 and O_2S for the sample treated with triple-cycled PWAC. Based on TOC values of overall 33% adsorption with single-cycled PWAC and 71% adsorption with triple-cycled PWAC, the O_3 species which has the highest sum of normalized intensities among other classes, reduced by 19% using single-cycled and by 61% using triple-cycled PWAC. Likewise, O_2, O_4, O_5, O_3S compound classes were decreased by 19%, 17%, 12%, 20% with single-cycled PWAC and 53%, 60%, 54% and 62% with triple-cycled PWAC respectively. This clearly demonstrates the effectiveness of using pore

widened activated carbons obtained via thermal cycling for the removal of NAFCs from OSPW. Note that distinct sulfur-containing compounds, including O_2S_2, O_3S_2, and O_2S, were extensively removed. The utilization of pore-widened activated carbons proved to be especially efficient in eliminating sulfur heteroatoms from NAFC extracts of OSPW.

Certain NAFC components exhibit resistance to adsorption. Notably, this includes a few residual components of the O_4 and O_3 classes. As noted above, the N containing classes are challenging to detect either because of their reduced ionization or possibly because of their reduced abundance, however we can still identify NO_3-NO_5 (as well as O_6-O_{10} species) which exhibited significant changes when exposed to activated carbon (AC), likely because of their higher polarity, preventing effective adsorption onto the hydrophobic surface of AC. Similarly, O_2-O_4 and SO_2-SO_4 compounds, being less oxygenated and less polar, make AC sorption more effective, establishing it as a beneficial treatment strategy for these substances.

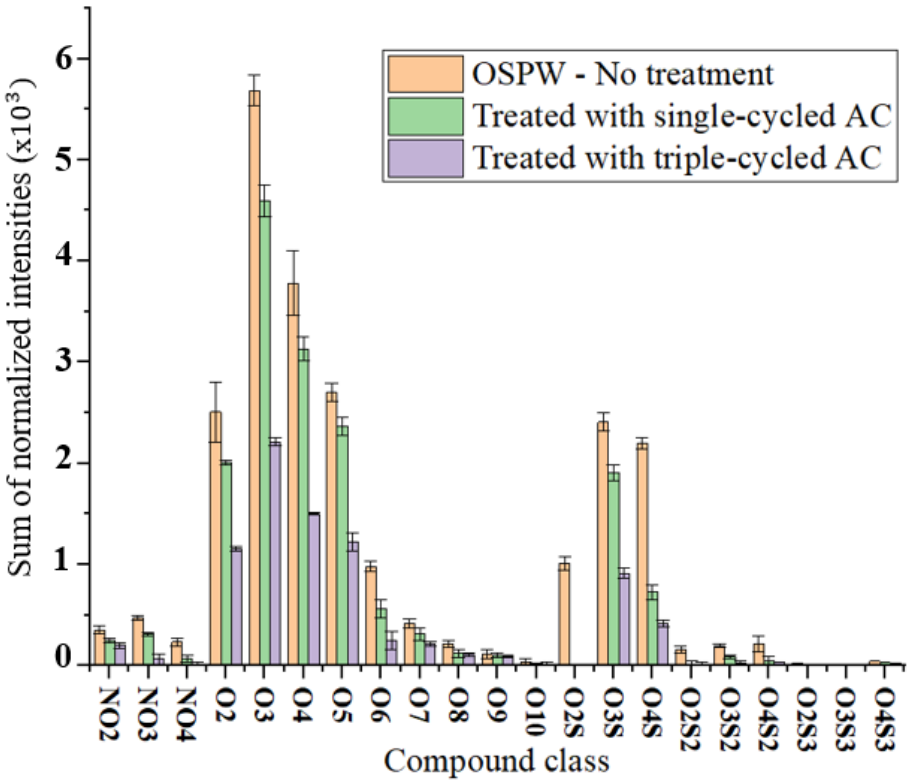

Figure 5.3. Negative ion ESI-FT-ICR-MS heteroatom class distribution for OSPW, treated OSPW with single-cycled AC and triple-cycled AC. the relative standard deviation based on triplicate run of the same sample was less than 10% of the measured values.

Isoabundance plots, which display the distribution of double-bond equivalents (DBEs, representing the sum of rings and double bonds to carbon) with color-coded contours against carbon number, offer a quick and effective means to visually explore the compositional diversity within a specific heteroatom class [50,94]. As shown in Figure 5.4, a plot of DBE vs. C number of O_2, O_3, O_4, O_2S and O_3S classes are given for OSPW and treated OSPW with single or triple cycled PWAC. Panels a-e in Figure 5.4 illustrate a decrease in DBE values for both O_x and O_xS species after being subjected to AC treatments. O_2 compounds, as depicted in Figure 5.4(a) which are commonly referred to as classical NAFCs ($C_nH_{2n+z}O_2$), exhibit a DBE range of 1-12 and carbon numbers spanning from 10 to 40. In untreated samples, the most prominent peaks are

found within the DBE range of 2-7. It is important to note that the carbon number range remains consistent across all classes. By introducing a single cycled AC treatment, it becomes apparent that the majority of the NA compounds have extensively removed, and the most abundant intensities are concentrated within the range of 6-7 (Z= -10 and Z= -12). When treating OSPW with triple cycled AC, the DBE values narrow down even further, with a reduction to just 4 (Z= -6). The utilization of a triple-cycled PWAC treatment proved to be highly efficient in eliminating more complex and larger NA compounds, resulting in a reduction of the carbon number range from 10-20 following the treatment.

Figure 5.4(b) shows that in the untreated OSPW, O_3 compounds exhibit a range of DBE values from 1 to 12, with the highest concentration observed at DBE values of 3 to 7. Following the treatment of OSPW with a single cycled AC, the DBE values decreased by approximately 1 unit. Moreover, with the introduction of a triple cycled AC, the predominant compounds are now centered around a DBE value of 3 which primarily correspond to tricyclic compounds or other compounds with the same DBE value. As depicted in Figure 5.4(c), the DBE values for the O_4 class range from 2 to 12, and the carbon number range remains consistent at 10-40 across the sample set. In the untreated sample, the most prevalent compounds are found within a DBE range of 4-8 (with Z values ranging from -6 to -14). When a single cycle of AC treatment is applied, this range narrows down to DBE values of 6-7. The total number of NA compounds and their concentrations have noticeably decreased, but larger compounds still persist in the sample.

For triple cycled AC treatment, Figure 5.4(c) shows that the most prominent compounds have a DBE value of between 2 and 4 (with Z values ranging from -2 to -6). This is consistent with an adsorption by the triple AC of species with higher DBE values leaving relatively small concentrations of low-aromatic, dicarboxylic acids. These O_4 compounds consist of two

carboxylic acids in their structure, making them highly polar. The triple cycle of AC treatment has demonstrated its ability to remove even polar compounds and adsorb them onto the surface of the AC.

As shown in Figure 5.4(d), the concentration of a few O_2S compounds decreased when exposed to the single-cycled PWAC and were extensively removed after exposure to the triple-cycled PWAC. This is possibly due to their hydrophobicity and resulting high affinity for the AC surface particularly the triple cycled AC with its increase in pore size and hydrophobicity. Note that these species exhibited features consistent with those of thiophenic compounds[91].

In Figure 5.4(e), the presence of O_3S compounds is observed, and these are recognized as petroleum sulfonates commonly utilized as emulsifiers in the bitumen recovery process[95]. Following a single cycle of AC treatment, some of the O_3S species are removed from the untreated OSPW. While the range of DBE values for the most abundant compounds remains unchanged, the addition of a triple-cycled PWAC treatment leads to a significant reduction in their intensities and DBE values as demonstrated by absence of highly concentrated peaks within the carbon number range of 10- 40. The plots displaying DBE versus carbon number clearly indicate that the concentration of compounds in the untreated sample decreases when subjected to the single-cycled PWAC treatment. The triple-cycled PWAC treatment proves even more effective in removing the larger compounds present in the original sample likely due to a greater proportion of mesoporosity and increased surface hydrophobicity, resulting in the enhanced adsorption of nonpolar compounds onto the surface.

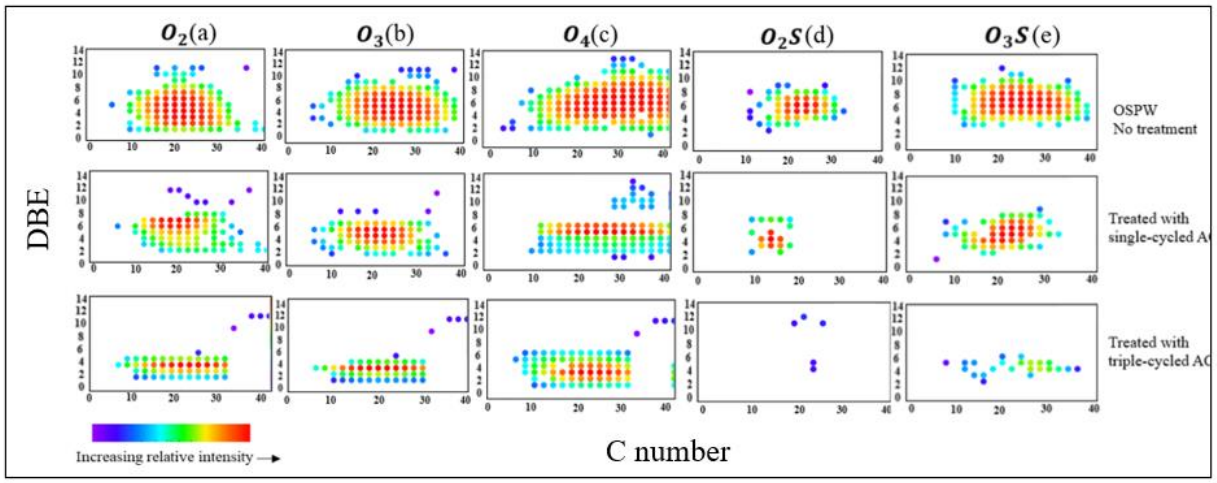

Figure 5.4. Comparison of OSPW treated with single and triple cycled ACs with non-treated OSPW for the 5 most abundant NAFC classes as follows: a) O2; b) O3; c) O4; d) O2S and e) O3S in Negative-ion ESI-FT-ICR-MS analysis.

5.4 Conclusion

In summary, the efficacy of single- and triple-cycled activated carbons in eliminating naphthenic acid components from complex mixtures, such as oil sands process-affected water (OSPW) assessing with TOC analyzer was investigated to determine the overall adsorption extent of NAs and utilizing FT-ICR-MS for thorough characterization of residual naphthenic acid from OSPW. By comparing TOC reduction percentages with changes in the FT-ICR-MS spectra, the effectiveness and selectivity of ACs in adsorbing NAs from OSPW is determined. before and after treatment.

Within the negative mode ionization, oxygenated NAFCs, specifically O_x and O_xS_y, dominated in terms of the sum of normalized intensities. DBE vs. C number plots displayed an enhanced removal of NAFCs over a large range of abundant DBE values following treatment with a single-cycled and triple-cycled PWAC. However, the greatest reduction of individual compounds was evident after employing a triple-cycled PWAC. This emphasizes the importance

of enlarging pore sizes for increased mesoporosity and highlights the role of surface functionality in activated carbons, even at the cost of lower specific surface areas. Furthermore, it is noteworthy that the O_2S and O_2S_2 classes of NAFCs were eliminated from OSPW after undergoing treatment with triple-cycled AC. Using FT-ICR-MS analysis and normalizing intensities to the intensity of the internal standard, we were able to show the differences in relative abundances and characterization of NAFCs which is essential to identifying treatment strategies of recalcitrant oil sands contaminants.

Chapter 6 – Conclusion

6.1 General Conclusion

This thesis provides a comprehensive exploration of the adsorption behavior of naphthenic acids (NAs) on various activated carbons (ACs), with a focus on optimizing the removal of these persistent organic contaminants from oil sands process-affected water (OSPW). Through a series of systematic investigations, the study has elucidated key factors influencing adsorption efficiency, including the physicochemical properties of both the adsorbent and the adsorbate, the role of surface functionalities, and the effects of structural modifications on adsorption dynamics.

The research highlights the diverse adsorption affinities of different naphthenic acid species to activated carbons, revealing critical insights for identifying NAs that are resistant to adsorption. The significance of physicochemical properties, particularly hydrophobicity, was found to be crucial in dictating adsorption efficiency, suggesting that physisorption is the dominant mechanism. The findings demonstrated that while hydrophobic surface interactions enhance adsorption, hydrogen bonding with surface oxygenated groups also plays a crucial role. This was particularly evident in the lower adsorption rates observed for NAs on heat-activated carbon (HAC) compared to other carbons, attributed to the presence of oxygenated species on the carbon surface. Future research should focus on enhancing surface functionalities to improve the adsorption of recalcitrant NA species, thereby optimizing ACs for environmental remediation.

Further investigation into the impact of heat treatment on the adsorption behavior of naphthenic acids revealed that increased heat treatment enhances mesoporosity and accelerates adsorption rates, particularly for heptanoic acid. By employing the m-exp model to evaluate adsorption half-life times, a consistent pattern emerged, indicating that the improved adsorption

performance was primarily due to physical modifications rather than chemical alterations. Despite these structural changes, the surface chemistry of the carbons remained stable, underscoring the potential of optimizing activated carbons through heat treatment to enhance their efficiency in removing naphthenic acids from OSPW. This represents a significant advancement in the development of more effective water treatment solutions.

The study also focuses on the efficacy of single and triple-cycled activated carbons in removing naphthenic acid components from complex mixtures such as OSPW. Utilizing total organic carbon (TOC) analysis and Fourier-transform ion cyclotron resonance mass spectrometry (FT-ICR-MS), the research assessed the overall adsorption extent and provided a detailed characterization of residual naphthenic acids. The results revealed that while both single-cycled and triple-cycled powdered activated carbons (PWACs) were effective in reducing TOC and removing NAFCs, the triple-cycled PWAC showed superior performance in eliminating a wider range of NAFCs, including the O_2S and O_2S_2 classes. This enhanced removal was attributed to the increased mesoporosity and optimized pore sizes, which facilitated greater adsorption efficiency despite a reduction in specific surface area. The use of FT-ICR-MS analysis, normalized to the internal standard, allowed for precise quantification of changes in the relative abundances of NAFCs, providing critical insights into the development of targeted treatment strategies for persistent oil sands contaminants.

Overall, this thesis demonstrates that the optimization of activated carbons for the removal of naphthenic acids from OSPW is a multifaceted challenge that requires a nuanced understanding of the interactions between adsorbent properties and adsorbate characteristics. The findings emphasize the importance of both structural and chemical modifications to activated carbons, suggesting that a combination of enhanced mesoporosity and tailored surface functionalities can

significantly improve adsorption performance. The research outcomes contribute valuable knowledge to the field of environmental remediation and offer practical guidance for developing more effective water treatment technologies to address the persistent issue of NA contamination in oil sands processed water. Future work should continue to explore novel approaches for enhancing the adsorption capabilities of ACs, particularly in targeting recalcitrant NA species, to further advance the sustainability and effectiveness of environmental cleanup efforts.

6.2 Future Work

- **Explore Advanced Surface Modifications**: Investigate the effects of different chemical treatments or functionalization techniques on the surface of activated carbons to enhance the adsorption of recalcitrant naphthenic acid species.
- **Optimize Pore Structure for Selective Adsorption**: Conduct studies on optimizing the pore size distribution and surface area of activated carbons to target specific naphthenic acid compounds, particularly those that are resistant to adsorption.
- **Evaluate Regeneration and Reusability of Activated Carbons:** Investigate the regeneration potential and reusability of single- and multi-cycled activated carbons to assess their long-term viability and cost-effectiveness for large-scale water treatment applications.
- **Study Adsorption Mechanisms in Realistic Environmental Conditions:** Perform experiments under varying environmental conditions (i.e. different pH levels, temperatures, and salinity) to better understand the adsorption mechanisms of naphthenic acids in natural waters.
- **Integrate Adsorption with Other Treatment Methods:** Research the integration of activated carbon adsorption with other water treatment technologies, such as advanced

oxidation processes or biological treatments, to enhance the overall removal efficiency of naphthenic acids and other contaminants.

- **Investigate Long-Term Environmental Impacts:** Conduct long-term studies on the environmental impacts of using activated carbons for naphthenic acid removal, including potential secondary pollution and the fate of adsorbed contaminants.

6.3 Contributions to Science

6.3.1 Publications

- A manuscript titled “Removal of Naphthenic Acids from OSPW Using Pore-Widened Activated Carbons: An FT-ICR-MS Study” has been published in the journal Energy & Fuels.
- Together with Oliver Strong and Dr. Tyler Roy, we have published the article “Transforming Micropores to Mesopores by Heat Cycling KOH Activated Petcoke for Improved Kinetics of Adsorption of Naphthenic Acids” in the journal Heliyon.
- In collaboration with Dr. Tyler Roy, another publication titled “The Effect of Adsorbent Textural and Functional Properties on Model Naphthenic Acid Adsorption” has been published in the journal of Environmental Sciences.

6.3.2 Conferences

- Presenting a poster at Inorganic Discussion Weekend at UOIT in November 2019.
- Oral presentation (virtual) at the Trent Graduate Student Symposium (TGSS) online in August 2021.
- Oral presentation (virtual) at Canadian Chemistry Conference and Exhibition (CCCE) in August 2021.

- Oral presentation at Conference of Metallurgists (COM2022) in August 2022.
- Oral presentation at Canadian Chemistry Conference and Exhibition (CCCE) in June 2023.

References

(1) Wu, C.; De Visscher, A.; Gates, I. D. On Naphthenic Acids Removal from Crude Oil and Oil Sands Process-Affected Water. *Fuel*. Elsevier Ltd October 1, 2019, pp 1229–1246. https://doi.org/10.1016/j.fuel.2019.05.091.

(2) Li, C.; Fu, L.; Stafford, J.; Belosevic, M.; Gamal El-Din, M. The Toxicity of Oil Sands Process-Affected Water (OSPW): A Critical Review. *Science of the Total Environment* **2017**, *601–602*, 1785–1802. https://doi.org/10.1016/j.scitotenv.2017.06.024.

(3) Allen, E. W. Process Water Treatment in Canada's Oil Sands Industry: II. A Review of Emerging Technologies. *Journal of Environmental Engineering and Science* **2008**, *7* (5), 499–524. https://doi.org/10.1139/S08-020.

(4) Honarvar, A.; Dinara, J. R.; Thorn, M.; Carlos, W.; Murillo, A.; Walden, Z. *Economic Impacts of New Oil Sands Projects in Alberta (2010--2035)*; 2011.

(5) Arshad, M.; Khosa, M. A.; Siddique, T.; Ullah, A. Modified Biopolymers as Sorbents for the Removal of Naphthenic Acids from Oil Sands Process Affected Water (OSPW). *Chemosphere* **2016**, *163*, 334–341. https://doi.org/10.1016/j.chemosphere.2016.08.015.

(6) Seyedy Niasar, H.; Xu, Dr. C. (Chunbao); Ray, Dr. M. Treatment of Oil Sands Process-Affected Water Using Activated and Surface Modified Petroleum Coke for Organic Compounds Recovery. *Chemical and Biochemical Engineering* **2017**, *Doctor of* (September), 190.

(7) Zubot, W. A. *Removal of Naphthenic Acids from Oil Sands Process Water Using Petroleum Coke.*; Library and Archives Canada = Bibliothèque et Archives Canada, 2011.

(8) Zubot, W.; MacKinnon, M. D.; Chelme-Ayala, P.; Smith, D. W.; Gamal El-Din, M. Petroleum Coke Adsorption as a Water Management Option for Oil Sands Process-Affected Water. *Science of the Total Environment*. 2012, pp 364–372. https://doi.org/10.1016/j.scitotenv.2012.04.024.

(9) University of Calgary PRISM Repository Https://Prism.Ucalgary.ca Removal of Naphthenic Acid from Water Using Biomass-Based Activated Carbon Iranmanesh, Sobhan Iranmanesh, S. (2013). Removal of Naphthenic Acid from Water Using Biomass-Based. https://doi.org/10.11575/PRISM/27627.

(10) Azad, F. S.; Abedi, J.; Iranmanesh, S. Removal of Naphthenic Acids Using Adsorption Process and the Effect of the Addition of Salt. *J Environ Sci Health A Tox Hazard Subst Environ Eng* **2013**, *48* (13), 1649–1654. https://doi.org/10.1080/10934529.2013.815457.

(11) Charlottetown, K. R. *Mechanisms of Naphthenic Acid Toxicity*; 2020.

(12) Clemente, J. S.; Fedorak, P. M. A Review of the Occurrence, Analyses, Toxicity, and Biodegradation of Naphthenic Acids. *Chemosphere* **2005**, *60* (5), 585–600. https://doi.org/10.1016/j.chemosphere.2005.02.065.

(13) Martinez Iglesias, A.; Madhumita Ray, S.; Iglesias, M. *Treatment of Synthetic Oil Sands Tailing Water with Activated Carbon Recommended Citation*; 2015. http://ir.lib.uwo.ca/etd.

(14) Brown, L. D. *Biological Treatment of Naphthenic Acids and Other Organic Compounds in Oil Sands Process-Affected Waters*.

(15) Headley, J. V.; McMartin, D. W. A Review of the Occurrence and Fate of Naphthenic Acids in Aquatic Environments. *J Environ Sci Health A Tox Hazard Subst Environ Eng* **2004**, *39* (8), 1989–2010. https://doi.org/10.1081/ESE-120039370.

(16) Rogers, V. V.; Liber, K.; MacKinnon, M. D. Isolation and Characterization of Naphthenic Acids from Athabasca Oil Sands Tailings Pond Water. *Chemosphere* **2002**, *48* (5), 519–527. https://doi.org/10.1016/S0045-6535(02)00133-9.

(17) Small, C. C.; Small, C. C. University of Alberta Activation of Delayed and Fluid Petroleum Coke for the Adsorption and Removal of Naphthenic Acids from Oil Sands Tailings Pond Water by Master of Science in Civil and Environmental Engineering Examining Committee Dr . Zaher Hashisho . **2011**.

(18) Masliyah, J.; Zhou, Z.; Xu, Z.; Czarnecki, J.; Hamza, H. Understanding Water-Based Bitumen Extraction from Athabasca Oil Sands. *Canadian Journal of Chemical Engineering*. Canadian Society for Chemical Engineering 2004, pp 628–654. https://doi.org/10.1002/cjce.5450820403.

(19) Martinez-iglesias, A.; Seyedy, H.; Charles, C. Adsorption of Model Naphthenic Acids in Water with Granular Activated Carbon. **2015**, 881–894. https://doi.org/10.1260/0263-6174.33.10.881.

(20) Afzal, A. *University of Alberta Application of Advanced Oxidation Processes for Treatment of Naphthenic Acids in Oil Sands Process Water*.

(21) Islam, M. S.; McPhedran, K. N.; Messele, S. A.; Liu, Y.; Gamal El-Din, M. Isotherm and Kinetic Studies on Adsorption of Oil Sands Process-Affected Water Organic Compounds Using Granular Activated Carbon. *Chemosphere*. 2018, pp 716–725. https://doi.org/10.1016/j.chemosphere.2018.03.149.

(22) Rogers, V. V; Wickstrom, M.; Liber, K.; Mackinnon, M. D. *Acute and Subchronic Mammalian Toxicity of Naphthenic Acids from Oil Sands Tailings*; 2002.

(23) Small, C. C.; Ulrich, A. C.; Hashisho, Z. Adsorption of Acid Extractable Oil Sands Tailings Organics onto Raw and Activated Oil Sands Coke. *Journal of Environmental Engineering* **2012**, *138* (8), 833–840. https://doi.org/10.1061/(asce)ee.1943-7870.0000543.

(24) Pourrezaei, P. *Physico-Chemical Processes for Oil Sands Process-Affected Water Treatment*.

(25) Islam, M. S.; Zhang, Y.; McPhedran, K. N.; Liu, Y.; Gamal El-Din, M. Mechanistic Investigation of Industrial Wastewater Naphthenic Acids Removal Using Granular Activated Carbon (GAC) Biofilm Based Processes. *Science of the Total Environment* **2016**, *541*, 238–246. https://doi.org/10.1016/j.scitotenv.2015.09.091.

(26) Niasar, H. S.; Li, H.; Kasanneni, T. V. R.; Ray, M. B.; Xu, C. C. Surface Amination of Activated Carbon and Petroleum Coke for the Removal of Naphthenic Acids and Treatment of Oil Sands Process-Affected Water (OSPW). *Chemical Engineering Journal* **2016**, *293*, 189–199. https://doi.org/10.1016/j.cej.2016.02.062.

(27) Sarkar, B.; Tong, S.; Jia, C. Q. Adsorption of Single-Ring Model Naphthenic Acid from Oil Sands Tailings Pond Water Using Petroleum Coke-Derived Activated Carbon. *Materials Science and Technology Conference and Exhibition 2013, MS and T 2013* **2013**, *3*.

(28) Brown, L. D.; Ulrich, A. C. Oil Sands Naphthenic Acids: A Review of Properties, Measurement, and Treatment. *Chemosphere*. 2015, pp 276–290. https://doi.org/10.1016/j.chemosphere.2015.02.003.

(29) Bauer, A.; Dixon, Dr. G. Identification of Oil Sands Naphthenic Acid Structures and Their Associated Toxicity to Pimephales Promelas and Oryzias Latipes. **2013**, *Master of*, 116.

(30) Grewer, D. M.; Young, R. F.; Whittal, R. M.; Fedorak, P. M. Naphthenic Acids and Other Acid-Extractables in Water Samples from Alberta: What Is Being Measured? *Science of the Total Environment* **2010**, *408* (23), 5997–6010. https://doi.org/10.1016/j.scitotenv.2010.08.013.

(31) Scott, A. C.; MacKinnon, M. D.; Fedorak, P. M. Naphthenic Acids in Athabasca Oil Sands Tailings Waters Are Less Biodegradable than Commercial Naphthenic Acids. *Environ Sci Technol* **2005**, *39* (21), 8388–8394. https://doi.org/10.1021/es051003k.

(32) Havre, T. E.; Sjöblom, J.; Vindstad, J. E. Oil/Water-Partitioning and Interfacial Behavior of Naphthenic Acids. *J Dispers Sci Technol* **2003**, *24* (6), 789–801. https://doi.org/10.1081/DIS-120025547.

(33) Hsu, C. S.; Dechert, G. J.; Robbins, W. K.; Fukuda, E. K. Naphthenic Acids in Crude Oils Characterized by Mass Spectrometry. *Energy and Fuels* **2000**, *14* (1), 217–223. https://doi.org/10.1021/ef9901746.

(34) Small, C. C.; Hashisho, Z.; Ulrich, A. C. Preparation and Characterization of Activated Carbon from Oil Sands Coke. *Fuel* **2012**, *92* (1), 69–76. https://doi.org/10.1016/j.fuel.2011.07.017.

(35) Brown, L. D.; Ulrich, A. C. Chemosphere Oil Sands Naphthenic Acids : A Review of Properties , Measurement , and Treatment. **2015**, *127*, 276–290. https://doi.org/10.1016/j.chemosphere.2015.02.003.

(36) Headley, J. V; Barrow, M. P. MASS SPECTROMETRIC CHARACTERIZATION OF NAPHTHENIC ACIDS IN ENVIRONMENTAL SAMPLES : A REVIEW. **2009**, 121–134. https://doi.org/10.1002/mas.

(37) Quagraine, E. K.; Peterson, H. G.; Headley, J. V. In Situ Bioremediation of Naphthenic Acids Contaminated Tailing Pond Waters in the Athabasca Oil Sands Region - Demonstrated Field Studies and Plausible Options: A Review. *J Environ Sci Health A Tox Hazard Subst Environ Eng* **2005**, *40* (3), 685–722. https://doi.org/10.1081/ESE-200046649.

(38) Toor, N. S.; Franz, E. D.; Fedorak, P. M.; MacKinnon, M. D.; Liber, K. Degradation and Aquatic Toxicity of Naphthenic Acids in Oil Sands Process-Affected Waters Using Simulated Wetlands. *Chemosphere* **2013**, *90* (2), 449–458. https://doi.org/10.1016/j.chemosphere.2012.07.059.

(39) Peng, J.; Headley, J. V; Barbour, S. L. Adsorption of Single-Ring Model Naphthenic Acids on Soils. *Canadian Geotechnical Journal* **2002**, *39* (6), 1419–1426. https://doi.org/10.1139/t02-098.

(40) Bataineh, M.; Scott, A. C.; Fedorak, P. M.; Martin, J. W. Capillary HPLC/QTOF-MS for Characterizing Complex Naphthenic Acid Mixtures and Their Microbial Transformation. *Anal Chem* **2006**, *78* (24), 8354–8361. https://doi.org/10.1021/ac061562p.

(41) Mohamed, M. H.; Wilson, L. D.; Headley, J. V; Mohamed, M. H.; Wilson, L. D.; Headley, J. V. Screening of Oil Sands Naphthenic Acids by UV-Vis Absorption and Fluorescence Emission Spectrophotometry Screening of Oil Sands Naphthenic Acids by UV-Vis Absorption and Fluorescence Emission Spectrophotometry. **2008**, *4529*. https://doi.org/10.1080/10934520802330255.

(42) Scott, A. C.; Young, R. F.; Fedorak, P. M. Chemosphere Comparison of GC – MS and FTIR Methods for Quantifying Naphthenic Acids in Water Samples. **2008**, *73*, 1258–1264. https://doi.org/10.1016/j.chemosphere.2008.07.024.

(43) Meshref, M. N. A.; Ibrahim, M. D.; Huang, R.; Yang, L.; How, Z. T.; Klamerth, N.; Chelme-Ayala, P.; Hughes, S. A.; Brown, C.; Mahaffey, A.; Gamal El-Din, M. Fourier Transform Infrared Spectroscopy as a Surrogate Tool for the Quantification of Naphthenic Acids in Oil Sands Process Water and Groundwater. *Science of the Total Environment* **2020**, *734*. https://doi.org/10.1016/j.scitotenv.2020.139191.

(44) Yen, T.; Marsh, W. P.; Mackinnon, M. D.; Fedorak, P. M. Measuring Naphthenic Acids Concentrations in Aqueous Environmental Samples by Liquid Chromatography. **2004**, *1033*, 83–90. https://doi.org/10.1016/j.chroma.2004.01.030.

(45) Bowman, D. T.; Warren, L. A.; Slater, G. F. Isomer-Specific Monitoring of Naphthenic Acids at an Oil Sands Pit Lake by Comprehensive Two-Dimensional Gas Chromatography–Mass Spectrometry. *Science of the Total Environment* **2020**, *746*, 140985. https://doi.org/10.1016/j.scitotenv.2020.140985.

(46) Brunswick, P.; Shang, D.; Aggelen, G. Van; Hindle, R.; Hewitt, L. M.; Frank, R. A.; Haberl, M.; Kim, M. Trace Analysis of Total Naphthenic Acids in Aqueous Environmental Matrices by Liquid Chromatography / Mass Spectrometry-Quadrupole Time of Flight Mass Spectrometry Direct Injection. **2015**, *1405*, 49–71.

(47) Munjanja, B. K. *Liquid Chromatography Mass Spectrometry (LC-MS)*; 2019; Vol. 1. https://doi.org/10.1201/9781315118352-7.

(48) MacLennan, M. S.; Peru, K. M.; Swyngedouw, C.; Fleming, I.; Chen, D. D. Y.; Headley, J. V. Characterization of Athabasca Lean Oil Sands and Mixed Surficial Materials: Comparison of Capillary Electrophoresis/Low-Resolution Mass Spectrometry and High-Resolution Mass Spectrometry. *Rapid Communications in Mass Spectrometry*. 2018, pp 695–702. https://doi.org/10.1002/rcm.8093.

(49) Headley, J. V.; Peru, K. M.; McMartin, D. W.; Winkler, M. Determination of Dissolved Naphthenic Acids in Natural Waters by Using Negative-Ion Electrospray Mass Spectrometry. *J AOAC Int* **2002**, *85* (1), 182–187.

(50) Barrow, M. P.; Headley, J. V.; Peru, K. M.; Derrick, P. J. Fourier Transform Ion Cyclotron Resonance Mass Spectrometry of Principal Components in Oilsands Naphthenic Acids. *J Chromatogr A* **2004**, *1058* (1–2), 51–59. https://doi.org/10.1016/j.chroma.2004.08.082.

(51) Marshall, A. G.; Rodgers, R. P. Petroleomics: Chemistry of the Underworld. *Proc Natl Acad Sci U S A* **2008**, *105* (47), 18090–18095. https://doi.org/10.1073/pnas.0805069105.

(52) Barrow, M. P.; McDonnell, L. A.; Feng, X.; Walker, J.; Derrick, P. J. Determination of the Nature of Naphthenic Acids Present in Crude Oils Using Nanospray Fourier Transform Ion Cyclotron Resonance Mass Spectrometry: The Continued Battle against Corrosion. *Anal Chem* **2003**, *75* (4), 860–866. https://doi.org/10.1021/ac020388b.

(53) Headley, J. V.; Armstrong, S. A.; Peru, K. M.; Mikula, R. J.; Germida, J. J.; Mapolelo, M. M.; Rodgers, R. P.; Marshall, A. G. Ultrahigh-Resolution Mass Spectrometry of Simulated Runoff from Treated Oil Sands Mature Fine Tailings. *Rapid Communications in Mass Spectrometry* **2010**, *24* (16), 2400–2406. https://doi.org/10.1002/rcm.4658.

(54) Headley, J. V.; Peru, K. M.; Armstrong, S. A.; Han, X.; Martin, J. W.; Mapolelo, M. M.; Smith, D. F.; Rogers, R. P.; Marshall, A. G. Aquatic Plant-Derived Changes in Oil Sands Naphthenic Acid Signatures Determined by Low-, High- And Ultrahigh-Resolution Mass Spectrometry. *Rapid Communications in Mass Spectrometry* **2009**, *23* (4), 515–522. https://doi.org/10.1002/rcm.3902.

(55) Barrow, M. P.; Witt, M.; Headley, J. V.; Peru, K. M. Athabasca Oil Sands Process Water: Characterization by Atmospheric Pressure Photoionization and Electrospray Ionization Fourier Transform Ion Cyclotron Resonance Mass Spectrometry. *Anal Chem* **2010**, *82* (9), 3727–3735. https://doi.org/10.1021/ac100103y.

(56) Gamal El-Din, M.; Fu, H.; Wang, N.; Chelme-Ayala, P.; Pérez-Estrada, L.; Drzewicz, P.; Martin, J. W.; Zubot, W.; Smith, D. W. Naphthenic Acids Speciation and Removal during Petroleum-Coke Adsorption and Ozonation of Oil Sands Process-Affected Water. *Science of the Total Environment* **2011**, *409* (23), 5119–5125. https://doi.org/10.1016/j.scitotenv.2011.08.033.

(57) Pereira, A. S.; Islam, M. S.; Gamal El-Din, M.; Martin, J. W. Ozonation Degrades All Detectable Organic Compound Classes in Oil Sands Process-Affected Water; An Application of High-Performance Liquid Chromatography/Obitrap Mass Spectrometry. *Rapid Communications in Mass Spectrometry* **2013**, *27* (21), 2317–2326. https://doi.org/10.1002/rcm.6688.

(58) Sophia A., C.; Lima, E. C. Removal of Emerging Contaminants from the Environment by Adsorption. *Ecotoxicol Environ Saf* **2018**, *150*, 1–17. https://doi.org/10.1016/j.ecoenv.2017.12.026.

(59) Iranmanesh, S.; Harding, T.; Abedi, J.; Seyedeyn-Azad, F.; Layzell, D. B. Adsorption of Naphthenic Acids on High Surface Area Activated Carbons. *J Environ Sci Health A Tox Hazard Subst Environ Eng* **2014**, *49* (8), 913–922. https://doi.org/10.1080/10934529.2014.894790.

(60) Han, X.; Scott, A. C.; Fedorak, P. M.; Bataineh, M.; Martin, J. W. Influence of Molecular Structure on the Biodegradability of Naphthenic Acids. *Environ Sci Technol* **2008**, *42* (4), 1290–1295. https://doi.org/10.1021/es702220c.

(61) Mônaco, F. S.; de Aguiar, D. V. A.; Oliveira, G. de A. R.; Vaz, B. G.; Lião, L. M.; de Andrade, L. A.; Ostroski, I. C. Adsorption of Organic Acids from Offshore Produced Water Using Microporous Activated Carbon from Babassu Pericarp: A Low-Cost Alternative. *Chem Eng Commun* **2022**. https://doi.org/10.1080/00986445.2022.2045281.

(62) Dawson, S. *Adsorption of Naphthenic Acids onto Activated Carbon Produced from Petroleum Coke*; 2011.

(63) Fisher, K. S.; Vreugdenhil, A. J. Adsorption of Chromium (VI) Using an Activated Carbon Derived from Petroleum Coke Feedstock. *Int J Mol Sci* **2022**, *23* (24). https://doi.org/10.3390/ijms232416172.

(64) Niasar, H. S.; Das, S.; Xu, C. (Charles); Ray, M. B. Continuous Column Adsorption of Naphthenic Acids from Synthetic and Real Oil Sands Process-Affected Water (OSPW) Using Carbon-Based Adsorbents. *Chemosphere* **2019**, *214*, 511–518. https://doi.org/10.1016/j.chemosphere.2018.09.078.

(65) Kawano, T.; Kubota, M.; Onyango, M. S.; Watanabe, F.; Matsuda, H. Preparation of Activated Carbon from Petroleum Coke by KOH Chemical Activation for Adsorption Heat Pump. *Appl Therm Eng* **2008**, *28* (8–9), 865–871. https://doi.org/10.1016/j.applthermaleng.2007.07.009.

(66) Selwi A, A. Source Rock Evaluation Using Total Organic Carbon (TOC) and the Loss- On-Ignition (LOI) Techniques. *Oil & Gas Research* **2015**, *1* (1). https://doi.org/10.4172/2472-0518.1000105.

(67) Bansal, R. C.; Goyal, Meenakshi. *Activated Carbon Adsorption*; Taylor & Francis, 2005.

(68) Sing, K. S. W. *INTERNATIONAL UNION OF PURE AND APPLIED CHEMISTRY PHYSICAL CHEMISTRY DIVISION COMMISSION ON COLLOID AND SURFACE CHEMISTRY INCLUDING CATALYSIS SUBCOMMITTEE ON REPORTING GAS ADSORPTION DATA* REPORTING PHYSISORPTION DATA FOR GAS/SOLID SYSTEMS with Special Reference to the Determination of Surface Area and Porosity*; 1982; Vol. 54.

(69) Thommes, M.; Kaneko, K.; Neimark, A. V.; Olivier, J. P.; Rodriguez-Reinoso, F.; Rouquerol, J.; Sing, K. S. W. Physisorption of Gases, with Special Reference to the Evaluation of Surface Area and Pore Size Distribution (IUPAC Technical Report). *Pure and Applied Chemistry* **2015**, *87* (9–10), 1051–1069. https://doi.org/10.1515/pac-2014-1117.

(70) Stevie, F. A.; Donley, C. L. Introduction to X-Ray Photoelectron Spectroscopy. *Journal of Vacuum Science & Technology A: Vacuum, Surfaces, and Films* **2020**, *38* (6). https://doi.org/10.1116/6.0000412.

(71) Expansion of the Analytical Window for Oil Spill Characterization by Ultrahigh Resolution Mass Spectrometry_ Beyond Gas Chromatography.

(72) Marshall, A. G.; Hendrickson, C. L.; Jackson, G. S. Fourier Transform Ion Cyclotron Resonance Mass Spectrometry: A Primer. *Mass Spectrom Rev* **1998**, *17* (1), 1–35. https://doi.org/10.1002/(SICI)1098-2787(1998)17:1<1::AID-MAS1>3.0.CO;2-K.

(73) Cho, Y.; Ahmed, A.; Islam, A.; Kim, S. Developments in FT-ICR Ms Instrumentation, Ionization Techniques, and Data Interpretation Methods for Petroleomics. *Mass Spectrom Rev* **2015**, *34* (2), 248–263. https://doi.org/10.1002/mas.21438.

(74) Tuning Electrospray Ionization with Low-Frequency Sound.

(75) Reemtsma, T. Determination of Molecular Formulas of Natural Organic Matter Molecules by (Ultra-) High-Resolution Mass Spectrometry. Status and Needs. *Journal of Chromatography A*. May 1, 2009, pp 3687–3701. https://doi.org/10.1016/j.chroma.2009.02.033.

(76) Tran, H. N.; You, S. J.; Hosseini-Bandegharaei, A.; Chao, H. P. Mistakes and Inconsistencies Regarding Adsorption of Contaminants from Aqueous Solutions: A Critical Review. *Water Research*. Elsevier Ltd 2017, pp 88–116. https://doi.org/10.1016/j.watres.2017.04.014.

(77) Ntakirutimana, S.; Tan, W.; Wang, Y. Enhanced Surface Activity of Activated Carbon by Surfactants Synergism. *RSC Adv* **2019**, *9* (45), 26519–26531. https://doi.org/10.1039/c9ra04521j.

(78) *Eckhard Worch Adsorption Technology in Water Treatment*.

(79) Marczewski, A. W.; Seczkowska, M.; Deryło-Marczewska, A.; Blachnio, M. Adsorption Equilibrium and Kinetics of Selected Phenoxyacid Pesticides on Activated Carbon: Effect of Temperature. *Adsorption* **2016**, *22* (4–6), 777–790. https://doi.org/10.1007/s10450-016-9774-0.

(80) Ayawei, N.; Ebelegi, A. N.; Wankasi, D. Modelling and Interpretation of Adsorption Isotherms. *J Chem* **2017**, *2017*. https://doi.org/10.1155/2017/3039817.

(81) Foo, K. Y.; Hameed, B. H. Insights into the Modeling of Adsorption Isotherm Systems. *Chemical Engineering Journal* **2010**, *156* (1), 2–10. https://doi.org/10.1016/j.cej.2009.09.013.

(82) Wu, F. C.; Liu, B. L.; Wu, K. T.; Tseng, R. L. A New Linear Form Analysis of Redlich-Peterson Isotherm Equation for the Adsorptions of Dyes. *Chemical Engineering Journal* **2010**, *162* (1), 21–27. https://doi.org/10.1016/j.cej.2010.03.006.

(83) Eder, S.; Müller, K.; Azzari, P.; Arcifa, A.; Peydayesh, M.; Nyström, L. Mass Transfer Mechanism and Equilibrium Modelling of Hydroxytyrosol Adsorption on Olive Pit–Derived Activated Carbon. *Chemical Engineering Journal* **2021**, *404* (June 2020). https://doi.org/10.1016/j.cej.2020.126519.

(84) Roy, T. M.; Nazari, E.; Strong, O. K. L.; Pede, P. R.; Vreugdenhil, A. J. The Effect of Adsorbent Textural and Functional Properties on Model Naphthenic Acid Adsorption. *Journal of Environmental Sciences* **2025**, *148*, 27–37. https://doi.org/10.1016/j.jes.2024.01.003.

(85) Strong, O. K. L.; France, H. E.; Scotland, K.; Wright, K.; Vreugdenhil, A. J. Selenite Adsorption and Reduction via Iron(II) Impregnated Activated Carbon Produced from the Phosphoric Acid Activation of Construction Waste Wood. *Arch Environ Contam Toxicol* **2023**, *85* (4), 485–497. https://doi.org/10.1007/s00244-023-01032-y.

(86) Niasar, H. S.; Li, H.; Das, S.; Kasanneni, T. V. R.; Ray, M. B.; Xu, C. (Charles). Preparation of Activated Petroleum Coke for Removal of Naphthenic Acids Model Compounds: Box-Behnken Design Optimization of KOH Activation Process. *J Environ Manage* **2018**, *211*, 63–72. https://doi.org/10.1016/j.jenvman.2018.01.051.

(87) Strong, O. K. L.; Nazari, E.; Roy, T.; Scotland, K.; Pede, P. R.; Vreugdenhil, A. J. Transforming Micropores to Mesopores by Heat Cycling KOH Activated Petcoke for Improved Kinetics of Adsorption of Naphthenic Acids. *Heliyon* **2023**, *9* (2). https://doi.org/10.1016/j.heliyon.2023.e13500.

(88) Heidarinejad, Z.; Dehghani, M. H.; Heidari, M.; Javedan, G.; Ali, I.; Sillanpää, M. Methods for Preparation and Activation of Activated Carbon: A Review. *Environmental Chemistry Letters*. Springer March 1, 2020, pp 393–415. https://doi.org/10.1007/s10311-019-00955-0.

(89) Luo, Y.; Li, D.; Chen, Y.; Sun, X.; Cao, Q.; Liu, X. The Performance of Phosphoric Acid in the Preparation of Activated Carbon-Containing Phosphorus Species from Rice Husk Residue. *J Mater Sci* **2019**, *54* (6), 5008–5021. https://doi.org/10.1007/s10853-018-03220-x.

(90) Headley, J. V.; Barrow, M. P.; Peru, K. M.; Fahlman, B.; Frank, R. A.; Bickerton, G.; McMaster, M. E.; Parrott, J.; Hewitt, L. M. Preliminary Fingerprinting of Athabasca Oil Sands Polar Organics in Environmental Samples Using Electrospray Ionization Fourier Transform Ion Cyclotron Resonance Mass Spectrometry. *Rapid Communications in Mass Spectrometry* **2011**, *25* (13), 1899–1909. https://doi.org/10.1002/rcm.5062.

(91) Barrow, M. P.; Peru, K. M.; McMartin, D. W.; Headley, J. V. Effects of Extraction PH on the Fourier Transform Ion Cyclotron Resonance Mass Spectrometry Profiles of Athabasca Oil Sands Process Water. *Energy and Fuels* **2016**, *30* (5), 3615–3621. https://doi.org/10.1021/acs.energyfuels.5b02086.

(92) Headley, J. V.; Peru, K. M.; Barrow, M. P. Advances in Mass Spectrometric Characterization of Naphthenic Acids Fraction Compounds in Oil Sands Environmental Samples and Crude Oil - A Review. *Mass Spectrom Rev* **2016**, *35* (2), 311–328. https://doi.org/10.1002/mas.21472.

(93) Hughey, C. A.; Minardi, C. S.; Galasso-Roth, S. A.; Paspalof, G. B.; Mapolelo, M. M.; Rodgers, R. P.; Marshall, A. G.; Ruderman, D. L. Naphthenic Acids as Indicators of Crude Oil Biodegradation in Soil, Based on Semi-Quantitative Electrospray Ionization Fourier Transform Ion Cyclotron Resonance Mass Spectrometry. *Rapid Communications in Mass Spectrometry* **2008**, *22* (23), 3968–3976. https://doi.org/10.1002/rcm.3813.

(94) Colati, K. A. P.; Dalmaschio, G. P.; De Castro, E. V. R.; Gomes, A. O.; Vaz, B. G.; Romão, W. Monitoring the Liquid/Liquid Extraction of Naphthenic Acids in Brazilian Crude Oil Using Electrospray Ionization FT-ICR Mass Spectrometry (ESI FT-ICR MS). *Fuel* **2013**, *108*, 647–655. https://doi.org/10.1016/j.fuel.2013.02.007.

(95) Barrow, M. P.; Peru, K. M.; Fahlman, B.; Hewitt, L. M.; Frank, R. A.; Headley, J. V. Beyond Naphthenic Acids: Environmental Screening of Water from Natural Sources and the Athabasca Oil Sands Industry Using Atmospheric Pressure Photoionization Fourier Transform Ion Cyclotron Resonance Mass Spectrometry. *J Am Soc Mass Spectrom* **2015**, *26* (9), 1508–1521. https://doi.org/10.1007/s13361-015-1188-9.

(96) Rahman, M. M.; Muttakin, M.; Pal, A.; Shafiullah, A. Z.; Saha, B. B. A Statistical Approach to Determine Optimal Models for IUPAC-Classified Adsorption Isotherms. *Energies (Basel)* **2019**, *12* (23). https://doi.org/10.3390/en12234565.